



The
University
Of
Sheffield.

Acuity and binocularity of the fruit fly: behaviour in a virtual environment

Ben Scales

A thesis submitted for the degree of Doctor of Philosophy

Department of Biomedical Science

The University of Sheffield

December 2021

Acknowledgements

First, I would like to express my gratitude to my supervisor, Professor Mikko Juusola, for the opportunity to embark upon this PhD and for your knowledge, guidance and support to develop my early research skills.

I am thankful to the BBSRC Doctoral Training Partnership for funding me for over four years of study.

A special thank you to Dr Jouni Takalo, a key source of support and kindness throughout my studies. And to Joni, I am grateful for our mutual journey as we embarked on our PhDs together.

I want to thank all current and former members of our group, particularly Neveen, Keivan and James, for making a friendly and enjoyable atmosphere to collaborate. And, of course, play chess. In addition, I am grateful for the initial help and training using the flight simulator from Dr David Jacuich and Dr Narendra Solanki.

Thanks to my advisors, Dr Anton Nikolaev and Dr Martin Zeidler, who provided vital feedback, sound advice, and positive encouragement throughout my studies.

Thank you to all my family. Especially to my soon to be wife, Emma. A constant source of encouragement and inspiration to me throughout the highs and lows of our parallel PhD journeys.

Abstract

Despite minuscule eyes and tiny brains, flying insects successfully perform remarkable behaviours with their limited visual system. In this thesis, I have investigated how the fruit fly (*Drosophila melanogaster*) responds to visual stimuli of different sizes and depths in a virtual environment. For tethered flying *Drosophila*, I analyse the orientation and robustness of perception to small objects and square gratings during innate, voluntary, and conditioned behaviours. My research aims to understand whether fruit flies respond behaviourally to objects smaller than their optical resolution limit and whether binocularity is used for small object detection.

Recent work has highlighted that ultrafast photomechanical photoreceptor microsaccades beneath the lens may enhance the spatial resolution limit of the fly below the optical limit. Therefore, I investigated how fruit flies respond to extremely small singular objects and dark and light stripes (gratings) within their visual field. My results reveal that fruit flies respond behaviourally to stimuli smaller than the interommatidial angle (the angular separation between neighbouring lenses). Additionally, flies respond robustly to close and small patterns when the pattern subtends the same size on the retina but are presented as either *close-small* or *far-big*. Furthermore, flies show an innate attraction for a singular feature when presented with distinct 2D or 3D small objects (ranging between 1-4°). Finally, learning experiments confirm that they can discriminate between these objects, although they fail to learn when one eye is occluded. Taken together, this supports the theory that fruit flies possess higher spatial resolution than predicted by their optics and use binocularity in close range.

In summary, the results gathered in this thesis contribute to a new insight into the visually guided behaviours of insects in virtual environments. Among other findings, my results emphasise the importance of both eyes contribution to vision, enhancing the animals' ability to see their world.

Contents

Chapter 1	1
Introduction.....	1
1.1 Invertebrate vision.....	1
1.1.1 Invertebrate visual system.....	2
1.1.2 Spatial vision.....	9
1.1.3 Motion and active vision.....	13
1.1.4 Binocular vision	18
1.2 Measuring behaviour.....	21
1.2.1 Using virtual reality	21
1.2.2 The optomotor response.....	22
1.2.3 Object detection and fixation	27
1.2.4 Learning at the torque meter	29
1.3 Thesis overview.....	33
Chapter 2.....	35
Pattern size and distance predict optomotor behaviour in fruit flies	35
2.1 Introduction	36
2.2 Materials and Methods	38
2.2.1 Experimental animals.....	38
2.2.2 Flight simulator.....	39
2.2.3 Arena size.....	39
2.2.4 Experimental setup.....	41
2.2.5 Data analysis	44
2.2.6 Statistics	44

2.3	Results	44
2.3.1	Effect of distance on optomotor responses to small patterns.....	45
2.3.2	Large patterns elicit stable responses over two distances	46
2.3.3	Fruit flies respond to gratings smaller than the interommatidial angle	49
2.3.4	Optomotor reversal is dependant on velocity and binocularity	51
2.4	Discussion	54
	Distance and optomotor	54
	Optomotor reversal	55
	Future work.....	56
	Conclusions.....	57
Chapter 3	58
Small object detection and discrimination in fruit flies	58
3.1	Introduction	59
3.2	Materials and Methods	61
3.2.1	Experimental animals.....	61
3.2.2	Single object detection in fruit flies	62
3.2.3	Combining 3D with 2D visual cues	62
3.2.4	Small pattern learning	63
3.2.5	Deep pseudopupil imaging	66
3.2.6	Data analysis	66
3.2.7	Statistics	68
3.3	Results	69
3.3.1	A small single visual cue	69
3.3.2	The use of a small depth cue.....	73
3.3.3	Preference for single 2D and 3D small visual cues	77
3.3.4	Constant orientation throughout the flight.....	77
3.3.5	Learning small visual cues requires both eyes in fruit flies.....	81

3.3.6	Faulty microsaccades disrupt learning	87
3.3.7	Combination of inner and outer photoreceptors	93
3.4	Discussion	100
	Single object detection.....	100
	Small objects are more salient with depth cues	101
	Contrast and hyperacute vision.....	102
	Visual acuity of gratings and single objects	103
	Object size and attraction.....	103
	Less fixation for the ‘right section’	105
	Possible limitation of head restriction.....	106
	Effect of time on attraction	106
	Two eyes permit learning small visual cues	107
	Learning with normal or defective photoreceptor movements	108
	Both photoreceptor channels contribute to hyperacute vision.....	109
	The use of real object depth.....	109
	A behavioural need for high acuity and binocularity.....	111
	Conclusions.....	112
Chapter 4	113
Concluding remarks	113
	Future directions	114
	Impact in the field	115
Supplement figures	117
References	126

List of figures

Chapter 1

Fig. 1.1 The compound eye.....	3
Fig. 1.2 Two optical designs of compound eyes.....	8
Fig. 1.3 Two optical parameters that define visual acuity.	12
Fig. 1.4 <i>Drosophila</i> photoreceptor microsaccades enhance spatial resolving power.	17
Fig. 1.5 Depth cues in animals.....	20
Fig. 1.6 Examples of measuring invertebrate behaviour using virtual reality.	22
Fig. 1.7 Examples of measuring optomotor behaviour in animals.	24
Fig. 1.8 The moiré effect.....	26
Fig. 1.9 <i>Drosophila</i> at the torque meter.	26
Fig. 1.10 Visual learning in the flight simulator.	32

Chapter 2

Fig. 2.1 The experimental setup.....	41
Fig. 2.2 Optomotor protocol and stimuli.	45
Fig. 2.3 Example fly performed differently when tested at two distances.	45
Fig. 2.4 Small patterns elicit stronger optomotor responses when closer.....	47
Fig. 2.5 Large patterns elicit consistent optomotor responses.	48
Fig. 2.6 Fruit flies respond to hyperacute gratings.	50
Fig. 2.7 Optomotor reversal is velocity-dependent.....	53

Chapter 3

Fig. 3.1 Single object experiments.....	63
Fig. 3.2 Visual learning experiments.	65
Fig. 3.3 Detecting and using a singular small visual cue to direct orientation.	70

Fig. 3.4 Effect of dot position on orientation preference.	72
Fig. 3.5 Using a subtle depth cue within small objects for orientation.....	74
Fig. 3.6 Effect of pin position on orientation preference.	76
Fig. 3.7 Singular 2D or 3D objects, when tested separately, are equally salient.	78
Fig. 3.8 Stable fixation in time when viewing a small single visual cue.	79
Fig. 3.9 Stable fixation in time when viewing a small single 3D object.	80
Fig. 3.10 Visual learning of fruit flies using small visual cues.....	82
Fig. 3.11 Monocular vision inhibits visual learning of small cues.	84
Fig. 3.12 Fruit flies use both eyes for learning small visual cues.	86
Fig. 3.13 Fruit flies require photoreceptor microsaccades to learn small visual cues.	88
Fig. 3.14 Faulty photoreceptor microsaccades inhibit visual learning.	90
Fig. 3.15 Visual learning is dependent on functional microsaccades.	92
Fig. 3.16 Outer (R1-R6) photoreceptors elicit learning.	94
Fig. 3.17 Inner (R7/8) photoreceptors elicit learning.	96
Fig. 3.18 Pooled scores of mutants with inner (R7/8) photoreceptors.....	97
Fig. 3.19 Combined photoreceptor channels enhance the learning of small visual cues in fruit flies.....	99

Supplementary figures

Fig. S1 Optomotor responses of fruit flies presented gratings with different wavelengths at two distances under slow rotational velocity (45°/s).	117
Fig. S2 Optomotor responses of fruit flies presented gratings with different wavelengths at two distances under fast rotational velocity (300°/s).	118
Fig. S3 Example flies show a strong bias towards the small dot.	119
Fig. S4 Example flies of visual learning.	120
Fig. S5 Blind mutants confirm visual learning in fruit flies.	121
Fig. S6 Monocular vision type and learning performance.....	122
Fig. S7 Learning scores for all fly groups.....	123
Fig. S8 Direction of heat punishment effects visual learning.	124

Symbols and abbreviation list

$\Delta\rho$	Acceptance angle
AC	Amacrine cell
CS	Conditioned stimulus
CS+	Conditioned stimulus with US
CS-	Conditioned stimulus without US
\emptyset	Diameter
ERG	Electroretinogram
EMD	Elementary motion detector
F	Focal length
$\Delta\varphi$	Interommatidial angle
LMC	Large monopolar cells
LED	Light emitting diode
D	Lens diameter
LPTC	Lobula plate tangential cells
R	Radius curve
Rh	Rhodopsin
PI	Performance index
λ	Spatial wavelength
US	Unconditioned stimulus
UV	Ultraviolet

Chapter 1

Introduction

1.1 Invertebrate vision

In a world deluged with information, animals use their sensory systems to gather knowledge about their surroundings. While no sensory system functions in isolation, vision is the foremost sensory input for many animals, providing a rapid and constant source of information to the observer (Warrant and Nilsson, 2006). Consequently, selection pressures must have actively shaped the early organisms' visual organs (Land and Fernald, 1992; Fernald, 2000) for better perception of the environment, improving survival for those with superior vision (Cronin *et al.*, 2014). Indeed, the invertebrates – animals with no backbone – have been found to possess high-resolution vision (Nilsson, 2013) in fossils dated to the Cambrian explosion approximately 540 million years ago (Land and Nilsson, 2012).

To perform tasks and overcome visual challenges, animals use vision to guide their behaviour (Cronin *et al.*, 2014). Examples of different visual challenges include the interception and capture of insect prey by aerial predators (Wardill *et al.*, 2017); the detection and evasion of predators (de la Flor *et al.*, 2017); the pursuit of potential mates (Somanathan *et al.*, 2017); and the collection of nectar and pollen before relocating the nest in central place foragers (Goulson, 1999). Thus, the visual system and the visual behaviours are inextricably entwined (Endler, 1992). An animal's visually guided behaviours drive the selection pressures placed on the visual system, while the accuracy of the visual information mediates the effective execution of the behaviours.

Consequently, studying the visual system in the context of these visual behaviours is essential even when the animal is removed from the wild. Natural behaviours - the typical behaviour that an animal would exhibit in the wild - can be readily studied by observing freely moving animals in their natural surroundings. Regardless, as has been undertaken within this thesis,

many aspects of visually guided behaviour can be better investigated within a laboratory setting where the exact visual information can be better controlled.

This opening chapter explores the invertebrate visual system and the most relevant functional modalities of vision, to the use of virtual reality environments for measuring animal behaviour, and an overview of the aims and objectives of this thesis.

1.1.1 Invertebrate visual system

The insect visual system typically contains five visual organs; a pair of lateral compound eyes and a triplet of median ocelli (Buschbeck and Friedrich, 2008). This combination is characteristic of many insects, although an additional pair of visual organs - the H-B eyelet - are present in the fruit fly *Drosophila melanogaster* (Buschbeck and Friedrich, 2008). The ocelli are three (some species possess one or two) small single-chambered eyes located in the dorsal head cuticle as a small cluster (Yoon, Hirosawa and Suzuki, 1996). Historically, their exact function was difficult to determine (Wilson, 1978), though generally, it is now known that each forms a blurry image to aid in the animal's flight control (Stange *et al.*, 2002). However, compound eyes are the focus of this thesis.

Compound eyes

The compound eyes are two large, multi-purpose eyes that capture the vast majority of the visual information facilitating many invertebrate behaviours (Land & Nilsson, 2012). The exact form differs between and within species, though it is usually almost spherical and covers a large visual field. Fruit flies, for example, sample about 85% of visual space (Buchner, 1971). The eye comprises many small hexagonal "facets" that form a convex structure on the eye's surface. Each facet is the outer layer of an individual optical unit called the ommatidium (pl. ommatidia), consisting of a transparent cornea, crystalline cone and photoreceptor cells. The photoreceptor cells (or photoreceptors as they are often called) are characterised by their rod-like light-sensitive parts, the rhabdomeres, which in some species (with apposition eyes) fuse to form a single rod, the rhabdom (**Fig. 1.1**) (Land & Nilsson, 2012). The cornea focuses light - as an inverted image - from a small region of space onto the distal rhabdomere or rhabdom tips (their focal plane), with the rhabdomere/rhabdom functioning as a waveguide(s) maximising information capture from the incoming photon flux. Meanwhile, the crystalline cone is thought to function as a spacer due to its low and homogeneous refractive index.

Surrounding each ommatidium is a black screen of light-absorbing pigment to stop rays passing between ommatidia, thereby isolating each ommatidium (Yack *et al.*, 2007). Each isolated sampling unit codes light information from a small region of visual space. Customarily, this region has been considered analogous to the 'pixel' within a camera image. So neighbouring ommatidia are thought to sample light from adjacent regions of space, collectively sculpting a mosaic of pixels to form the overall image (Shaw, 1984).

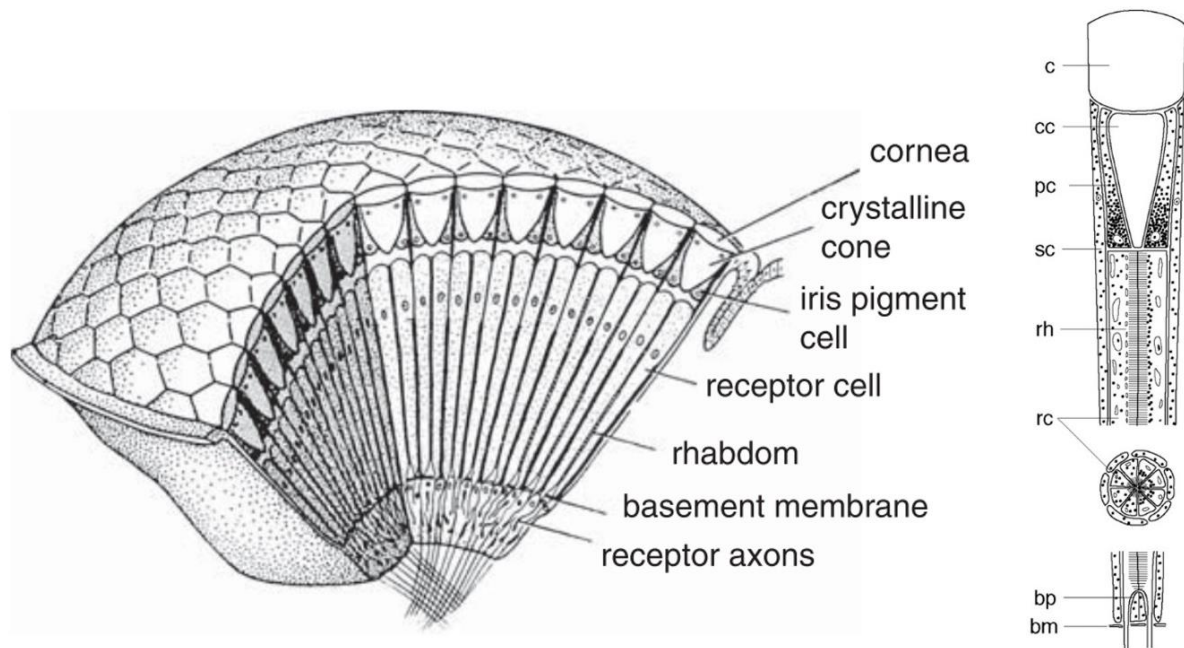


Fig. 1.1 The compound eye.

(left) Schematic of the overall structure of the compound eye, showing the arrangement of ommatidia (right) and a longitudinal cross-section of an ommatidium. Abbreviations show the cornea (c), crystalline cone (cc), pigment cell (pc), secondary pigment cells (sc), rhabdom (rh), retinula cells (rc), basal pigment cells (bp) and basement membrane (bm). Images adapted from Land & Nilsson, (2012) (left) and Warrant, (2019) (right).

Consequently, the greater the number and density of ommatidia an invertebrate can possess, the more detail is captured in the image. The dragonfly is an extreme example of high ommatidia numbers, with approximately 30,000 units per eye compared to the 750 or 5,500 found in the fruit fly and honeybee, respectively (Seidl and Kaiser, 1981; Srinivasan, 2011; Land and Nilsson, 2012). Such differences are presumably due to the ecological demands placed on the species. Indeed, the need to intercept prey mid-air is an evident selection pressure

for high acuity in dragonflies (Land, 1997). Resolvability is explored in more detail below (see 1.1.2 Spatial vision).

Photoreceptor cells

A rod-like photoreceptor rhabdomere contains tens of thousands of specialised bristle-like membrane foldings called the microvilli (Hardie and Juusola, 2015). For example, a typical *Drosophila* photoreceptor has about 30,000 microvilli aligned along its inner length, jointly forming its tapering rhabdomere (Juusola and Hardie, 2001). Each microvillus is a fully compartmentalised photon sampling unit (Song *et al.*, 2012). It contains all the necessary phototransduction molecules (G-protein cascade), including the light-sensitive pigment, rhodopsin, to convert photon absorptions to minute elementary electrochemical signals, the quantum bumps (Hardie and Juusola, 2015). Rhodopsin, which is abundant in microvilli, contains a colourless opsin protein, pocketing in a chromophore, retinal. In photon absorption, retinal photoisomerises while opsin tunes this reaction's spectral sensitivity (Briscoe and Chittka, 2001; Hardie and Juusola, 2015). Due to the high density of rhodopsin (Osorio, 2007) within the highly-dense microvilli, each rhabdomere or rhabdom has a higher refractive index than the surrounding medium (Shaw, 1984). Consequently, the rhabdomere/rhabdom encloses light within it, acting as a waveguide (Shaw, 1984; Hardie and Raghu, 2001).

During light stimulation, the quantum bump waveforms, amplitudes and numbers across a photoreceptor's microvilli adapt rapidly to sum up its macroscopic response, i.e. a graded voltage change (Henderson, Reuss and Hardie, 2000; Juusola and Hardie, 2001; Juusola *et al.*, 2017). These graded voltage responses across the compound eyes represent the light patterns in the visual environment and are essential for forming images of the world and detecting motion (Land & Nilsson, 2012). As light enters the distal tip(s) of the rhabdomeres or a rhabdom and travels down the structure, it is contained by internal reflection (Land & Nilsson, 2012). However, in the conventional theoretical models that assume an immobilised eye with static structures, the spatial information of the image is lost for each ommatidium as it travels down the rhabdom. In reality, the local photomechanical photoreceptor contractions across the eyes significantly reduce this spatial information loss, enabling more acute perception (Juusola *et al.*, 2017; Kemppainen *et al.*, 2022; see 1.1.3. Active vision, below). With each rhabdom only discriminating the intensity of the incident light, and each ommatidium only discriminating average intensity and colour (and often the polarisation) of the light in respect

to its neighbours (Warrant and McIntyre, 1993), insect compound eyes have been thought to provide a mosaic-like view of the world as mentioned above.

The number of photoreceptor cells within an ommatidium varies between species, though it is common for an insect to possess eight cells (R1-R8). For example, *Drosophila* have the typical eight cells while honeybees have an additional cell (Land and Nilsson, 2012). The rhabdomeres of the six larger peripheral (outer) photoreceptor cells (R1-R6) extend the entire span of the cell body. In contrast, the rhabdomeres of the two narrower (inner) photoreceptors (R7-R8) at the ommatidium centre are arranged in tandem with R7 distal and R8 proximal (Warrant and Nilsson, 2006). Thus, there are only seven cells at any cross-section of the ommatidium (Fig. 1.2D) (Braitenberg, 1967).

If the rhabdomeres are arranged as a single waveguide, this is called a fused rhabdom (Fig. 1.2B), as found in bees. This is when all the separate rhabdomeres are fused centrally. In contrast, if the rhabdomeres remain separated and transfer the light separately, this is called an open rhabdom (Fig. 1.2D), as found in flies (Osorio, 2007) (the differences in eye design are discussed more below). The open rhabdom increases exposure to light sevenfold with no loss in spatial resolution (Kirschfeld, 1967), beneficial for a crepuscular insect with bi-modal activity profiles such as fruit flies (Pegoraro *et al.*, 2020). Thus they can gain an advantage over their predators and competitors during dawn and dusk (Land & Nilsson, 2012).

In *Drosophila*, the outer photoreceptors (R1-R6) are thought to participate in various visual tasks, primarily motion vision and orientation mediating behaviours such as course control and landing (Braitenberg, 1967; Heisenberg and Buchner, 1977; Vogt and Desplan, 2007). In contrast, the inner pair of photoreceptors (R7-R8) primary function is presumably to differentiate colours (Trujillo-Cenóz, 1965), although they also contribute to motion perception (Wardill *et al.*, 2012). The receptors share the same visual field and contribute information from the same point in space to the rhabdom, yet they do not necessarily supply the same information. The R1-R6 receptors express Rh1, which has peak sensitivities at 360 nm and 480 nm (Stavenga, 2010) and specialises in vision at low light levels (Hardie, 1985). In contrast, R7 expresses one of two UV-sensitive rhodopsin (Rh3 or Rh4), and R8 can be sensitive to either blue light (Rh5) or green light (Rh6).

In honeybees, the photoreceptors are sensitive to various wavelengths of light and categorised according to their spectral sensitivity. With a visual spectrum spanning 300 to 650nm (Frisch,

1914; Kühn & Pohl, 1921; Kühn, 1927), two receptors are maximally sensitive to ultra-violet (UV) light (340 nm), two are blue-sensitive (463 nm), and four yellow-green-sensitive (530 nm) photoreceptors (Peitsch *et al.*, 1992; Briscoe and Chittka, 2001). This variety seen in photoreceptor sensitivity ultimately enables insects to discriminate "colours," i.e. different light wavelengths (Briscoe and Chittka, 2001). Thus, flies and bees are trichromats, consistent with humans and many other insect species, although their spectral sensitivity is shifted towards shorter wavelengths of light (Menzel, 1979; Chittka, 1996).

The optic lobes of flies comprise the lamina, medulla and lobula (Dyer, Paulk and Reser, 2011). To guide behaviour, neuronal circuits within the insect brain form perceptions from the visual information received from the sensory neurons (Behnia and Desplan, 2015). The axons from the R1-R6 photoreceptors project to neural columns and are received by large monopolar cells (LMCs) and the amacrine cell (AC) (Shaw, 1984). The larger L1 and L2 cells mediate key pathways for motion detection as they respond to on an off moving edges. Albeit in opposing directions with L1 perceiving back-to-front motion and L2 front-to-back (Vogt and Desplan, 2007). The information is then transferred from the lamina innervating at different layers via several cell types to the medulla (Morante and Desplan, 2008). The R7-R8 cells circumvent this neuropil and make synaptic connections with their corresponding medulla column where motion and colour information integrate (Kirschfeld, 1967; Morante & Desplan, 2005). From this point, the information is carried throughout the rest of the visual pathway: lobula, lobula plate and central brain (Borst, 2009). The lobula plate has been studied extensively (Borst and Egelhaaf, 1989; Krapp, Hengstenberg and Egelhaaf, 2001). Lobula plate tangential cells (LPTC) are present in layers of the lobula plate and are sensitive to horizontal or vertical motion (Schnell *et al.*, 2012; Borst and Helmstaedter, 2015) and so are associated with optomotor responses (Fujiwara *et al.*, 2017; Kim *et al.*, 2017).

Eye designs

Different optical designs evolve by natural selection due to different light intensities exerting selection pressure. Each design is categorised according to the structure and function of the optics and retina. The two most widespread designs are the focal apposition compound eye (and its variants) (Fig. 1.2) and the superposition compound eye (Land & Nilsson, 2012).

Apposition eyes gather rays from a particular direction by focussing light from a single lens onto its fused rhabdom below (Fig. 1.2A and B). This design is commonplace among diurnal species living in bright habitats, like honeybees. Rays from a different origin are absorbed

within the screening pigment of the cell, functionally isolating the ommatidia from each other (Yack *et al.*, 2007). In a trade-off between resolution and sensitivity, this eye design generally favours resolution and lacks sensitivity. In contrast, the superposition eye captures rays from multiple lenses and focuses them onto a single rhabdom (Land and Fernald, 1992). This design facilitates higher sensitivity levels and so is unsurprisingly typical of nocturnal species encountering low light levels (Frederiksen and Warrant, 2008). However, it is challenging for the optics to perfectly superimpose multiple images, limiting resolution (for review, see Warrant, 2017). *Drosophila* possess a variant of the apposition eye called the neural superposition compound eye (Fig. 1.2C). This design somewhat removes the limitations of the other eye types by possessing similar optics to the apposition eye, yet superimposing the images using neural mechanisms akin to the superposition eye. The neural superposition eye of *D. melanogaster* is of interest to this thesis. Since the above section (see *Compound eyes*) generally discussed the structure and function of the apposition eye, I shall provide more insight into the neural superposition eye.

In the fly eye, the neural signals of eight receptor cells (R1-R8) from seven neighbouring ommatidia superimpose together in the same second-order cell of the lamina (Kirschfeld, 1976; Borst, 2009). This is possible as the fields of view of the six peripheral rhabdomeres in one ommatidium share the same view as the central rhabdomere of one of the neighbouring ommatidia. Likewise, the angle between adjacent ommatidia is identical to the angle of adjacent rhabdomeres within an ommatidium. However, this eye type does have a constraint. The separation between the distal tips of the rhabdomeres within an ommatidium has to be identical to the angle separating adjacent ommatidia. Because the rhabdomeres are very narrow, considerable light energy occurs outside the light-guide, i.e. 'leakage'. Consequently, there needs to be a substantial separation between rhabdomeres to prevent 'cross-talk' (Wijngaard and Stavenga, 1975).

This eye design is the only design found within the Brachycera order - characterised by their reduced antennae segmentation – a suborder of Dipterans (higher flies) (Nilsson and Ro, 1994) to which the Drosophilidae family belongs (Wiegmann *et al.*, 2003). An interesting optical phenomenon in *Drosophila* is the "deep pseudopupil". Each lens forms an upright virtual image of the seven distal rhabdomere endings in its focal plane (Franceschini, 1972). This phenomenon allows the analysis of the movement of photoreceptor microsaccades, as discussed in chapter 3.

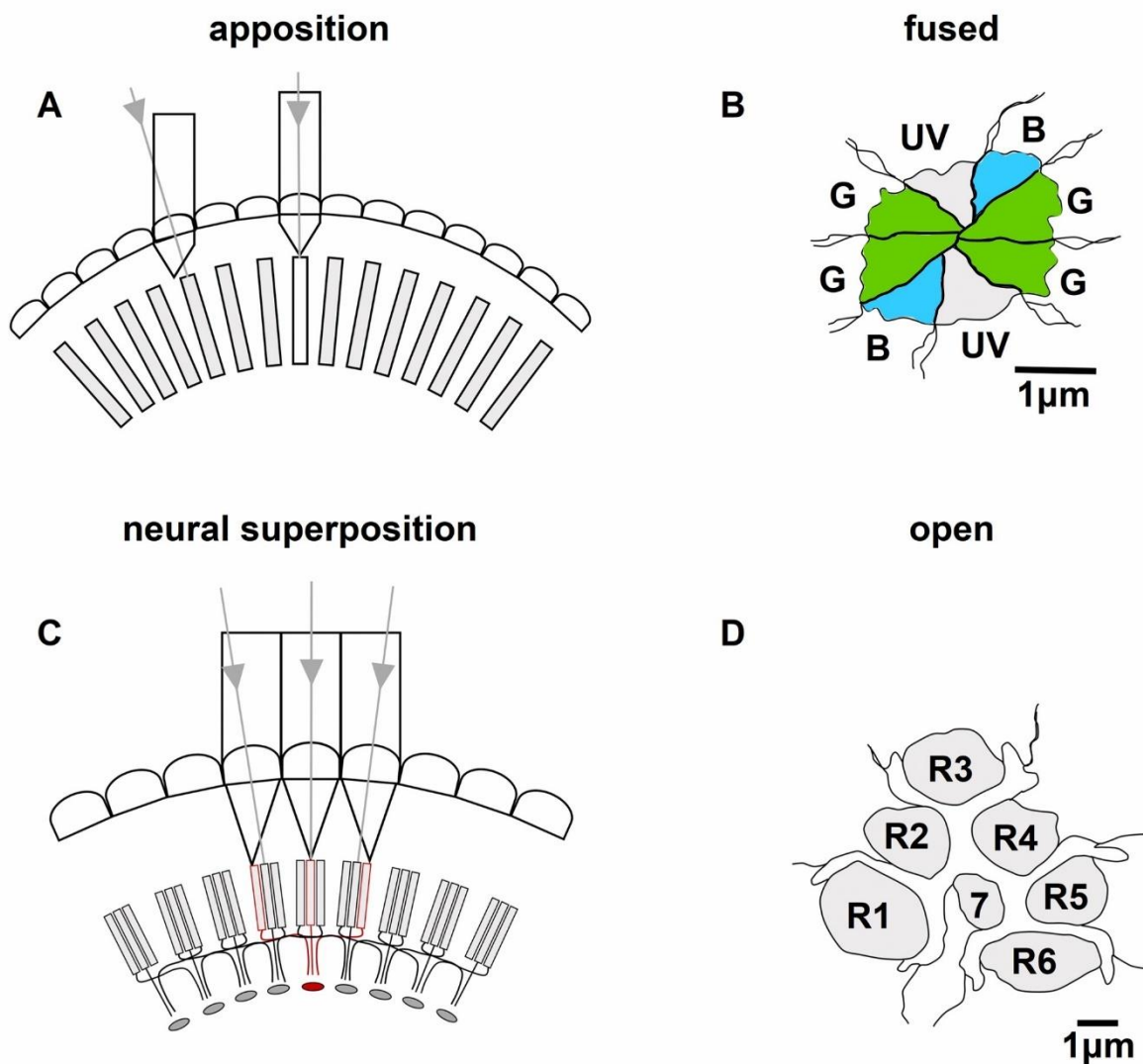


Fig. 1.2 Two optical designs of compound eyes.

(A) The focal apposition compound eye with (B) a fused rhabdom, typical of diurnal insects such as the honeybee *Apis mellifera*. (C) The neural superposition compound eye with (D) an open rhabdom, as found in the fruit fly *Drosophila melanogaster*. This design superimposes the neural signals of eight receptor cells from seven neighbouring ommatidia together in the lamina, this is possible as the six peripheral rhabdomeres in one ommatidium share the same field of view as the central rhabdomere of one of the neighbouring ommatidia. This facilitates higher sensitivity levels for the fruit fly which is active at dawn and dusk. Image redrawn and modified from Land & Nilsson, (2012).

1.1.2 Spatial vision

Many behaviours are mediated by visual acuity, defined as the minimum angle that the eye can resolve spatial information. High acuity increases the image's resolution and thereby provides fine spatial detail. However, the two principal components of the eye - the optics and the retina - cause numerous physical limitations to the spatial resolving power of the eye (Warrant and McIntyre, 1993; Gonzalez-Bellido, Wardill and Juusola, 2011). Furthermore, light availability is a significant limitation since the eye's capability is irrelevant if insufficient photon capture, i.e. photon noise, restricts any discernible spatial detail. This is because any ambiguity over the intensity of a stimulus concurrently provides uncertainty about its spatial location (Warrant and McIntyre, 1993).

Optical limitations

Mallock (1894) first proposed that the arthropod eye produces a relatively poor image due to its small and imperfect optics. The poorer the optics, the worse the retinal image and consequent spatial resolving power of the eye. Optical limitations include spherical and chromatic aberration (Warrant and McIntyre, 1993). In both cases, parallel light rays are focused to a position behind the lens, i.e. the focal plane. However, due to the spherical surface of the lens, rays entering the periphery can focus closer behind the lens than rays entering at the centre, thereby focussing short of the focal plane and causing blurring and ultimately reducing image quality. Comparably, chromatic aberration can focus shorter wavelengths of light closer to the back of the lens than longer wavelengths to cause blurring (Warrant and McIntyre, 1993).

Additionally, since the compound eye consists of tiny lenses, they have the fundamental design problem of diffraction. This occurs when light passes through an aperture, as it will slightly bend (i.e. diffract) at the edges (Land & Fernald, 1992). This arises due to light photons' dual properties, which are particles that behave like waves (Broglie, 1924). The smaller the lens, the more significant the effect of diffraction as light rays will spread more and restrict resolvability due to its wave-like properties (Land & Nilsson, 2012). Consequently, there will be a blurred pattern of light within the retinal image referred to as the "airy disk" (Land and Nilsson, 2012). The airy disk will reach a threshold of being too large with decreasing facet diameter. Therefore, to limit diffraction, either the lens size can be increased or the wavelength reduced (Land, 1997). Besides diffraction, smaller lenses also limit acuity as they ultimately allow fewer photons to pass through and be captured by the photoreceptors below (Snyder, Stavenga and Laughlin, 1977; Nilsson, 1989).

Photoreceptor limitations

The size and number of rhabdoms are critical to the overall visual acuity of the insect. Spatial resolution is improved with narrow rhabdomeres since they collect light from a smaller receptive field within the scene. How rhabdom size influences acuity was studied in a comparative study of two miniature dipteran species, the fruit fly and the predatory killer fly (*Coenosia attenuata*) (Gonzalez-Bellido, Wardill and Juusola, 2011). The study highlighted that although the species have similar-sized lenses, the killer fly has three-to fourfold better acuity. Consequently, it is not the optical limitations influencing the differences in spatial resolution. Instead, as shown by electron microscopy, the much smaller rhabdomeres found in the killer fly contributed to their enhanced acuity, consistent with the ecological demand of their predatory lifestyle. Conversely, some photons will propagate outside the rhabdomere when very narrow (Snyder and Miller, 1977), potentially limiting the spatial resolving power.

Interommatidial angle and acceptance angle

The interommatidial angle ($\Delta\phi$) refers to the angular spacing between adjacent ommatidia (Fig. 1.3) (Land, 1981, 1997). Smaller angles indicate more densely packed rhabdoms which have the potential for the eye to facilitate high spatial resolution (Snyder, Stavenga and Laughlin, 1977). The precision in which light is split according to its direction of origin, i.e. resolution, determines how well an animal can see. The ratio of the facet diameter, D , compared to the eyes radius curvature, R , ($\Delta\phi \approx d/r$ radians), determines the interommatidial angle and consequent ommatidia density. To improve the resolvability of the compound eye, a larger eye radius and smaller facet size would elicit a higher density of ommatidia and enhance resolution (Kirschfeld, 1976; Land & Fernald, 1992), but since the eyes surface is a finite area, it cannot have adaptations that maximise both resolution and sensitivity. Thus to limit trade-offs between resolution and sensitivity, one solution would be to increase the size and quantity of the sampling units, yielding an overall larger eye (Land & Fernald, 1992). However, the required size of a compound eye to match the resolvability of a camera-type eye would be unsupportable and impede biological fitness (Kirschfeld, 1976).

In addition to the interommatidial angle, another critical parameter is the acceptance angle ($\Delta\rho$) (Fig. 1.3). The angle is defined as the half-width of the photoreceptors receptive field (angular sensitivity) for each ommatidium (Warrant and McIntyre, 1993) and determined by the ratio of the rhabdom diameter, d , and the focal length of the ommatidium, f , ($\Delta\rho \approx d/f$ radians) (Stavenga, 2003; Frederiksen and Warrant, 2008). Thus, the interommatidial angle would represent the angular spacing between pixels on a camera image, and the acceptance angle would be the

angular size of each pixel. Consequently, smaller angles in both would imply better spatial resolution.

A common approach is not to have a constant lens size across the eye but rather to vary the eye structure in different eye regions (Land, 1997). For example, when comparing interommatidial angles, in *D. melanogaster*, the angle ranges from 4° in the frontal area to 8° in the dorsal rim (Gonzalez-Bellido, Wardill and Juusola, 2011). Regions of smaller interommatidial angles and enlarged facets are called acute zones and are typically sex-specific. For example, male insects often possess acute zones to support chasing behaviour during sexual pursuit (Land & Eckert, 1985).

The structural and optical measurements provide valid estimates to determine the resolvability threshold of each species. This, along with the quality of the optics and the density of the sampling units. For example, the historical consensus is that *Drosophila* have low-resolution vision and experience considerable motion blur. Generally, this was believed due because of the limitations discussed above, including the interommatidial angle size, photoreceptor slow integration time (the speed of phototransduction reactions), and motion blur during saccadic behaviours (Land, 1997). Since the vast majority of the time the eye or the animal's surroundings are moving, motion blur restricts spatial resolution. The extent of blurring depends on the photoreceptors' integration time limit and the angular velocity of the eyes relative to their surroundings (Srinivasan and Bernard, 1975; Land, 1995). Many insects experience blurring with angular velocities over 50° per second (Laughlin and Weckström, 1993), which during flight is prevalent as high-speed movements can be up to thousands of degrees per second (Collett and Land, 1975). However, different adaptations have arisen to overcome the limitations brought about by motion blur. This includes acute zones (discussed above), saccadic and fixation behaviour (discussed below in *Body saccades*) and photomechanical contractions (microsaccades) (discussed below in *Photomechanical photoreceptor microsaccades*). Consequently, neural or physiological mechanisms may aid the optics and thereby enhance acuity beyond what is predicted by the optics alone.

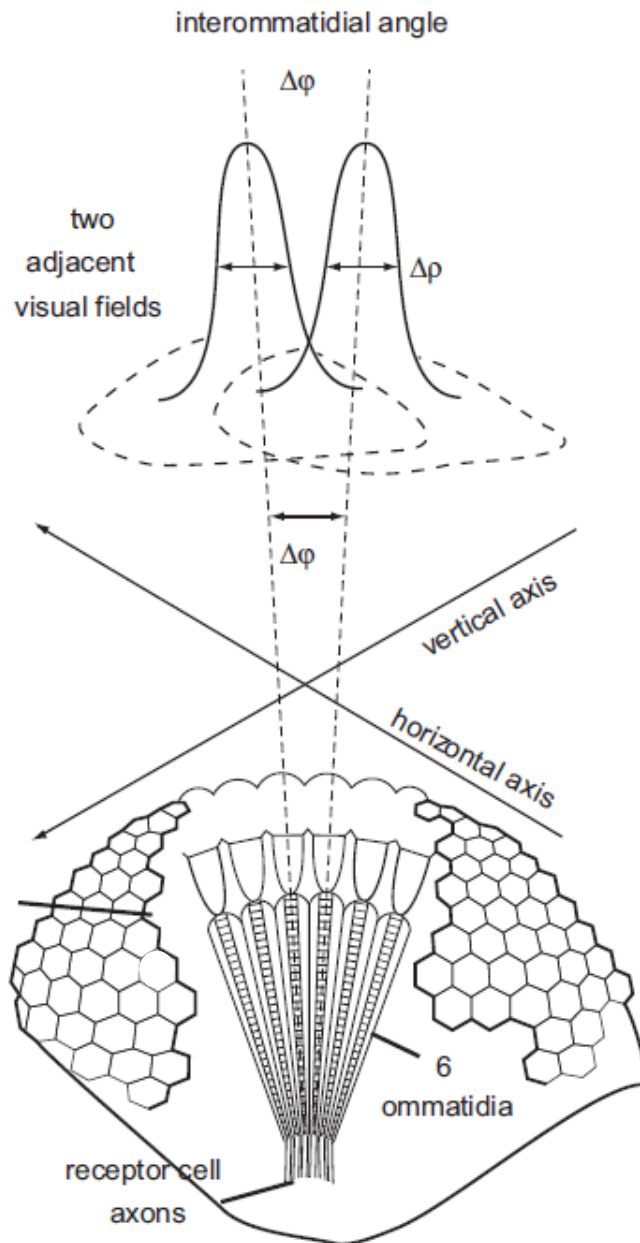


Fig. 1.3 Two optical parameters that define visual acuity.

The interommatidial angle ($\Delta\phi$) is the angular spacing between adjacent ommatidia. The acceptance angle ($\Delta\rho$) is the half-width of the angular sensitivity curve. Image reproduced with permission from Horridge, (2009).

Spatial wavelength

Various stimuli can be utilised for the behavioural assessment of an animal's visual system. Behavioural studies to determine the finest grating or single object thresholds an eye can detect can generally be referred to as the “minimum separable” or “minimum visible” (Land, 1997). First, linear square gratings are extended source stimuli of equally sized dark and light bars

repeating. The variability of the size and contrast of the bars is a valuable tool for testing the visual system of an animal (Warrant and McIntyre, 1993). The bar's size is commonly referred to as the spatial wavelength, the angle in degrees in which one cycle of the bars, i.e. one dark and one light pairing, subtends the eye, i.e. degrees/cycle. The animal will only resolve individual bars if each bar is projected onto separate photoreceptors (Land, 1997). The spatial frequency is the reciprocal of the spatial wavelength. Therefore, high spatial frequency gratings contain more inherent spatial detail as smaller bars are more tightly packed together, while low spatial frequency gratings contain less detail with coarser bars. Testing the limit of the visual system to respond to high spatial frequency bars is a useful experimental approach to measure the spatial resolution of the eye.

Second, the smallest detectable single object can sometimes define acuity instead of the finest grating. This is because detecting small objects and small gratings offers different challenges and situations for the eye. In its natural environment, a single object, for example, maybe a virgin queen sighted by a drone, a grating, on the other hand, could be compared to general flora. Consequently, the smallest single object detectable by the eye is not necessarily identical to the finest grating visible.

1.1.3 Motion and active vision

Motion perception is the most studied visual modality in fruit flies. The elementary motion detector (EMD) was one of the earliest models on motion detection. Pioneered and first proposed by Hassenstein and Reichardt (1956), the generalised model computes motion direction centred on a non-linear correlation of the response between two adjacent photoreceptors to temporal luminance changes (Geurten *et al.*, 2007). This is achieved by direction-selective amplification of the directional responses of the adjacent receptors after one has been delayed (Behnia and Desplan, 2015). Two pathways compute this, one detects light edges while the other detects dark edges (Maisak *et al.*, 2013). The response is predicted by the model to not increase continuously with increasing velocity, but rather after going beyond the optimum velocity to then decrease in response. Additionally the model predict that this optimum velocity is not fixed but rather varies in response to the spatial wavelength of the pattern's (Borst, 2000). As parameters were modified to fit new experimental observations then new models originated. The Barlow-Levick-model' is almost identical (Barlow and Levick, 1965), except brightness signal comparisons to calculate the direction of image velocity are

achieved by having two adjacent image points arrive simultaneously through a veto gate. The detectors null direction therefore corresponds with the motion direction, e.g. from right to left. Motion vision has many functions for an animal. As the animal moves through its environment the retinal image is in constant motion. The distribution of motion vectors, optic flow, depends on the specific movement that the animal performs, such as moving forward or sideways. Optic flow therefore is an invaluable source of information for visual course control (Lawson and Srinivasan, 2018).

Vision can generally be divided into two types of systems, passive and active. Passive refers to object movement and the energy generation independent of the animal observer (Nelson and MacIver, 2006). Examples include the use of celestial visual cues to guide their behaviour. The dung beetle (*Scarabaeus satyrus*), for instance, has been found on a starlit night to use the Milky Way for straight-line orientation (Dacke *et al.*, 2013). However, either as an alternative or combined with passive cues, the animal can also use their self-generated energy to extract information from their environment.

Many examples of active sensing can be found in nature. For example, bats and dolphins have used 'sound' for echolocation by emitting sound energy (biosonar) into their environment to help with navigation and prey capture (Au and Simmons, 2007). 'Touch' has been utilised by many insects species, including stick insects (*Carausius morosus*) and crickets (*Gryllus campestris*, *Gryllus bimaculatus*) through their antennal movements (Horseman, Gebhardt and Honegger, 1997; Dürr, König and Kittmann, 2001). More to the point, there are numerous examples of animals utilising 'vision' for active sensing of their environment. I shall first discuss how animals use the self-generated energy of their body and head movements for active vision. I will then explore the more recent finding of photoreceptor microsaccades in *Drosophila melanogaster*, as this discovery is the motivation for the experiments in chapters 2 and 3.

Body saccades

Human eyes can move independently from the head and body, using a fixate-and saccade (or gaze-and-shift) strategy (Land, 1992). However, unlike vertebrates, insects cannot move their eyes independently from their head as their eyes are fixed on the external surface of the head. However, this does not mean that invertebrates cannot achieve active vision. Flying or walking insects also perform fixation and saccadic behaviour by moving their entire head and body (Geurten *et al.*, 2014; Mongeau and Frye, 2017). This entails rapid periods of stabilised gazing

intermittent with rapid shifts in gaze location (Collett and Land, 1975; Schilstra and Van Hateren, 1999; Van Hateren and Schilstra, 1999).

Drosophila (and other flying insects) use head movements to stabilise the wide-field image, which helps steady the visual input and reduce motion blur (Hardcastle and Krapp, 2016). Fox and Frye (2014) found that head fixation impairs object fixation when the object is presented alongside ground motion. Wing steering responses follow both the figure and ground whilst the head follows only the ground. Suggesting the head movements are necessary for stabilising the image of ground motion during a visual tracking task (Fox and Frye, 2014). Additionally, these head movements shape and coordinate the flight motor response in flies during flight. Cellini and Mongeau (2020) found that head movements increase the wing gain and coordinate steering responses. Furthermore, head responses occur 40 ms sooner than wing responses, suggesting a temporal order of the head gathering visual information (through the compound eyes) to elicit the appropriate behaviour response (downstream wing steering responses). In addition to head and body movements, it has recently been shown that a pair of muscles within the eye cause saccade-like movement that may enhance vision (unpublished work presented by Lisa Fenk at the Fourth International Conference on Invertebrate Vision 2019). Furthermore, recent work has shown that *Drosophila* possess photomechanical photoreceptor movements as another form of active vision, to some extent comparable to the saccades of the vertebrate eye (Juusola *et al.*, 2017).

Photomechanical photoreceptor microsaccades

Juusola and colleagues (2017) demonstrated that fruit fly photoreceptor cells rapidly contract to light *in vivo* (in intact living flies), as had been previously shown by Hardie and Franze (2012) *ex vivo* (in a petri dish). These contractions (or microsaccades) occur by cleaving PIP₂, e.g. phototransduction, so photon capture self generates this form of active sensing (Hardie and Franze, 2012; Juusola *et al.*, 2017). The contractions occur beneath the rigid optics (**Fig. 1.4**) and swing the photoreceptors backwards, forward, and side to side in a piston-like motion. Such cell contractions and elongations dynamically shift the x,y position and adjust the receptive field size, further focussing the light input spatially and temporally. Specifically, the phasic responses indicate an object's movement over one photoreceptor's receptive field to the next, thus encoding space in time. These findings suggest that fruit flies possess "hyperacute vision", defined as spatial resolving power better than what is predicted by the optical resolution limit. Notably, these *local* photomechanical microsaccades differ from the *global*

eye-muscle-induced micro-movements as intraocular muscles would move the retina as a whole in a single movement (Franceschini *et al.*, 1991; Franceschini, 1997) which inspired the construction of hyperacute artificial light-sensors (Viollet, 2014) that has applications within visual stabilization and target tracking (Colonnier *et al.*, 2015).

The ultrafast microsaccade dynamics would then have the added effect of reducing image blur, an essential feature for continuously sampling light during the head and body's saccadic and fixation behaviour. However, this behaviour generates rapid angular velocity changes (Srinivasan and Bernard, 1975), which, together with *Drosophila's* relatively slow photoreceptor integration time (Juusola and French, 1997), suggests a blurred image. Indeed, the previous consensus is that flies would have essentially been blind during this behaviour because of this motion blur (Land, 1999). Nevertheless, the previously unknown mechanism of photoreceptor contractions explains the fly's potential ability to see a clear and high-resolution image (Juusola *et al.*, 2017). When a fly was presented with high contrast bursts (rapid light changes and static periods) resembling a naturally lit scene, intracellular recordings revealed that R1-R6 captured up to four times more information than previous estimates (Juusola and Hardie, 2001).

Furthermore, behavioural experiments investigating their optomotor response showed the adult female *Drosophila* responded to gratings as fine as 1.16° , approximately four times smaller than their interommatidial angle, and consistent with the intracellular recordings. The implications are that *D. melanogaster* spatial vision might be four-fold better than previously believed. Following from this research (Juusola *et al.*, 2017), how the mechanics of the contractions occur globally over each eye has now been explored for the first time, suggesting that these contractions also provide short-range binocularity in *Drosophila*, to be discussed in more detail below (1.1.4 Binocular vision).

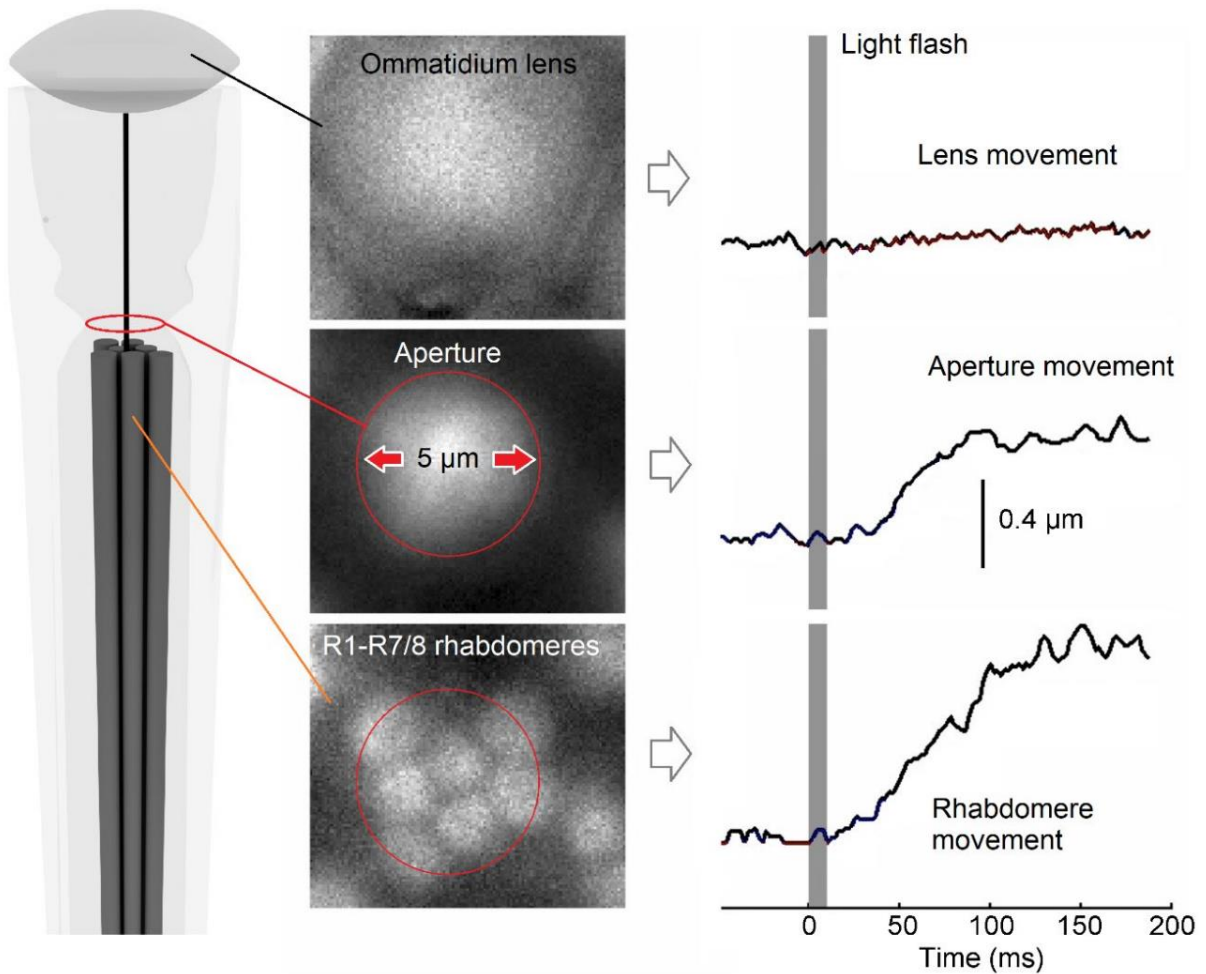


Fig. 1.4 *Drosophila* photoreceptor microsaccades enhance spatial resolving power.

In vivo recordings show the lens is immobile (top) while the photoreceptors below contract to light input (bottom). The contractions occur beneath the rigid optics and swing the photoreceptors backwards, forward, and side to side in a piston-like motion. Such cell contractions and elongations dynamically shift the x,y position and adjust the receptive field size, further focussing the light input spatially and temporally. Grey bar indicates a light flash stimulation. Image reproduced with permission from Kemppainen et al., (2022).

Indeed, numerous studies support Juusola's (2017) theory and go against the traditional view that *Drosophila* only see blurred low-resolution images. For example, Schneider *et al.* (2018) demonstrate with machine learning and modelling that *Drosophila* have visually distinct features that conspecifics can use for re-identifying each other. And Cruz, Pérez and Chiappe, (2021) (e.g. their Fig. 6C) show free-walking *Drosophila* reacting robustly and consistently to hyperacute 1° and 2.5° objects. Consequently, there is growing support that *Drosophila*

perform feats beyond the optical limit. This is perhaps unsurprising given the above factors and other behavioural examples of animals detecting objects smaller than the interommatidial angle, such as robber flies (Wardill *et al.*, 2017) and killer flies (Wardill *et al.*, 2015).

So while head movements serve to stabilise the gaze to elicit wing steering responses (Cellini and Mongeau, 2020), photoreceptor movements seemingly serve to enhance the retinal image beyond the structural limitations, though their exact functional role remains to be investigated.

1.1.4 Binocular vision

Depth perception

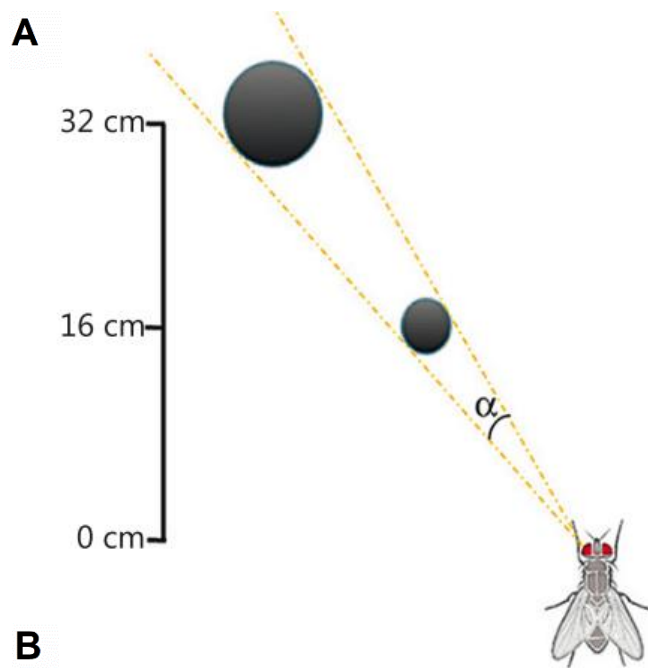
In a three-dimensional world, the ability to perceive depth is essential for many species. To identify whether an object is a target of interest, the animal must evaluate its properties and decide on the appropriate behavioural response dependent on its distance. For example, a predator needs to decide whether it is a suitable prey item, and the prey needs to decide whether it is predatory species it needs to evade (Prete and Mc Lean, 1996; Combes *et al.*, 2012; Haselsteiner, Gilbert and Wang, 2014; Wardill *et al.*, 2015). To evaluate this, the animal must first determine whether the object is small and close or large and far away, as either scenario can subtend the same angular size on the retina (**Fig. 1.5A**). Conversely, a small object, either close or far away, would subtend very different sizes on the retina (**Fig. 1.5B**). However, the images sampled by the retina are collected by a two-dimensional array of photoreceptors. Therefore, the "lost" three-dimensional (3D) information must be reconstructed perceptually from 2D retinal images by extrapolating depth cues that signify differences in object distance. These cues can be either monocular (one eye) or binocular (two eyes) and typically fit into three distinct categories; light transport, perspective and triangulation (Banks *et al.*, 2016). Light transport involves shading and occlusion, while perspective includes looming and relative size. The latter category of triangulation entails motion parallax and binocular disparity. Motion parallax is the most common mechanism reported in invertebrates. The perceived speed an object moves across an animal's visual feed is determined by its distance from the observer. Thus, objects closer to the animal will appear to move faster and further than those farther away.

Invertebrate stereopsis

In general, binocular disparity for depth perception in animals is much less common or demonstrated. Thus, its occurrence in invertebrate species is much less known. Stereopsis, or stereo vision, functions to calculate object depth using the binocular disparity between two eyes. Thus, each eye simultaneously acquires a slightly different two-dimensional retinal image. These differences between images become evident once fused neuronally. From this, the object's distance can be calculated. However, this mechanism has been demonstrated in relatively few species. Traditionally, research into stereo vision has focussed on primates and other mammals (Nityananda and Read, 2017), encompassing both predatory (Ptito, Lepore and Guillemot, 1991) and prey species (Timney and Keil, 1999).

Until recently, stereopsis had only been suggested in a single insect order, the mantises (Maldonado and Rodriguez, 1972). Utilising anaglyph glasses, Nityananda *et al.* (2016) demonstrated that praying mantis will attempt hunting behaviour when the observed stimulus is perceived to be within its catching range. However, inspired by the approach used in mantis, cuttlefish have been tested with anaglyph glasses and presented virtual prey items. Feord *et al.* (2020) found that cuttlefish detected and positioned themselves to strike prey more efficiently when binocular vision remained intact. Cuttlefish stereopsis is a much more recent finding (Feord *et al.*, 2020), and so it is much less clear and the underlying mechanisms less understood.

In both cases of invertebrate stereopsis, the animal utilised binocular mechanisms for the fundamental function of prey capture. Further investigation is needed to determine whether stereopsis appears in other invertebrate species. It may be surprising that recent theory suggests that the fruit fly may utilise stereo vision for short-range distance estimation (Kemppainen *et al.*, 2022). The photoreceptor contractions that enhance acuity (Juusola *et al.*, 2017) may also provide the fly with binocularity over a short range due to the global mechanics of the contractions. Kemppainen *et al.* (2022) show how microsaccades contract mirror-symmetrically across both eyes in a back-to-front motion which calculates object distance via phasic disparity signals correlating into neural distance temporally.



B
Sampling properties of the compound eye

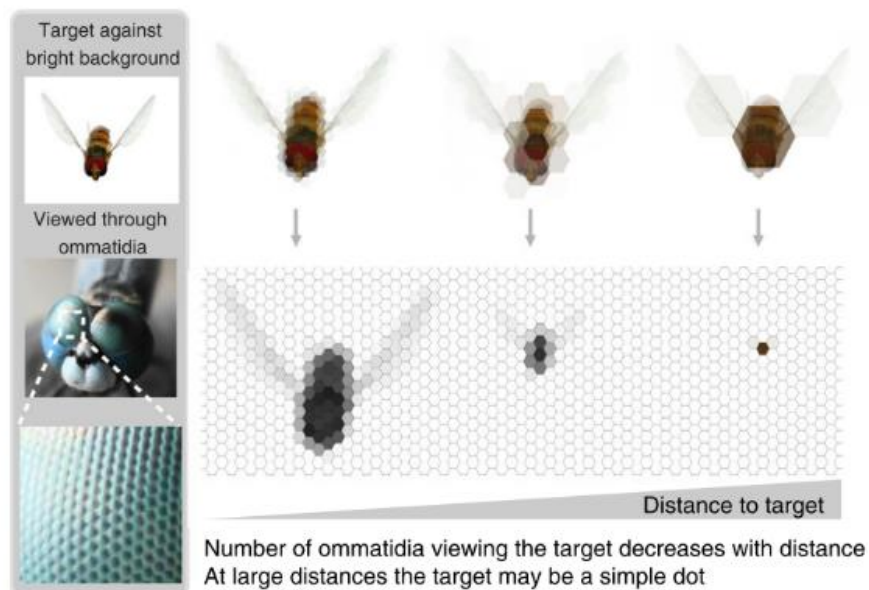


Fig. 1.5 Depth cues in animals.

(A) Close-small and far-big objects subtend the same angular size on the retina. This therefore makes it difficult to distinguish the distance to the object which animals need to overcome to minimize metabolic costs. (B) When close to the observer, more sampling units capture the object than when it is far away. As distance increases fewer 'pixels' will cover the object until it may only be covered by a single pixel. Images reproduced with permission from (A) Wardill *et al.*, (2015) and (B) Gonzalez-Bellido, Fabian and Nordström (2016).

1.2 Measuring behaviour

If the eyes are an instrument to *see* the world, then behaviours are a mechanism to *interact* with it. We can determine which visual cues they can perceive by measuring an animal's behavioural output. This section explores using virtual reality systems to isolate specific behaviours and visual cues from the optomotor response and object detection. In addition, to the ways, *Drosophila* can be conditioned to develop orientation preferences in a flight simulator.

1.2.1 Using virtual reality

Researchers can immerse animals in artificial environments through virtual reality (VR) systems to measure various visual behaviours (Schultheiss *et al.*, 2017) (Fig. 1.6). Typically, animals are fixed in space, and their responses to artificial stimuli are quantified. Though it restricts natural behaviour, this approach increases animal and stimulus presentation control to yield novel insights into many research areas (Chouinard-Thuly *et al.*, 2017). For example, understanding visual course control, the ability to select and sustain a specific orientation, and understanding motivation, i.e., the animal's goal by maintaining a particular orientation. The system of most relevance to this thesis is the flight simulator (see Chapter 2 & 3), which measures flying behaviour, which can be tested in both open and closed-loop paradigms (Schultheiss *et al.*, 2017).

A critical issue with behavioural observations of freely moving animals in a highly complex environment is demonstrating conclusively that the behaviour of interest results from specific stimuli and is not influenced by other factors. In this respect, the artificial setups of virtual reality systems have the advantage that well-defined stimuli can be presented to the animal, allowing a more systematic investigation into the different elements of visually guided behaviours. However, this comes at the price of understanding the animal's motivation and context-dependent behaviours performed in an artificial environment (Heisenberg and Wolf, 1984).

A useful setup, parallel to the measurements of attempted flight, is the use of a trackball to measure the walking behaviour of insects. Insects can engage their legs with the air-supported ball and attempt locomotion in response to the visual stimulus, whether presented within an LED matrix or light projected arena (Taylor *et al.*, 2015). However, LED arenas are not as helpful in studying acuity, with size restrictions often being close in size to the interommatidial

angle (e.g. 3.75° , Salem *et al.*, 2020). Thus, I used the torque meter with paper scenes, enabling much finer visual stimuli.



Fig. 1.6 Examples of measuring invertebrate behaviour using virtual reality.

Image of a tethered American cockroach *Periplaneta americana* mounted on an air-supported trackball in a bespoke virtual reality systems. Insects can engage their legs with the air-supported ball and attempt locomotion in response to the visual stimulus. Though it restricts natural behaviour, this approach increases animal and stimulus presentation control to yield novel insights into many research areas. Image reproduced with permission from Takalo *et al.*, (2012).

1.2.2 The optomotor response

An instinctive behaviour that is not easily observed in the wild - but is an essential aspect of motor control - is the optomotor response (Srinivasan, Poteser and Kral, 1999). Many animals can move their eyes (optokinetic) in the same direction as motion. Insects, however, cannot independently move their eyes and so turn the entire body (optomotor). The behaviour is an

automatic turning to follow the movement of wide-field stimuli. It functions as a form of course control whenever the animal encounters unexpected or sudden deviations from its heading (Srinivasan, Poteser and Kral, 1999). For example, this may be a gust of wind blowing a honeybee leftward during a flight. In this case, the animal's optic flow would rotate from left to right across both eyes. Optic flow provides information about motion direction and object distance (Cronin *et al.*, 2014). Insects typically encounter either translation (front-to-back optic flow) or yaw rotation (front-to-back in one eye, back-to-front in the other eye). Thus, to stabilise rotational optic flow, an insect will attempt to reduce the retinal slip of the flow field by maintaining a straight path (Götz, 1968). Therefore the honeybee example should fly rightward.

Regardless of the optomotor response's function and visibility in nature, its use in a laboratory setting is unquestionable. Its effectiveness is akin to using the proboscis extension response (PER) protocol in honeybee learning and memory experiments (Giurfa and Sandoz, 2012). The optomotor response has been utilised in vision research as an effective behavioural measure in controlled experiments for measuring various aspects of vision (Fig. 1.7), including the role of ocelli (Honkanen *et al.*, 2018), binocular interactions (Duistermars, 2012), the organisation of large-and small-field pathways (Duistermars *et al.*, 2007) and dim-light vision (Nuutila *et al.*, 2020). Furthermore, von Gavel (1939) also demonstrated that flies responded to gratings smaller than the interommatidial angle, the first indication that the optical resolution limit did not limit *Drosophila* spatial resolving power. It is a behavioural response that will be robustly performed as long as the animal can see the movement of the environment as tested in Chapter 2.

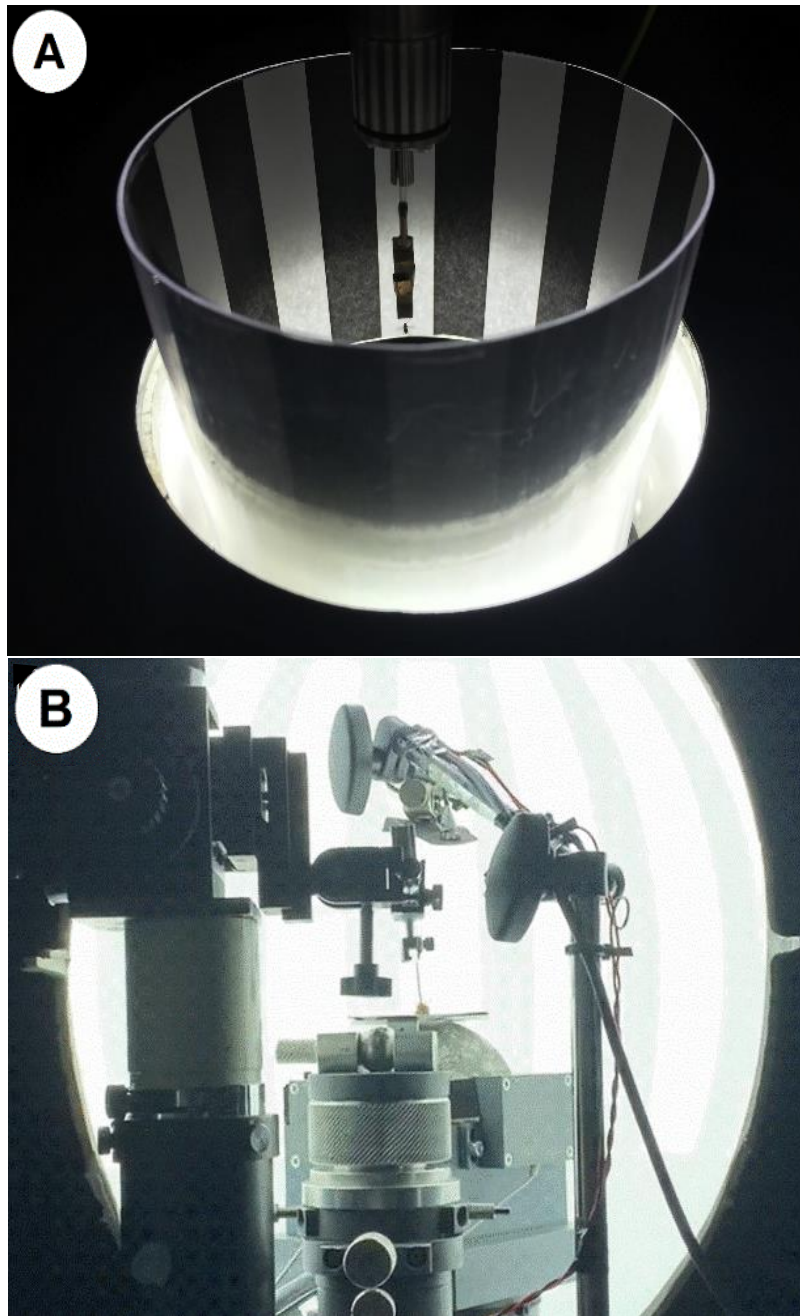


Fig. 1.7 Examples of measuring optomotor behaviour in animals.

Dark and light bars presented (A) to the fruit fly *Drosophila melanogaster* and (B) honeybee *Apis mellifera* that turn their entire body (optomotor) to follow the movement of wide-field stimuli. This is an innate response that functions as a form of course control whenever the animal encounters unexpected or sudden deviations from its heading. Presenting different sized bars is a useful tool for measuring visual acuity.

Historically, linear gratings (discussed above 1.1.2 Spatial vision (*Spatial frequency*)) have been used to elicit optomotor responses (Srinivasan, 1977). Early studies include von Gavel

(1939), who tested optomotor behaviour to different spatial wavelengths and contrasts. Interestingly, when the presented wavelength was approximately 9° , the turning response reversed as the flies turned in the opposite direction from the moving grating. In the dim light, this reversal shifted and now occurred with larger wavelengths. This reversal point was explained as a Moiré effect (Fig. 1.8). This phenomenon has been found in honeybees between 5° and 10° (Kunze, 1961). Aliasing occurs when overlapping periodic textures are offset by a slightly different wavelength or angle. In behavioural measures of acuity in insects, the moiré effect is occurring between the interommatidial angle and the grating which is induced by the rotation of the gratings, which are perceived by the animal as a slowed down image rotation which then reverses in the opposite direction (Horridge, 2009a).

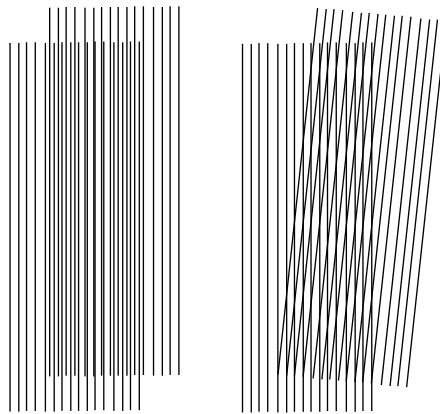


Fig. 1.8 The moiré effect.

Aliasing can occur when overlapping periodic textures are offset by varying spatial wavelengths or angles. When measuring acuity this can result in the animal perceiving movement in the opposite direction when viewing specific spatial wavelengths.

To study the optomotor response of *Drosophila* eye mutants, Götz (1964) developed the yaw torque compensator, or so-called "*Drosophila* flight simulator". By measuring their turning tendency, i.e. the amount of force the fly exerts in its attempt to control its flight course, Götz was able to study the motion perception of the fly. In this and subsequent experiments, the fly is tethered at the torque meter (Fig. 1.9), i.e. it is never really making actual turns or performing saccadic shifts, and therefore is receiving no visual feedback. The fly's behaviour is restricted to one degree of freedom (i.e. rotation around the vertical body axis). The setup is configured to open-loop where the grating was under the experimenter's control and therefore was unpredictable to the animal. So while the yaw torque of the animal does not control the stimulus as it does in a closed-loop setting, the fly's torque is nevertheless analysed to assess how well

the animal can see the specific stimulus parameters. Flies do not fly in smooth curves in nature. Instead, they zig-zag (saccades), corresponding to torque spikes when tethered at the torque meter. As the fly receives no visual feedback and seemingly fails to achieve any goals, the responses generally decline in strength over repetitions and must be averaged.

The simulator has been utilised to develop insight into visually guided behaviours. Such results are possible due to the fully automated control of the stimulus (e.g. speed, direction) in response to the precise torque output of the fly (e.g. yaw, thrust, pitch, roll). Theoretically, lots of different behaviour can be performed by the animal. However, the literature has mainly focused on yaw torque, which has been studied for over 50 years (Götz, 1964). Blondeau and Heisenberg (1982) designed a simple torque meter to measure pitch and roll. Dill, Wolf and Heisenberg, (1995) introduced a novelty choice experiment, a visual paired-comparison task that does not provide any reinforcement, and later studied how the central complex and mushroom bodies mediate the behaviour (Solanki, Wolf and Heisenberg, 2015). More recently, Toepfer, Wolf and Heisenberg (2018) investigated orientation behaviour in a flight simulator system where the visual stimulus was ambiguous. This setup is traditionally used with an unambiguous stimulus, adding a second texture that rotated opposite to the first texture could see how the fly used each frame of reference when selecting cues for flight direction.

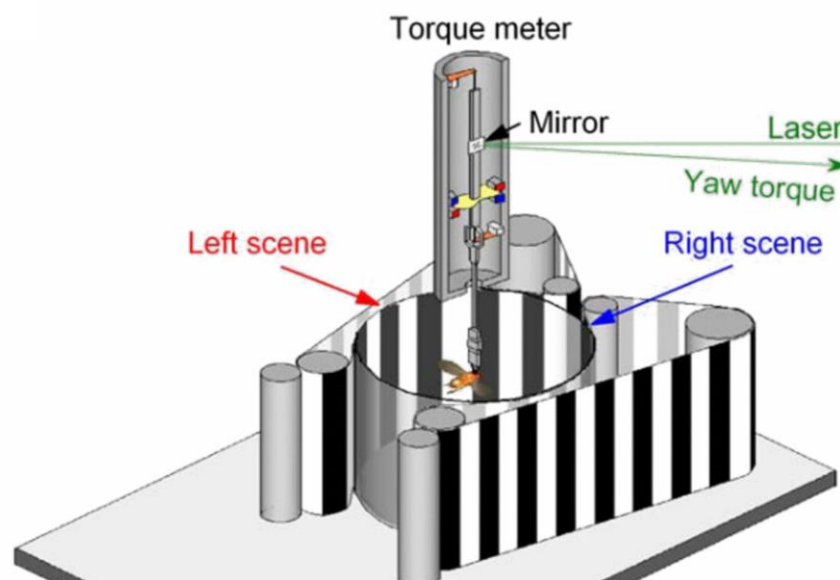


Fig. 1.9 *Drosophila* at the torque meter.

Schematic of a tethered flying *Drosophila* at the torque meter presented with competing left and right stimuli. The attempted turns to the left and right (yaw torque) by the fly are measured in response to the stimuli. Image reproduced with permission from Tang and Juusola (2010).

In addition to studying the optomotor response of flying *Drosophila*, devices have been designed to record the turning behaviour of walking *Drosophila*, such as the "tread compensator" (Götz and Wenking, 1973) and "styrofoam ball" (Buchner, 1976). For example, a recent study developed a spherical projection system fitted with a trackball using a fisheye lens to project visual stimuli to the sphere's inner surface (Takalo *et al.*, 2012). This was followed up by (Honkanen *et al.*, 2014), using the same setup to measure the optomotor response of cockroaches. More recently, Honkanen *et al.* (2018) showed that besides the compound eyes, the ocelli play a vital role in the mechanism that elicits the optomotor response in cockroaches. The spherical projection system described above has been adapted for cockroaches, but it may be utilised for a more comprehensive array of smaller invertebrates with minor adjustments.

1.2.3 Object detection and fixation

Distinguishing small singular objects (or targets) amongst a complex visual environment is a challenging visual task. Targets can be defined as a small object moving independently of its background, e.g. a fly moving through its environment, and can be tracked for various functions, including foraging or mating (Gonzalez-Bellido, Fabian and Nordström, 2016). Nevertheless, the compound eye with a relatively low spatial resolution still enables many insects to detect and then perform appropriate behavioural responses to the small object relative to its context. For example, during flight, animals perform a "gaze and saccade" strategy that includes periods of rapid movements (saccades) and fixations (gaze). When tracking a small object, either through saccades or fixations, the background image (wide-field) is shifted over the retina, creating an optic flow, while the object (small-field) remains relatively still on the retina as the animal attempts to track it.

Consequently, this process was believed to arise from two functionally distinct visual pathways. A wide-field pathway which responds to optic flow and is associated with behaviours such as the optomotor response (discussed above) (Reichardt, Poggio and Hausen, 1983) and a small-field pathway associated with smaller objects (Egelhaaf, 1985; Carroll, 1993; Nordström, Barnett and O'Carroll, 2006; Barnett, Nordström and O'Carroll, 2007; Duistermars *et al.*, 2007). These distinct visual pathways arise in early visual processing, diverging in lamina monocular cells (LMCs) directly downstream of the photoreceptors (Katsov and Clandinin, 2008).

Consequently, the insect visual system needs to segregate the relative movement of the object to distinguish it from the background (Nordström, Barnett and O'Carroll, 2006; Nordström and O'Carroll, 2009; Gonzalez-Bellido, Fabian and Nordström, 2016). Objects can remain obscured if it is stationary and matches the background texture, though if the object moves, it will suddenly become visible. Following on from the early optomotor experiments at the torque meter, this object detection has been shown behaviourally in *Musca* (Wehrhahn and Reichardt, 1973; Virsik and Reichardt, 1976; Reichardt and Poggio, 1979; Reichardt, Poggio and Hausen, 1983).

The theory of "object fixation" by Reichardt and Poggio (1976) describes how an animal chooses a particular orientation relative to a specific reference point. This behaviour, or orientedness, functions to collect as much information about its current situation by continually gathering sensory data about objects. The stabilisation of a vertical "stripe" in the frontal part of the visual field was shown in the fly *Musca* (Reichardt, 1973). The stripe stabilisation in other parts of the fly's visual field is called "non-fixation" or "anti-fixation". However, the same pattern can be attractive or aversive. For example, when the vertical stripe is bright, and the arena background is dark, the fly avoids the stripe most of the time and performs anti-fixation behaviour (Heisenberg and Wolf, 1984). Behavioural studies have shown in freely walking flies, *Drosophila melanogaster*, that stationary stripes induce fixation behaviour (Reichardt and Wenking, 1969; Horn and Wehner, 1975; Wehner and Horn, 1975; Horn, 1978). Flies had their wings cut and were placed within a circular arena which was uniform except for a vertical stripe on the periphery. In most cases, flies walked towards the stripe, although occasionally flies would walk in the opposite direction (Wehner, 1972).

In the flight simulator, the angular position of the pattern (a vertical stripe) is variable, while the fly's orientation is fixed in space. Flies have been shown to prefer flying towards vertical stripes (Heisenberg and Wolf, 1979), perhaps, due to the similarity with natural features from the world, such as plant stalks. This behaviour is independent of fly age, sex, and diet. It also does not depend on the contrast or intensity of the pattern but rather its size and shape (Wehner, 1972; Horn and Wehner, 1975; Horn, 1978). Overall, it has been shown that dark stripes have a restricted "attractiveness" for flies when they are fixed in position and are walking or flying. However, for freely walking flies, this attractiveness is higher.

In contrast to the attractiveness of stripes, when presented with small dots (or spots) (either circular or rectangular), flies have seemed to have an innate aversion to the stimulus (Maimon,

Straw and Dickinson, 2008; Cheng, Colbath and Frye, 2019). Small dots may be perceived as predators, despite small objects resembling attractive resources, such as a potential mate. Using an LED display, it has been reported that flies avoid a small target in odourless air. However, flies would reverse their aversion and steer towards the small target when paired with an attractive odour (Cheng, Colbath and Frye, 2019). Walking flies find a small black (10°x10°) square above the horizon as strongly repellent (Tanaka and Clark, 2020). The square pattern may not have the shape or angular velocity of a predatory species for the fly (e.g. dragonfly or bird), but the fly cannot pause to gather more knowledge about the object. We have seen that the same pattern can be attractive or aversive. Dot stimuli has typically been found to be innately repulsive, here I will test with smaller sized dots in chapter 3 to see whether the response is constant with size.

With the vast amount of sensory information being gathered by an animal at any given moment, the nervous system would quickly be overwhelmed if it were to treat all information with equal importance. Furthermore, the brain size would restrict the ability to analyse and respond. Consequently, the brain separates the critical information from the irrelevant or less important by limiting actions to a momentarily selected fraction of the sensory information. Such is how humans can shift their attention to any part of their visual field without actually moving their fixation point (Warren and Warren, 1968). *Drosophila* in the torque meter can perform similar selective attention (Tang and Juusola, 2010). Under specific parameters, the flies restrict their responses to particular parts of the visual field, whether spontaneous or in response to other sensory stimuli (Wolf and Heisenberg, 1980; Tang and Juusola, 2010).

It is difficult to understand the animal's motivational state when measuring spontaneous preferences for simple visual stimuli in a virtual reality system. One solution is to manipulate the animal's motivational state by conditioning a positive or negative attachment to the stimulus with learning assays.

1.2.4 Learning at the torque meter

There are multiple visual learning paradigms. Learning requires a closed-loop system. Consequently, yaw torque exerted by the fly to the left causes the clockwise rotation of the panorama, while yaw torque to the right causes anti-clockwise rotation ("negative" visual feedback for turning). The first to investigate operant pattern learning with flies tethered at the

torque meter was by Wolf and Heisenberg (1991) after experiments outside of the torque meter demonstrated associative learning in *Drosophila melanogaster* (Spatz, Emanns and Reichert, 1974; Folkers and Spatz, 1981). The original and standard paradigm at the torque meter is a heat conditioning experiment (Fig. 1.10). The panorama for visual learning carries four equally distributed patterns in the centre of four quadrants (Q1-4), this, therefore, surrounds the fly in an alternating sequence of two types of pattern, for example, T patterns (conditioned stimulus, CS) (Dill, Wolf and Heisenberg, 1993; Tang *et al.*, 2004; Liu *et al.*, 2006) with an upright T (e.g. Q1 or Q3) and inverted T (e.g. Q2 or Q4). To then investigate whether the fly can discriminate between the type types of pattern, the fly receives heat punishment (unconditioned stimulus, US) (via a laser beam) if the fly orientates towards one pattern type (e.g. inverted T, CS+). The fly can quickly learn to avoid the pattern with the punishing pattern. This is remembered, and the fly prefers to orientate towards the non-punishing pattern (e.g. upright T, CS-), even after the heat is switched off permanently (memory test) (Wolf and Heisenberg, 1991). The food composition and fly age are critical for learning (Guo *et al.*, 1996). This setting is wholly artificial and would not realistically occur in any context in free flight in the wild. However, flies can still learn an association between heat and a pattern or orientation (Brembs and Heisenberg, 2000).

Building on this, this same method has been used to continue studies into pattern learning (Dill, Wolf and Heisenberg, 1993, 1995; Dill and Heisenberg, 1995). Flies can discriminate between identical patterns (T), which are presented at differing heights (9° centre of gravity difference) (Dill, Wolf and Heisenberg, 1993). In addition to patterns, other features of learning demonstrated at the torque meter include a combination of patterns and colour (Brembs and Heisenberg, 2001) colour alone (Wolf and Heisenberg, 1997; Brembs and Hempel De Ibarra, 2006; Brembs and Wiener, 2006) and yaw torque (Heisenberg and Wolf, 1993; Brembs and Heisenberg, 2000).

This learning assay has been utilised to investigate other aspects for *Drosophila* vision, including the functional relationships in the brain (Dill, Wolf and Heisenberg, 1995; Wolf *et al.*, 1998; Liu *et al.*, 1999) and the learning and memory process (Xia *et al.*, 1997; Xia *et al.*, 1997; Wang *et al.*, 1998; Xia, Feng and Guo, 1998).

Operant learning (can also be referred to as outcome learning) is based around reward and punishment learning (Heisenberg, 2015). The animal responds to a particular action with a specific behavioural response depending on the outcome. In such case, the animal relies on its

expectation of the future for what the outcome will be, for example, if it expects to receive pain when flying towards a particular pattern, it will respond by avoiding this pattern if it is able to learn the association. Flies store numerous parameters including size, colour, and elevation of the panorama for up to 48 hours (Xia *et al.*, 1997). Wild-type flies are capable of generalizing pattern memory over different contexts (i.e. context-independent memory), which for flies with impaired mushroom-bodies is not possible (Liu *et al.* 1999). Mushroom bodies have been used in many studies of learning and memory in *Drosophila* and are necessary for associative olfactory conditioning (Belle and Heisenberg, 1994; Waddell and Quinn, 2001). The central complex in the invertebrate brain is considered to be the site of orientation behaviour, the integration of multiple sensory modalities and other ‘high-order’ processes (Liu *et al.*, 2006; Ofstad, Zuker and Reiser, 2011). By silencing neurons that have projections to the ellipsoid body (a substructure of the central complex) the ability for visual learning is greatly impaired (Ofstad, Zuker and Reiser, 2011), therefore specific circuits within the ellipsoid body are essential for visual learning. In general, little is known about the underlying neural circuits that mediate these behaviours, such as associative learning at the torque meter, but *Drosophila* is a powerful model organism for determining how such complex behaviours are driven by circuits in the brain.

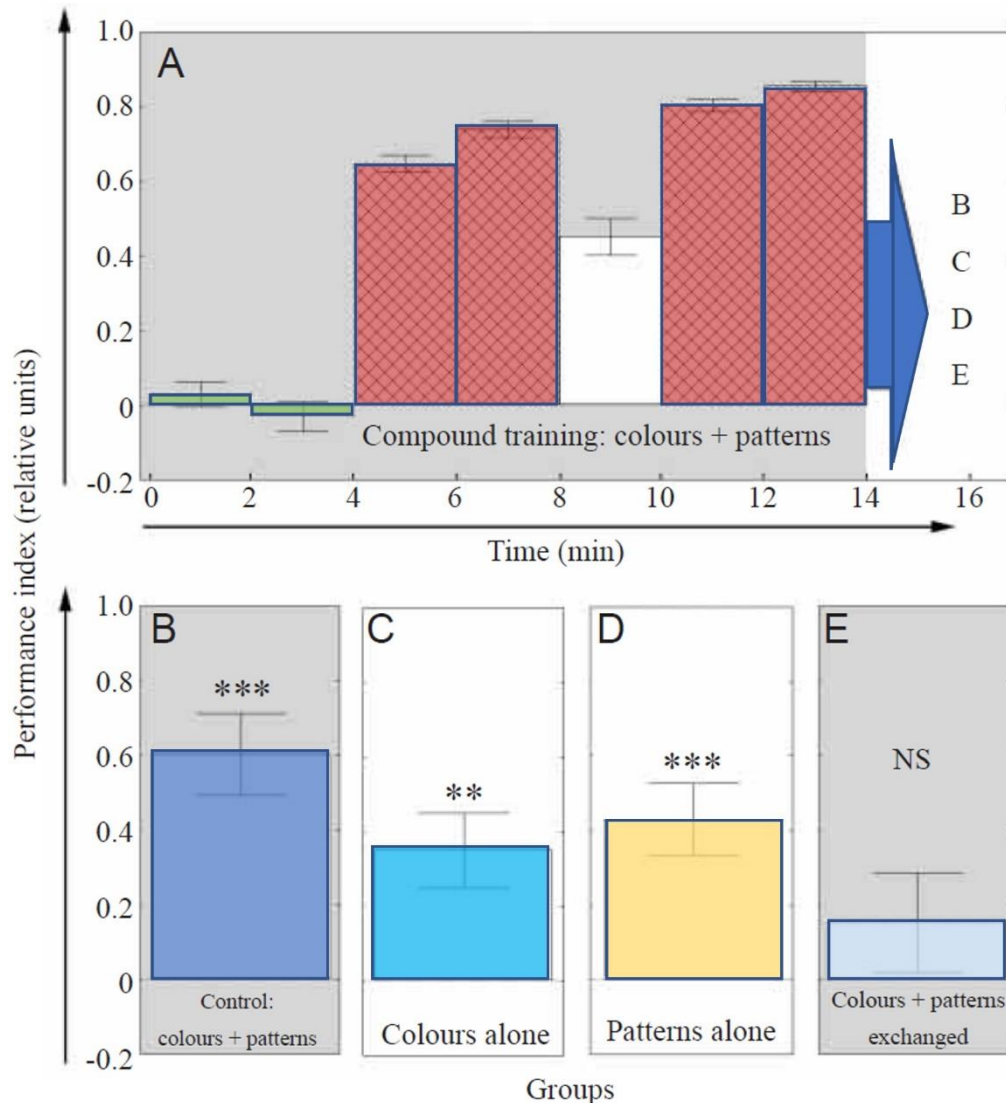


Fig. 1.10 Visual learning in the flight simulator.

Visual pattern learning of upright and inverse T-shaped black patterns using both colour and pattern stimuli to train associations to fly towards the CS- after receiving heat punishment. **(A)** The performance index (PI) shows no initial pattern preference during pre-training (green bars). During training (red checked bars), heat is delivered to the head and thorax of the fly for the CS+ (e.g. upright Ts). **(B-E)** During the memory test, the learning scores (PI 8/9) show that flies have a conditioned orientation preference for the CS- (e.g. inverse Ts) after learning associations of **(B)** colours and patterns presented together, **(C)** colours alone, **(D)** patterns alone, **(E)** or colours and patterns exchanged. This shows that when presenting patterns and colours together, the different stimuli can elicit similar learning association strengths. Image modified from Brembs and Heisenberg, (2001).

1.3 Thesis overview

Visual information is a primary source of sensory input for many animals. Despite their tiny eyes and brains, insects acquire and process a vast amount of information to guide their behaviour (Warrant and McIntyre, 1993). Due to their species-specific adaptations, the fruit fly *Drosophila melanogaster* can perform its required behavioural tasks. But how specifically do the eyes help guide the animal's behaviour?

My research aims to understand how insects use the images generated from both their eyes to enhance their perception of the world and whether *D. melanogaster* see the world with higher resolution than previously believed. The fruit fly may seem an unlikely candidate for high acuity visual tasks, but it is possible to study their flying behaviour as they are very amenable to behavioural experiments and have already been shown to see fine patterns. Specific questions are: Does the optomotor response of the fly change in response to high-frequency gratings in different environment proximities? Is the fly's single target acuity comparable to the minimum separable threshold shown with gratings? Can the fly discriminate between small 2D and 3D objects at close proximity, and are both eyes required for perceiving these changes in object depth? My overall research aim is to understand whether fruit fly acuity depends on the behavioural context and how insects use both eyes to enhance their detection of objects in their environment with behavioural analysis.

An insect experiencing rotation will innately compensate by rotating itself in the same direction. This simple reflex stabilises the animal's vision when experiencing unexpected deviations within the environment. The relative difference in the strength of the optomotor response reflects the specific visual stimulus parameters used, i.e. its temporal frequency, with larger dark and light stripes, which are presumably easier to detect, eliciting more robust responses from the insect. However, the effect of changes in the object's proximity within the environment while maintaining the gratings' at a constant angular size is unknown. Thus, changing the viewing distance at which optomotor responses are measured may lead to interesting new insights into fly vision. In [Chapter 2](#), I investigate the effect of temporal frequency and environment proximity on the dynamics of the optomotor response in the fruit fly. My results reveal that the fly responds to high spatial frequencies beyond the limits of the interommatidial angle, and when viewed at a closer distance, these higher frequencies elicit a more robust rotation. This ability allows flies to detect objects which subtend smaller angles in

the visual field with finer detail when the proximity of object is closer, indicating that they may possess myopic vision

Most studies investigating fruit fly visual acuity have been conducted with gratings, and relatively little is known about their capacity for single target detection, particularly for small objects. In **Chapter 3**, I first investigate whether singular hyperacute objects (ranging from 1° to 4°) generates a behavioural response in fruit flies. Flies were presented with either a singular dot or a singular 3D object alongside two 2D dots. I found that flies would perform slight fixation behaviour towards a single hyperacute dot placed amongst a light bar within dark and light stripes. I also found that when flies were presented with one 3D object with the same area and contrast of two 2D objects, the 3D object was seemingly more salient to a fly than the 2D object. These results suggest that fruit flies can see small objects and distinguish their differing depths.

To further investigate the perception of hyperacute objects in **Chapter 3**, I condition orientation preferences in fruit flies using similar 2D and 3D stimuli as the single object experiment. In addition to dots, I investigate the effect with a vertical bar (or stripes). The results demonstrate that slight differences in object depth were detectable for the insect. Flies discriminated between small 2D and 3D objects during conditioning, similar to the T-patterns control, even though it was presumably more difficult for the insect to discriminate hyperacute patterns. When one eye was occluded, the flies could still learn the control but failed to discriminate between the 2D and 3D objects. Furthermore, mutant flies with either the inner or outer photoreceptors non-functional were still able to learn in all conditions. These results support the hypothesis that fruit flies can perceive small objects within their environment and discriminate between changes in the object's depth. Moreover, that all photoreceptor cells contribute to this perception. Thus, in parallel with Chapter 2 and the first section of chapter 3, it suggests that fruit flies detect smaller environments with much more clarity than distal environments, advantageous for an insect experiencing highly cluttered environments.

Chapter 2

Pattern size and distance predict optomotor behaviour in fruit flies

Abstract

Flying insects must acquire depth information for navigating a three-dimensional world. By perceiving the absolute distance of an object, the animal can then perform the appropriate behavioural response. For example, by eliciting pursuit and courtship behaviour for close-small objects (as in potential mates) or escape responses for far-big objects (as in predators). Optomotor behaviour has been thoroughly studied in virtual environments on tethered animals, yet little is known about the effect of environment proximity on the characteristics of the optomotor response. Here, I investigate whether fruit flies – with recently proposed short-range binocular mechanisms – respond more robustly to close-small stimuli, despite constant angular size cues between the tested distances. By performing open-loop experiments on tethered fruit flies within two different sized arenas, I found that the fly varies its optomotor behaviour depending on changing distance and temporal frequency. When square gratings are presented physically closer, the flies strengthen their optomotor response, but only for smaller spatial wavelengths (2.4° and 4.8°). This result shows that the eye's distance from a nearby surface influences the perception of gratings that subtend small angles in the visual field. Thus, the fruit fly may possess myopic vision and see nearby conspecifics more clearly, than further away potential predators.

2.1 Introduction

In a three-dimensional world, animals must acquire depth information to perform appropriate behavioural responses. This information can then help discriminate between small objects nearby or large objects far away (Nityananda *et al.*, 2016). For example, a flying insect must acquire depth information to identify whether an object is a potential mate nearby or a large predator far away, which may subtend the same angle on the retina. Subject to calculating an object's distance, an animal can then infer the size of any other object within its visual field (Cartwright and Collett, 1979). It can then reduce any potential risk from predators and minimize the metabolic cost associated with poor decision making (Maimon, Straw and Dickinson, 2008). However, this process is complicated as depth information is not intrinsically present within retinal images (Land & Nilsson, 2012).

Many insects have specialised mechanisms encompassing monocular and binocular cues for distance estimation (Nityananda and Read, 2017). For example, stereopsis uses a binocular disparity cue between two retinal images to calculate the distance to an object. This correspondence has been well studied for vertebrate species, particularly in primates (for review, *see* Heesy, 2009). In contrast, only a few invertebrate groups have been shown to use their binocular overlap for stereopsis. Most notably, praying mantis use stereopsis to perform striking behaviours when prey is within its catch range (Nityananda, Tarawneh, *et al.*, 2016). Much more recently, Feord *et al.* (2020) demonstrated that cuttlefish utilise binocular cues to speed up prey capture. Thus, it is unclear whether stereopsis is more common amongst insects than previously believed. However, most insects utilise other depth cues for depth perception. As such, the underlying mechanisms for stereopsis remain much less understood in insects (Land, 1999). Indeed, for insects, the dominant depth cue is considered to be motion parallax (Lehrer *et al.*, 1988; Sobel, 1990), a monocular cue in which the animal's self-motion changes the viewing perspective and displaces the images of nearby objects. Locusts, for example, perform peering behaviour before jumping towards an object (Sobel, 1990), while honeybees (Lehrer and Collett, 1994) and bumblebees (Riabinina *et al.*, 2014) use motion parallax during learning flights to learn the position of the nest. Fruit flies also exploit it during walking (Wehner and Horn, 1975) and flying (Carbrera and Theobald, 2013) behaviours.

The fruit fly *Drosophila melanogaster* is a model species within vision research. In classic studies, a flight simulator has been used to assess the visual capabilities of the fly (Götz, 1964; Heisenberg, Wonneberger and Wolf, 1978; Heisenberg and Wolf, 1979). Behavioural

experiments in tethered flies show that optomotor behaviour is performed in response to rotating dark and light gratings (Götz, 1964). Recently, the fruit fly has been shown to respond to gratings with a spatial wavelength as small as 1.16° (Juusola *et al.*, 2017), which should not be possible when determined by the interommatidial angle of 4.5° (Gonzalez-Bellido, Wardill and Juusola, 2011). However, the fly uses ultrafast photomechanical photoreceptor microsaccades and stochastic refractory photon sampling, which enhances phasic contrast differences between objects, to see their environment with higher acuity than predicted by the optics (Juusola *et al.*, 2017).

Moreover, recent physiological experiments show that fly photoreceptor contractions sweep mirror symmetrically from back to front, and that the frontal photoreceptors' receptive fields overlap at approximately 23.5° (Kemppainen *et al.*, 2022). This overlap suggests the possible use of stereopsis (neural combination of the two retinal images from each eye) in fruit flies which would aid their depth perception for the nearby world (<70 mm). This effect is theorised to diminish at a range beyond 70mm as the error rate increases. Therefore, fruit flies potentially elicit a form of myopic vision where close objects are seen with more spatial details than blurred distance objects.

Thus, while optomotor behaviour and depth perception have been investigated extensively, the use of optomotor behaviour to investigate an animal's depth perception has not previously been reported. For example, in a flight simulator, the fly is fixed in space and unable to acquire typical depth cues associated with more natural flight conditions, such as translation cues from motion parallax. Therefore, the fly would have to utilise other depth cues to estimate the distance to an object.

Despite their tiny eyes, flying insects utilise visual information to guide various behaviours, from flight control and navigation to locating mates and resources. One fundamental aspect of visual acuity is spatial resolution, traditionally measured as the eye's capacity for resolving the gratings of dark and light bars (Warrant and McIntyre, 1993). For an animal to resolve a grating, adjacent dark and light bars (one cycle) must project onto the receptive fields of adjacent sampling units (Land and Nilsson, 2012). When presented with a finer grating, images of both the dark and light bars will fall on the same receptive field, thereby reducing its perceived contrast, which will cause the overall image to appear uniformly grey. Grating acuity is thus the spatial resolution of fine detail within the visual scene.

This study examined tethered fruit flies' optomotor responses to oscillating dark and light gratings of varying amplitudes and frequencies, presented at two physical distances from the fly. The responses are compared for differences in strengths at two distances combined with a change in spatial wavelength. Because of the predicted stereo range in *D. melanogaster*, it is hypothesised that the optomotor responses performed at two distances would elicit variations as fruit flies may see the proximal grating surface with hyperacute stereopsis and the more distant grating surface in blurred 2D. For the 25 mm distance, the gratings were presented well within *Drosophila*'s estimated stereo vision range (0-70 mm) (Kemppainen *et al.*, 2022). In contrast, for the 50 mm distance, the gratings are on the outer limit of the range. I predicted that fruit flies perform more robust optomotor responses to higher spatial frequencies when viewing from closer proximity.

2.2 Materials and Methods

2.2.1 Experimental animals

Wild-type Berlin (WTB) *Drosophila* were provided by Björn Brembs (University of Regensburg). The flies were reared at 25°C with a 12-h light / 12-h dark cycle and fed on a molasses-based medium. 3-10 day old females were cold-anaesthetised for approximately 10 min and then placed on a bespoke Peltier cooling stage. Here, individuals were tethered dorsally to a small copper-wire hook (0.06 mm Ø) positioned at the top of the thorax. The hook was at an approximate 20°-30° angle along the fly's longitudinal body axis. This allows the fly to be suspended at an angle that replicates their free-flight aerodynamics (Dickinson and Muijres, 2016). A droplet of UV-light sensitive glue (Loctite) was positioned between the thorax and head to hold the hook and restrict independent head movements. Each fly was inspected under magnification for precise tethering and head restriction before being isolated in a small vial for a minimum 30 min recovery.

Immediately before the hook tethering, a small group of flies had the left or right eye painted with non-toxic black acrylic paint (Winsor & Newton, Winton Oil Colour, Ivory Black – 1414331). The paint covered the medial eye section to create quasi-monocular vision, as this section would be needed for binocular vision (stereopsis). Despite the occlusion, many flies could fly immediately after the preparation. Some flies, however, demonstrated visible

discomfort due to the paint and would repetitively rub the paint with their legs (during active flight or dangling). Consequently, these flies were excluded from the dataset.

2.2.2 Flight simulator

Experiments were performed using a bespoke flight simulator system utilising a torque meter (Wardill *et al.*, 2012). The torque meter was positioned centrally in the upper opening of a cylindrical arena (transparent plastic cup; The University of Sheffield, Department of Chemical and Biological Engineering workshop) within the centre of the flight simulator. From the vantage point of the fly, this upper opening leaves some gap in the visual coverage, but all objects outside the arena were blacked out and not considered visible to the fly.

A small clamp holds the fly's hook (secured onto the thorax) to connect with the torque meter. The fly is now in a stationary position with a fixed orientation (Götz, 1964), unable to acquire visual feedback through translation or rotation. However, it can still freely beat its wings and move its legs, halteres, abdomen, and antennae. The fly's attempted body rotations to the left or the right, i.e. its yaw torque, are transduced by the torque meter into an electrical voltage signal (1 kHz sampling rate). Then, a computer provides feedback to a stepping-motor attached beneath the arena's base, generating a bi-directional arena rotation surrounding the fly. On the inner surface of the arena wall, a high-resolution paper stimulus is presented. Data can then be analysed using custom-written software (Biosyst) (Juusola and Hardie, 2001).

Surrounding the arena is a light diffuser in front of an outer ring-shaped light tube (spectral full-band: 350-900nm; Imperia fluorescent circular lamp 22 W 6,500 °K), providing uniform illumination of the stimuli without generating shadows. The system was mounted on a vibration isolation table and held within a Faraday cage which provided structural support for a black roller curtain to block outside light and enable access to the system.

2.2.3 Arena size

To investigate whether the optomotor behaviour of the fruit fly was affected by pattern distance, gratings were presented in two different sized arenas but kept at an almost identical angular size. Typically, a fly will perform visual course control behaviour (e.g. optomotor response) when receiving rotational movement signals. First, a group of flies ($n = 15$) were tested in a small arena (50 mm \varnothing), with the fly suspended centrally approximately 25 mm from the pattern. Second, flies ($n = 15$) were tested in a large arena (100 mm \varnothing), doubling the distance between the fly's eye and pattern to approximately 50 mm. Both groups were

presented images that subtend azimuth $\pm 360^\circ$ coverage horizontally, and $\pm 38^\circ$ and $\pm 40^\circ$ vertically in the small and large arena, respectively. A single example fly was tested in both arenas. However, preliminary trials indicated that most flies could not perform consecutively in both arenas (due to energy expenditure), so this was not attempted during experiments. Larger females were selected by eye to ensure standardisation across all stimulus parameters in both groups. Large flies were chosen consistently (as opposed to small flies consistently) because they would fly better during the experiments (personal communication, Narendra Solanki). Additionally, with changing body size come pronounced differences in the optical quality between individuals as the optics dictate that the smaller the eye the poorer the vision (Land and Nilsson, 2012) with larger individuals having both superior sensitivity and resolution (Currea, Smith and Theobald, 2018).

The small arena presented the dark and light gratings with a 1.0 contrast as seen from the fly. Contrast is defined as the physical contrast of a simple image such as gratings that assigns a contrast value between light and dark stripes. However, the large arena cannot be as brightly lit due to the structural limits of the flight simulator. The top portion of the large arena protrudes above the ring-light surrounding the arena, producing a lower contrast in this top region. Consequently, rotations in the large arena may theoretically produce weaker optomotor responses than the small cup because of dimmer light (Honkanen *et al.*, 2014). However, in both arenas, flies were tethered at a constant height in relation to the ring-light (elevated 20 mm from the arena base). Therefore, the flies would have experienced similar light intensities in both arenas and would not have been influenced by the dimmer top portion. More so, it is unlikely that flies will be overly sensitive to this slight contrast change within a particular region, as overall, it is a very bright light (Duistermars *et al.*, 2007).

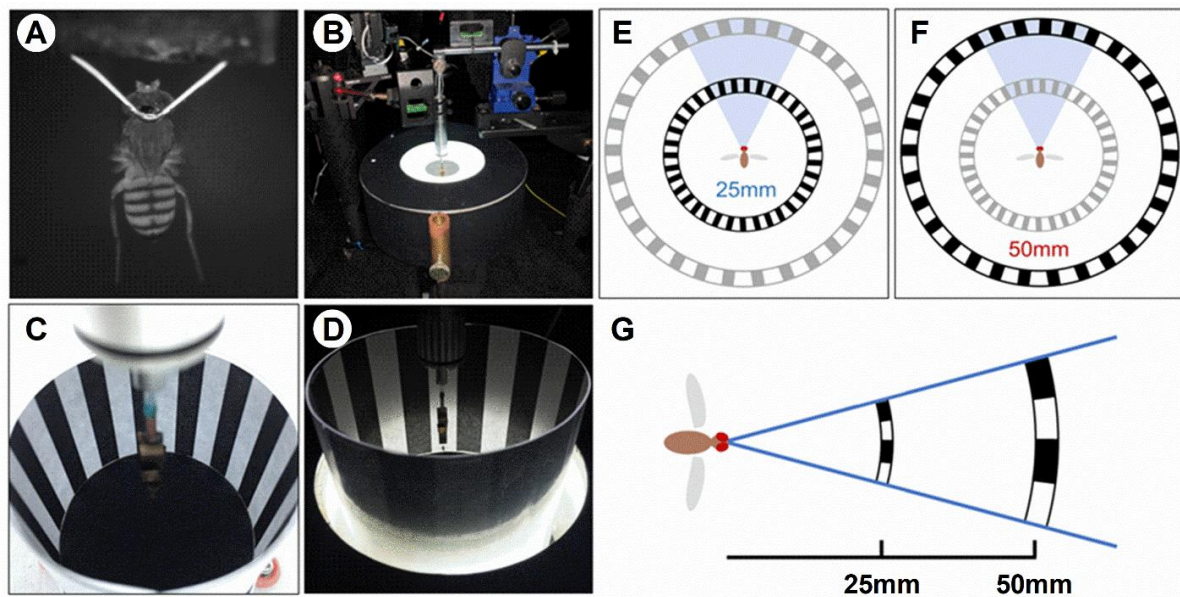


Fig. 2.1 The experimental setup.

(A) A flying female fruit fly is tethered to a thin copper-wire hook between the head and thorax and connected to the torque meter within the centre of the flight simulator. (B) The flight simulator system shows the small arena, uniformly lit by the right-shaped light tube with diffusers. (C, D) Images of the small and large arenas, (C) gratings on the inner surface of the small arena approximately 25 mm from the fly's eye, and (D) gratings presented in the large arena 50 mm from the fly's eye. (E-G) Schematic illustration of how small-close patterns subtend the same angular size as big-far patterns.

2.2.4 Experimental setup

The flight simulator system was configured to an open-loop setting, meaning the experimenter controls pattern movement. One experimental run consisted of 8 s of interleaved rotation (Fig. 2.2). Initiated with a 1 s static stimulus, followed by 2 s of rotational movement to the right (clockwise), then static again for 2 s, before 2 s of leftward rotational movement (anti-clockwise), before concluding with another 1 sec static stimulus. Each 8 s stimulus was repeated 10-25 times. Trials were excluded if flies stopped flying or behaved erratically. There was no pause between trials other than preparing the subsequent stimulus resolution, approximately 30 s stimulus changeover time.

The flies were presented with an extended source stimulus, i.e., a continuous panoramic grating of vertical dark and light bars. The bars were printed in black with a resolution of $1,200 \times 1,200$ dots per inch (Sharp MX-5141) onto white paper of consistent quality. The visual stimulus was

then positioned on the inner surface of the arena. Thus, the pattern forms a 360° panorama along each fly's vertical axis and rotates in the fly's horizontal plane. For each unique stimulus, flies were first tested with a slow (45°/s) pattern rotation followed by a fast (300°/s) rotation. In the small arena, flies were presented patterns with five spatial wavelengths (2.3°, 4.7°, 6.4°, 12.9° and 25.7°). In the large arena, presented twice as far from the fly, five similar-sized spatial wavelengths were presented (2.4°, 4.9°, 6.9°, 13.8° and 27.7°). Thus, regardless of arena size, from each fly's perspective, the gratings would be an almost identical angular width and appear as the same size within the fly's visual field. The different stimuli were presented to each fly in a pseudorandom order. For clarity, these slightly different spatial wavelengths are labelled as the average 2.4°, 4.8°, 6.6°, 13° and 26°. In addition, two control stimuli (dark and light) were tested to confirm that airflow or other features did not influence optomotor behaviour. A white diffuser plastic arena was presented to a fly with or without white paper for the 'light' control, while in the 'dark' control, the same arena was presented but with the ring-light switched off to create complete darkness during the trials.

Yaw torque responses are measured for distance, spatial wavelength and temporal velocity. In total, two different distances were tested, showing five different spatial wavelengths with two controls, presented at two angular velocities. Thus, a typical fly would see fourteen unique stimulus combinations, yielding twenty-eight unique combinations for the single example fly tested in both arenas.

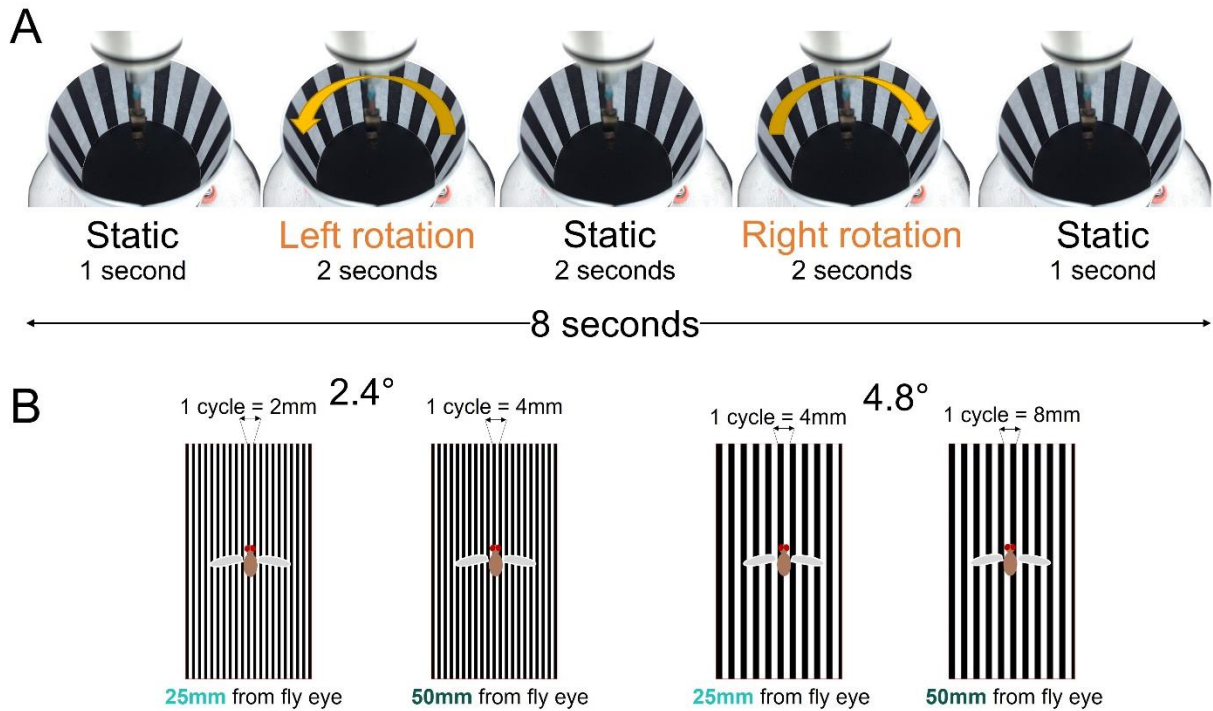


Fig. 2.2 Optomotor protocol and stimuli.

(A) One experimental run consisted of 8 s of interleaved rotation. Initiated with a 1 s static stimulus, followed by 2 s of rotational movement to the right (clockwise), then static again for 2 s, before 2 s of leftward rotational movement (anti-clockwise), before concluding with another 1 sec static stimulus. (B) (left) A flying female views the 2.4° stimulus from 25mm which has a physical size of 2mm for one cycle (one dark and one light bar) and is 4mm for the large arena (50mm). (right) The 4.8° stimulus has a physical size of 4mm in the small arena and 8mm when use din the large arena.

2.2.5 Data analysis

A fly's optomotor behaviour expresses as a syn-directional, bi-phasic yaw torque response. The response peak is at the cessation of the first rotational movement before it gradually returns to its baseline, typically over a few seconds. However, since this return is not immediate and the static stimuli separating the two rotational movements is only 2 s, the torque response is only marginally recovered (10-70%) during the initiation of the second rotation. The second rotational movement is therefore not as robust as the first. Consequently, I analysed the maximum range (or peak-to-peak) of the yaw torque responses from each trial. This then gave the value of the range between the maximum response to the left rotation and the maximum response to the right rotation. All trials were pooled and averaged to make a single fly recording for each stimulus, reducing noise and arbitrary trends found within individual trials. For each fly, the stimulus were scaled by normalising to whichever stimulus elicited the most potent response. The normalised values were then averaged for the population for each stimulus. This approach helps to reveal the response's underlying strength, as an individual's response will vary over multiple repetitions to the same stimulus. The population responses for each stimulus can then be compared for differences.

2.2.6 Statistics

All statistical tests were performed using SPSS (IBM SPSS Statistics 26). Data were tested for normality using the Shapiro-Wilk test. To test whether flies responded to hyperacute patterns differently to the dark control, I used a one-way ANOVA with Dunnett's *post hoc* test. To test between the different sized arenas, I used an independent samples t-test if there was a normal distribution. Otherwise, a Mann-Whitney test was used. A post hoc power analysis was conducted using G*Power version 3.1 (Faul *et al.*, 2007) using the obtained sample size and effect size to determine the study's power in [Fig. 2.4](#). To investigate the effect of velocity on the turning direction for the 6.6° spatial wavelength, I used a paired-samples t-test.

2.3 Results

To study the effect of environment proximity on *Drosophila* optomotor behaviour, I analysed the torque responses of wild-type Berlin flies in two different sized arenas within a traditional, *Drosophila* flight simulator. Tethered flies attempt to prevent images from slipping on their retinae by following field rotations which generate yaw torque responses. The simulator was

arranged in an open-loop configuration, and the torque responses were pooled and averaged for each fly.

2.3.1 Effect of distance on optomotor responses to small patterns

To investigate the effect of distance on the fruit flies response to varying spatial wavelengths, flies were presented stimuli in a small (25 mm) or large (50 mm) arena. A single example fly was tested in both groups at both distances (Fig. 2.3). During slow rotation, the fly strengthened its response to hyperacute stimuli at shorter distances (Fig. 2.3B). In contrast, with fast rotation the larger arena elicited more robust optomotor responses (Fig. 2.3C and D).

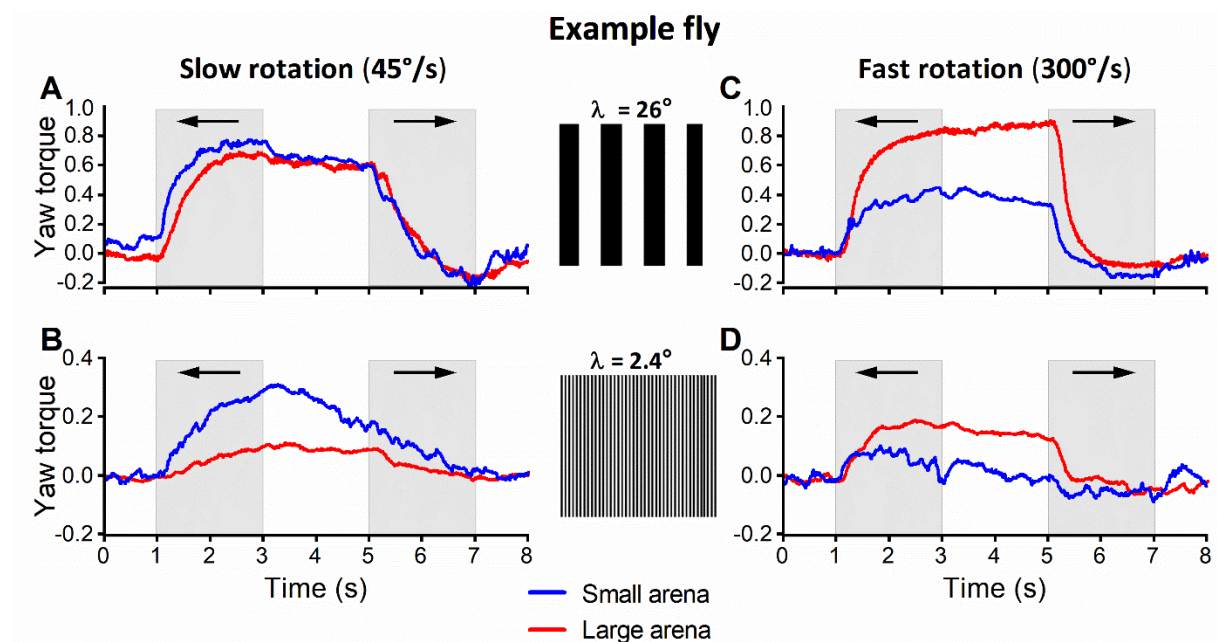


Fig. 2.3 Example fly performed differently when tested at two distances.

A single fruit fly was tested for all stimuli at distances of 25 mm (blue line) and 50 mm (red line). (A, B) Under slow rotation (45°/s), the fly exhibits similar responses to the large pattern (A, 26°) but shows stronger responses to the small pattern (2.4°) when physically closer (B). (C, D) Under fast rotation (300°/s), the fly shows more robust responses to both patterns when tested in the large arena. Grey shading indicates the rotational period. Black arrows show the direction of rotation as viewed by the fly.

The two groups tested at either distance support this result (Fig. 2.4). The mean strength of the optomotor responses was stronger under slow rotation (Fig. 2.4A, C, E, G) when presented in

the smaller arena (teal line) compared to the large arena (green line) for both the 4.8° pattern (**Fig. 2.4A**) and the hyperacute pattern (2.4°; **Fig. 2.4A**). These results were statistically different (4.8°: independent-sample t-test: $t(28) = 3.02$, $P = 0.005$; **Fig. 2.4C**; 2.4°: independent-sample t-test: $t(28) = 3.17$, $P = 0.004$; **Fig. 2.4G**). In contrast, under fast rotation speeds the mean strength did not differ significantly (4.8°: independent-sample t-test: $t(28) = 0.57$, $P = 0.57$; **Fig. 2.4D**; 2.4°: independent-sample t-test: $t(28) = 0.4$, $P = 0.69$; **Fig. 2.4H**).

Taken together, this suggests that under slow rotation, arena size does significantly effect the optomotor response, while under fast rotation, this difference is removed. However, given the sample size ($n = 15$ per group), a post hoc power analysis for both **Fig. 2.4C** and **Fig. 2.4G** (effect size $d = 0.2$ and $\alpha = 0.05$) has shown if there were a difference between the small arena and large arena at fast rotation, as big as the difference observed under slow rotation, then I would have had a 13% chance of detecting it. It is therefore possible that the small sample size can explain why this difference was not observed under fast rotation.

2.3.2 Large patterns elicit stable responses over two distances

As predicted, the larger patterns, which are easily detected at both distances, do not elicit stronger optomotor responses when they are closer to the eye. This is consistent for both the slow (26°: Mann-Whitney test: $U = 117.50$, $P = 0.838$; **Fig. 2.5C**; 13°: Mann-Whitney test: $U = 76.00$, $P = 0.14$; **Fig. 2.5G**) and fast rotations (26°: Mann-Whitney test: $U = 117.00$, $P = 0.87$; **Fig. 2.5D**). However, although there is only a slightly stronger optomotor response for the larger arena for fast rotation for the 13° wavelength, it is statistically different (Mann-Whitney test: $U = 171.00$, $P = 0.015$; **Fig. 2.5H**).

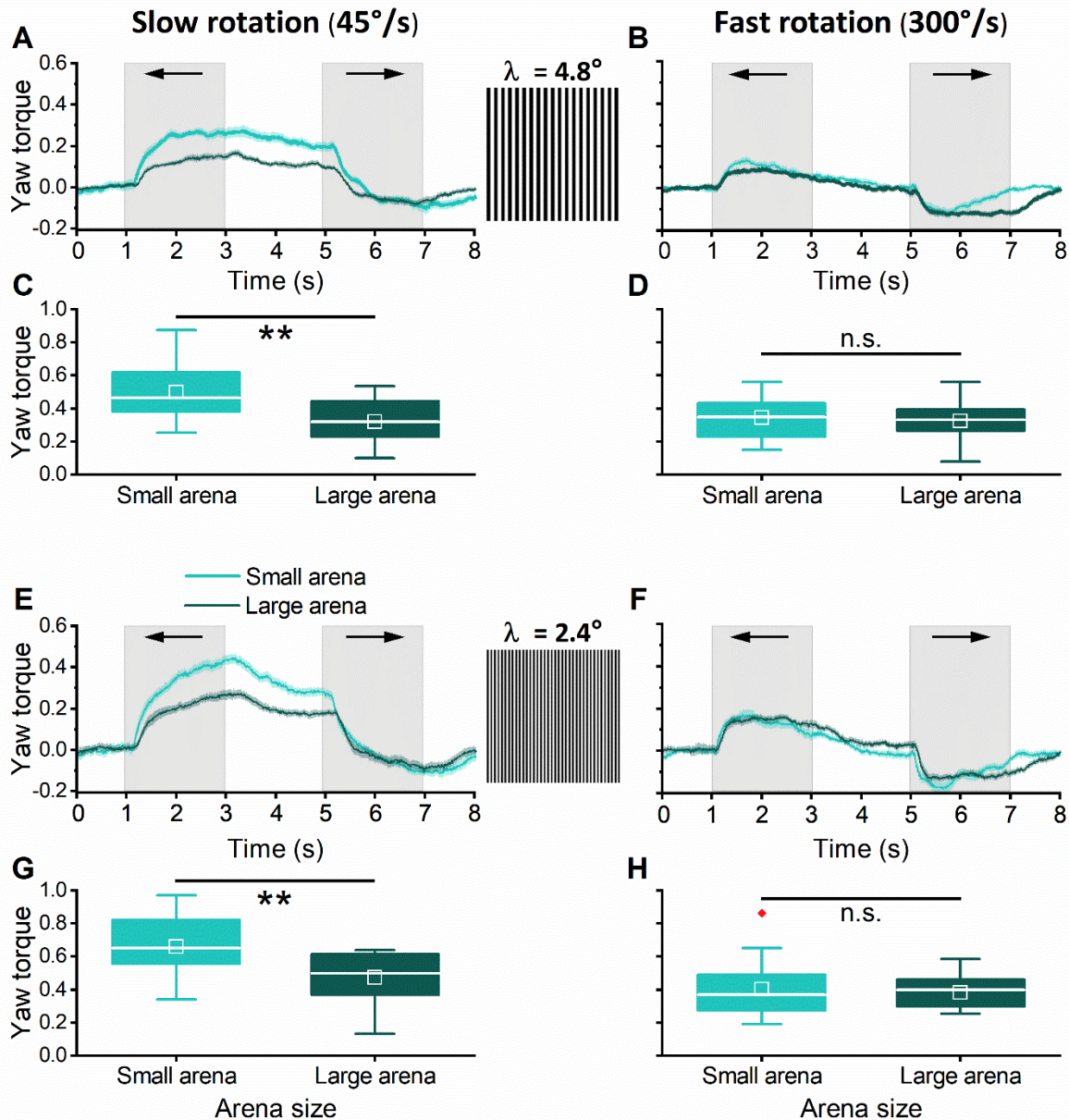


Fig. 2.4 Small patterns elicit stronger optomotor responses when closer.

The mean responses of fruit flies in different sized arenas ($n = 15$ small arena; $n = 15$ large arena) to 4.8° (A-D) and 2.4° (E-H) spatial wavelengths under slow rotation (left plots) and fast rotation (right plots). (A, C) Fruit flies exert more yaw torque when presented the 4.8° grating in the small arena (teal) compared to the large arena (green). (E, G) This is consistent with the 2.4° grating. (B, D, F, H) In contrast, there is no difference in the mean strength of responses for pattern distance under fast rotation. Grey shading indicates the rotational period. Black arrows show the direction of rotation as viewed by the fly. Boxes indicate the 25-75% interquartile range, the white line indicates the median, the white box is the mean, whiskers represent the entire data spread, and red diamonds represent outliers. Asterisks indicate the level of significance: * $P < 0.05$, ** $P < 0.01$, *** $P < 0.001$ and n.s. not significant.

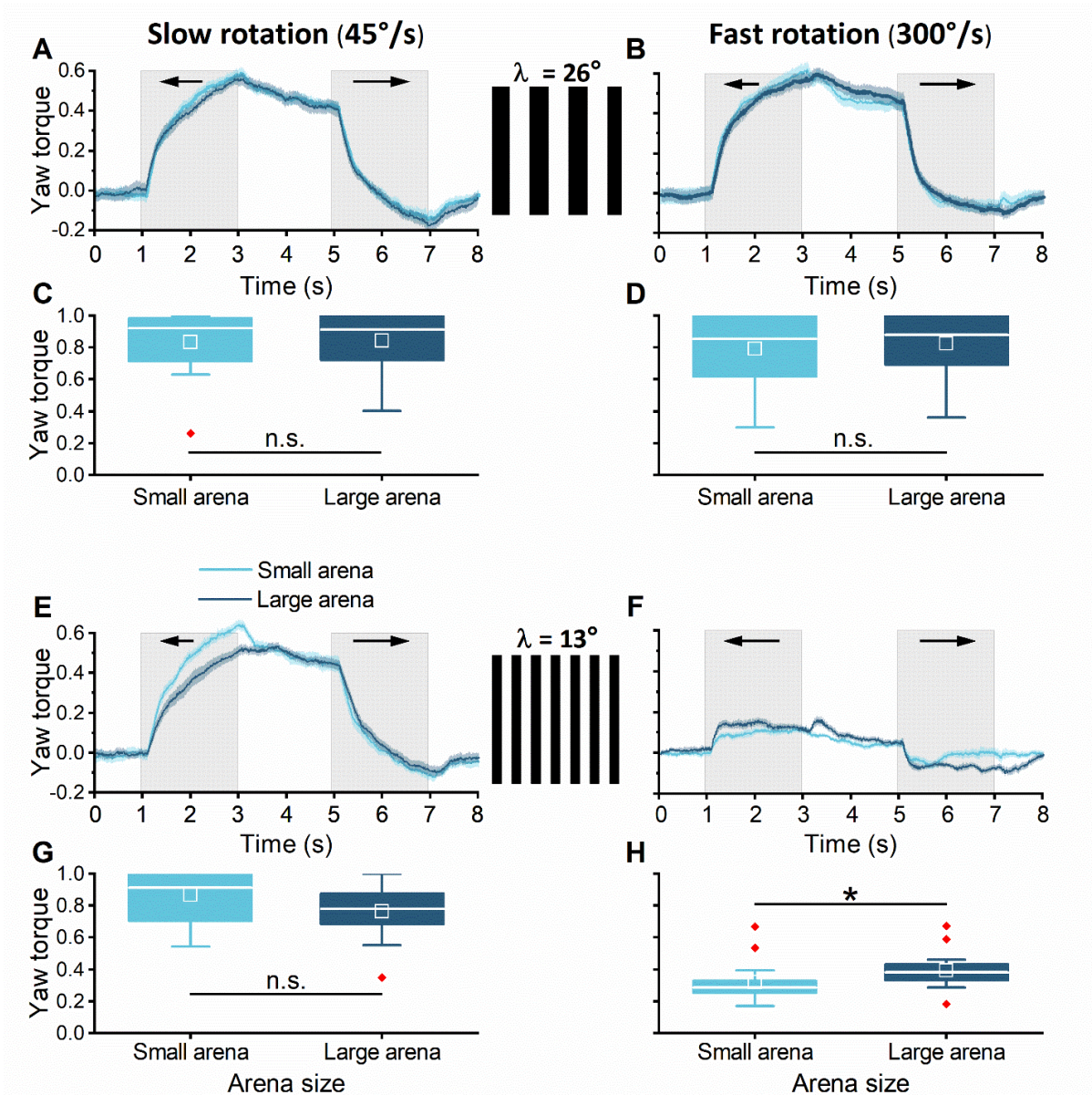


Fig. 2.5 Large patterns elicit consistent optomotor responses.

The mean responses of fruit flies in different sized arenas ($n = 15$ small arena; $n = 15$ large arena) to 26° (A-D) and 13° (E-H) spatial wavelengths under slow rotation (left plots) and fast rotation (right plots). (A-E, G) Fruit flies show similar optomotor responses to the changing wavelengths and speeds when viewing the patterns at different distances. (F, H) In contrast, although the results are similar to the other stimulus parameters, there is a statistical difference for stronger responses in the large arena for the 13° pattern (F). Grey shading indicates the rotational period. Black arrows show the direction of rotation as viewed by the fly. Boxes indicate the 25-75% interquartile range, the white line indicates the median, the white box is the mean, whiskers represent the entire data spread, and red diamonds represent outliers. Asterisks indicate the level of significance: * $P < 0.05$, ** $P < 0.01$, *** $P < 0.001$ and n.s. not significant.

2.3.3 Fruit flies respond to gratings smaller than the interommatidial angle

This study confirmed the results of Juusola and colleagues (2017) as fruit flies performed optomotor responses to gratings smaller than the interommatidial angle (**Fig. 2.6**). This was statistically different to the dark control (One-way ANOVA: $F(2, 42) = 1.26$, $P \leq 0.001$; **Fig. 2.6C**) for both the 2.4° (Post-hoc Dunnett: $P \leq 0.001$) and 4.8° (Post-hoc Dunnett: $P \leq 0.001$). Additionally, for the large arena, flies responded stronger to small stimuli than for the dark control (One-way ANOVA: $F(2, 34) = 9.72$, $P \leq 0.001$; **Fig. 2.6D**), which differed statistically for the 2.4° pattern (Post-hoc Dunnett: $P \leq 0.001$) and 4.8° wavelength (Post-hoc Dunnett: $P = 0.011$).

In contrast, the dark and light control stimuli (**Fig. S1** and **S2**) evoked minimal responses. This result also confirms classic results that slow field rotations generate stronger responses than fast field rotations (blue vs green line) (Götz, 1964; Blondeau and Heisenberg, 1982). However, it is worth noting that slow field rotations were constantly tested before fast rotations (as different velocities were not the focus of the study), so less motivation or energy may be a factor in the fast rotation results.

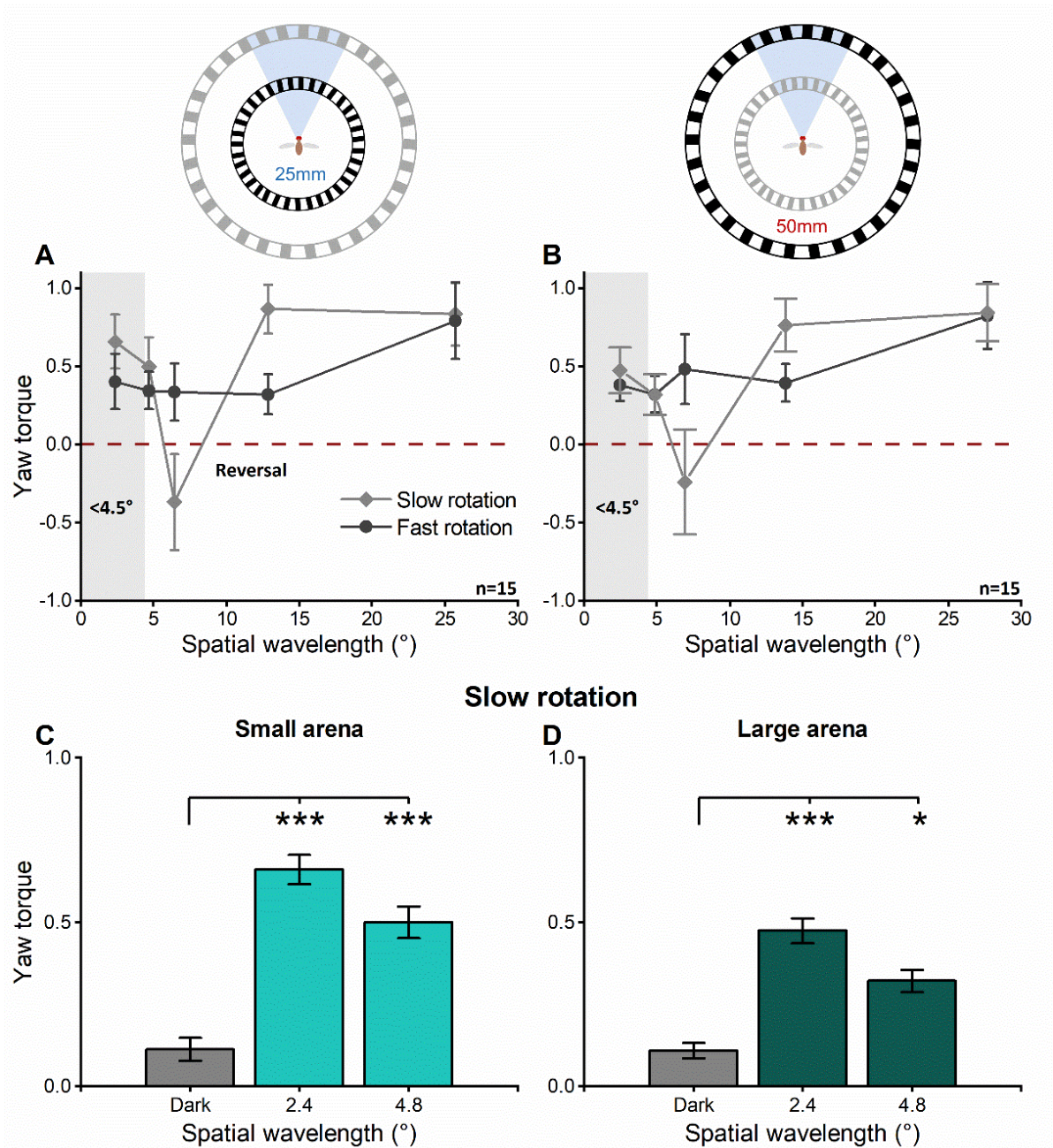


Fig. 2.6 Fruit flies respond to hyperacute gratings.

The strength of the optomotor response depends on the rotational velocity and spatial wavelength of the stimuli. (**A**, **B**) Slow rotations ($45^\circ/\text{s}$; green line) elicit more robust responses than fast rotations ($300^\circ/\text{s}$; blue line). Large patterns (26°) elicited the most robust responses at either rotational velocity or pattern distance ($n = 15$ small arena; $n = 15$ large arena). Grey shading indicates sizes smaller than interommatidial angle. (**C**, **D**) The mean responses and SEM show that small patterns (2.4° and 4.8°) elicit stronger optomotor responses than the dark control. Asterisks indicate the level of significance: * $P < 0.05$, ** $P < 0.01$, *** $P < 0.001$ and n.s. not significant.

2.3.4 Optomotor reversal is dependant on velocity and binocularity

To study the turning direction of fruit flies with respect to a 6.6° pattern wavelength, I compared the optomotor response while the animal experienced various distances, velocities, and binocular or monocular vision (Fig. 2.7). In contrast to the other tested wavelengths, the 6.6° pattern generated optomotor response dynamics in the opposite direction (reversal) of the field rotations at both distances under slow rotation (green line; Fig. 2.7A and B). It is essential to distinguish that these were not weak optomotor responses. Instead, they were strong responses against the patterns rotation direction. This finding was unsurprising as similar results have been previously reported and explained as spatial aliasing (Land and Nilsson, 2012). Elementary motion detectors (Hassenstein and Reichardt, 1956) were previously believed to be subject to spatial aliasing due to their underlying architecture (Buchner, 1976) which was used to explain optomotor reversal behaviour. In contrast though, Tammero, Frye and Dickinson, (2004) show how EMDs in the front and rear field of view mediate responses with similar spatial properties which cannot be explained by spatial aliasing. However, the differences observed during slower field rotations was not observed during the faster rotation, and so there was a statistical difference between the two velocities for the small arena (paired-sample t-test: $t(14) = -6.39$, $P \leq 0.001$; Fig. 2.7C) and large arena (paired-sample t-test: $t(14) = -6.76$, $P \leq 0.001$; Fig. 2.7D).

Furthermore, when monocular flies ($n = 9$; Fig. 2.7E) were presented to the slow ($45^\circ/s$) rotation, they ceased to reverse and instead performed normal responses. This was consistent for flies who had either the left eye ($n = 5$) or right eye ($n = 4$) painted. When the left eye is painted and the right eye is able to follow grating rotation leftward it is able to follow the movement more robustly than when the right eye is painted. This result is consistent with the finding that photoreceptor microsaccades globally sweep from back to front (Kemppainen *et al.*, 2022). By painting the left eye whose saccades are moving against the pattern rotation, the fly now follows the rotation rather than turning in the opposite direction. When the right eye is painted the same effect occurs although less robustly. As the rightward rotation (where right eye painted flies would perform best) occurs a couple seconds after the leftward rotation, the response is not as strong because the fly has not returned to its baseline. Nevertheless, covering one eye of the fly consistently removes the reversal behaviour shown by normal flies. There is a significant effect when we compared the binocular flies to these monocular flies (Independent-sample t-test: $t(24) = 4.79$, $P = 0.022$; Fig. 2.7F).

During faster rotation (300°/s), flies perform typical syn-directional optomotor responses, consistent with expected behaviour. Therefore, to explore the effect of velocity more fully, a few flies (n = 4) were also tested with additional rotational velocities (100°/s, 200°/s and 500°/s; **Fig. 2.7G**), although the sample size was small and the strength of the response was weak due to the fast rotation and relatively small wavelength, the flies clearly showed a normal turning response. This finding is important as it suggests that it is not only the spatial wavelength that predicts the reversal (aliasing) behaviour but also the rotation speed, as it only occurred under a particular rotational velocity. Therefore, if spatial aliasing caused the optomotor reversal, it should occur similarly at all tested velocities. Clearly, this is not the case with *Drosophila*.

Taken together (**Fig. 2.7H**), the results show that only with binocular vision at slow rotation do the majority of flies reverse (87%), under all other parameters (albeit with smaller sample sizes), nearly all flies (75% to 100%) perform normal responses. The percentage of animals turning with or against the grating direction was not significantly different between stimuli (chi-square test: $\chi^2(5, 51) = 0.47$, $P = 0.052$; **Fig. 2.7H**). These results suggest that it is not spatial aliasing because this should theoretically cause reversal behaviour for the 6.6° wavelength regardless of velocity and monocular vision. Instead, both eyes simultaneously viewing the pattern rotating at 45°/s is the crucial factor. Coincidentally, the mirror-symmetrical global movements of the photoreceptor microsaccades sweep from back to front at a similar velocity (45°/s - 50°/s). This suggests that rather than the size of the optics causing spatial aliasing, the speed of the photomechanical microsaccades moving mirror-symmetrically (at the opposite directions) in the left and right eye is causing perceptual aliasing when the grating rotation happens to match its velocity.

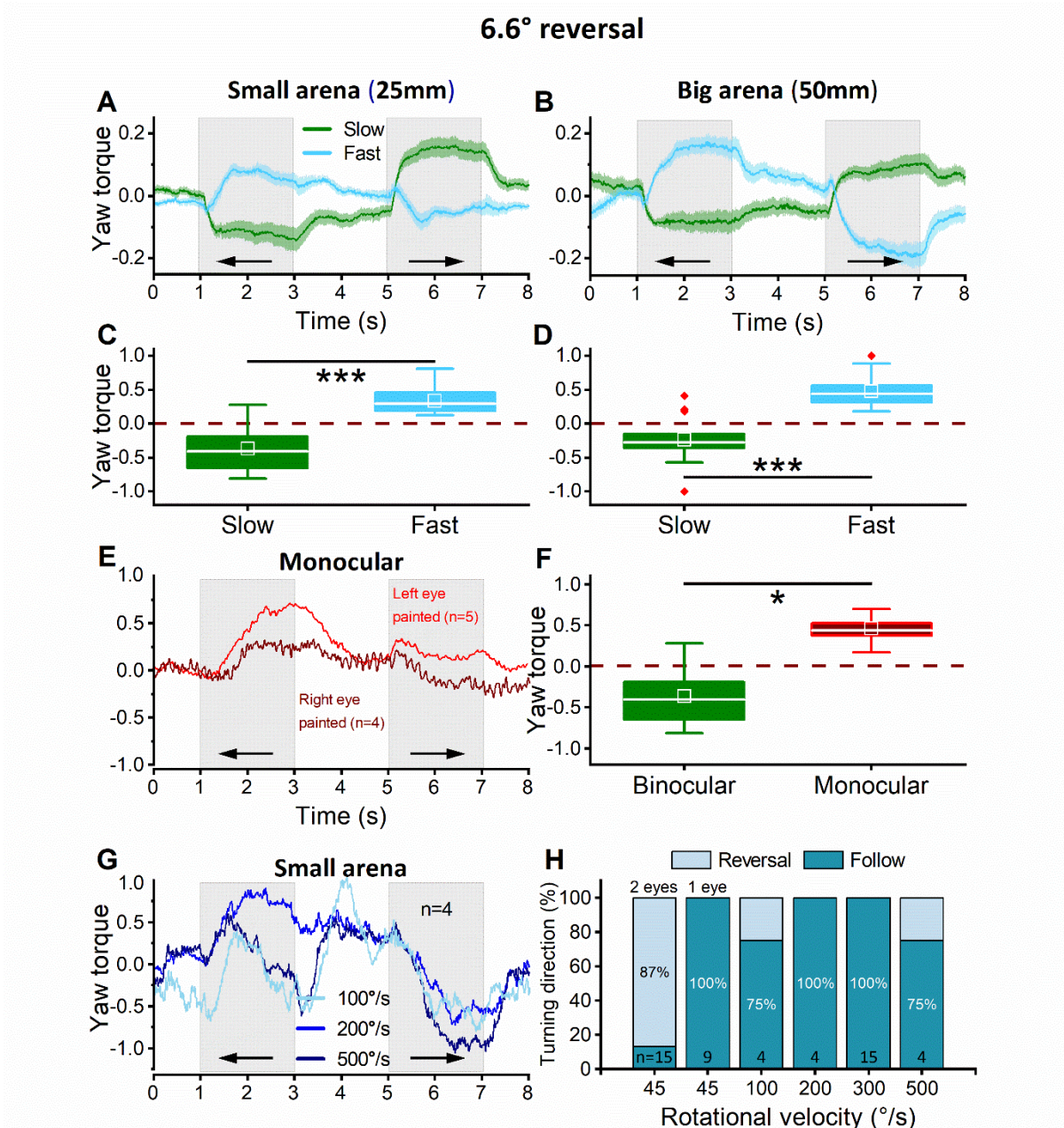


Fig. 2.7 Optomotor reversal is velocity-dependent.

(A-D) When fruit flies ($n = 15$) view the 6.6° stimulus, the mean optomotor response is in the reversed direction during slow rotation (green) but is in the normal turning direction under fast rotation (blue). (E) Monocular flies ($n = 9$) viewing the $45^\circ/\text{s}$ (slow) rotational velocity undertook normal optomotor responses with either the left eye (red, $n = 5$) or right eye painted (dark red, $n = 4$). (F) There was a significant difference between the optomotor response of binocular flies (green) and monocular flies (red) when tested in the small arena with slow rotation. (G) For a small group of flies ($n = 4$), the stimulus was also rotated at $100^\circ/\text{s}$, $200^\circ/\text{s}$ and $500^\circ/\text{s}$, which showed the normal turning direction. (H) Binocular flies viewing the slow rotation predominantly reverse their turning direction (87%). In contrast, all other groups predominantly

perform following turning responses. If the reversal were explained by spatial aliasing, all groups should have turned in the opposite direction. Grey shading indicates the rotational period. Black arrows show the direction of rotation as viewed by the fly. Boxes indicate the 25-75% interquartile range, the white line indicates the median, the white box is the mean, whiskers represent the entire data spread, and red diamonds represent outliers. Asterisks indicate the level of significance: *P < 0.05, **P < 0.01, ***P < 0.001 and n.s. not significant. Figure F 'binocular' data is replotted from E 'slow' data.

2.4 Discussion

In a previous experiment, behavioural results showed that tethered fruit flies performed optomotor turning responses to grating patterns of 1.16° at the torque meter (Juusola *et al.*, 2017). The data presented here confirm the validity of these findings as fruit flies elicited clear turning responses to follow the wide-field stimuli of 2.4° gratings (Fig. 2.6). Importantly, although a larger pattern, this is still considerably smaller than the interommatidial angle of 4.5° in fruit flies (Gonzalez-Bellido, Wardill and Juusola, 2011). Therefore, approximately two pairs of light and dark bars will fall within the visual field of a single photoreceptor. Hence, dark and light bars do not need to fall on adjacent photoreceptors as predicted by the optics for eliciting optomotor behaviour. This result suggests that the minimum visual detection of gratings is well below the optical resolution limit.

Distance and optomotor

More importantly, for this study, the optomotor response was different at 25 mm and 50 mm for the 2.4° and 4.8° (Fig. 2.4). This would indicate a range of short-sightedness (or myopic vision) in *Drosophila*, where flies see the nearby world with more spatial resolving power. The fly cannot utilise motion parallax with head movements as the head is fixed. Otherwise, the patterns would move further and faster across the retina in the small arena. Indeed, with their theoretical model, Kemppainen and colleagues (2022) predict a < 70mm range where binocularity enhances acuity, which diminishes with distance as error rate increases (Kemppainen *et al.*, 2022), thereby facilitating binocularity for short-range tasks before rapidly receding to monocular cues. The left and right eye microsaccades' global mirror-symmetric (back-to-front) dynamic occurs at approximately $45^\circ/\text{s}$ - $50^\circ/\text{s}$ (Kemppainen *et al.*, 2022). It is perhaps no coincidence that walking speed in *Drosophila* is as low as 1.5 cm/s and a typical fast run is 3.8 cm/s (Strauss and Heisenberg, 1990), which at a distance of 25 mm is

approximately $34^\circ/\text{s}$ to $88^\circ/\text{s}$ respectively, suggesting that this is adapted for visual courtship behaviours tracking the relatively small and slowly moving conspecifics. Indeed, since fruit flies are prey species, any pursuit behaviour or mate selection- requiring depth estimation - would likely be during courtship behaviour, which can assume the moving object's constant size and velocity. Indeed, the results for large patterns further suggest changes in acuity for changes in the proximity of the environment. Larger patterns that are considerably easier to detect promoted stable turning responses at both distances (**Fig. 2.5**). Supporting the idea that fruit fly photoreceptor microsaccades optimise vision for close-small objects without losing the ability to accurately respond to more coarse optic flow changes (Kempainen *et al.*, 2022).

On the other hand, the fruit fly grating acuity may be superior within the laboratory setting. The flight simulator is a highly artificial experience for naïve fruit flies, and the stimulus is very simplistic and tested at high contrast. Therefore, the behaviour in this situation is unlikely to be ecologically the most relevant. In another experiment, a flight simulator is placed outdoors to enhance natural conditions for testing the migratory flight behaviour of the nocturnal Australian Bogong moth (Dreyer *et al.*, 2018). This approach helps promote the desired natural conditions whilst unwanted sensory stimuli are best controlled. It would now be interesting to test the grating acuity (and single target acuity, chapter 3) in fruit flies if they were to be tested with respect to natural light levels outdoors. For example, as a crepuscular insect, the fruit fly could be tested in an outdoor flight simulator at dawn and dusk to compare behavioural performance to the laboratory conditions.

Optomotor reversal

The results show reversal behaviour for the 6.6° wavelength (**Fig. 2.7**). Since the early study on fruit flies by Lotte von Gavel (1939), it has been reported that a wavelength near 9° causes a reversal in their optomotor response. Indeed, similar findings have been found in other species. For example, the response reverses between 5° and 10° in honeybees (Kunze, 1961)). However, this has always been explained as a Moiré effect among the interommatidial angle and grating (Land and Nilsson, 2012). An alternative explanation is that the global dynamics of the photomechanical photoreceptor microsaccades influence the gratings' perception. Since the back to front dynamics of the microsaccades occurs at approximately $45^\circ/\text{s}$ - $50^\circ/\text{s}$ coincides with the slow rotational velocity of $45^\circ/\text{s}$. Consequently, as the microsaccades of one eye theoretically move in unison with the pattern rotation, the microsaccades in the other eye are moving against the pattern. This may cause a neural imbalance in the rotational optic flow

perception as one eye is velocity locked. This eye therefore has a much weaker signal with little contrast, while the eye moving against the pattern has high contrast and stronger signal. It is, therefore, possible that the reversal response originates from neural processes eliciting perceptual aliasing.

Therefore, covering one eye of the fly should not inhibit the reversal response even though it may weaken it as the fly compensates for the defect. Regardless, the results show no weakened response but rather demonstrate a robust normal turning response to a 6.6° wavelength, i.e. occluding one eye reverses the reversal (**Fig. 2.7E**). This is supported by the monocular flies with different eyes painted. With the left eye occluded, the right eye is able to follow the leftward rotation more robustly than when the right eye is occluded. As expected for the rightward rotation there is the opposite effect as having the right eye occluded allows the left eye to follow the rotation. Albeit the second rotational movement is not as robust as the first since the torque response is only marginally recovered during the initiation of the second rotation due to the short 2 second interlude. Future studies can alter which direction the gratings are rotated towards first, so as to see directly compare the response for the initial stronger optomotor responses. Additionally, increasing the rotational velocity seemingly inhibits the reversed response and causes flies to innately perform the typical syn-directional response (**Fig. 2.7E**). Optomotor responses to different rotational velocities have been described previously (Götz, 1964). However, it has not been applied to exploring optomotor reversal to the best of my knowledge. Instead, studies have focused on the spatial wavelength and different light levels with the shifting of reversal behaviour (Hecht and Wald, 1934). Consequently, a Moiré effect caused by the matched sampling of the interommatidial angle to the grating wavelength is unlikely to be the definitive explanation for this phenomenon.

Future work

Structural limits of this bespoke flight simulator system limited the arena size to a 100 mm diameter (i.e. the ‘large’ arena presenting patterns 50 mm from the eye). However, other sizes within this range could be tested in the future besides the 50 mm arena (i.e. the ‘small’ arena presenting patterns 25 mm from the eye). For example, the arena’s could increase by 5 mm increments (eye to pattern) to test the responses between these values and further understand the dynamics of distance and optomotor responses. On the other hand, arenas could become gradually smaller to investigate whether strengthened turning responses to small stimuli correlate with increasing proximity.

Furthermore, testing a wider variety of grating patterns smaller than the optical resolution limit would enhance the current findings. I tested approximately 2.4° in both arenas, and Juusola and colleagues (2017) tested 1.16° in a 25 mm arena, neither study did exploratory tests to determine the absolute detectable limit eliciting optomotor responses. However, preliminary data for fruit flies on a trackball suggests it may be as low as 0.5° (unpublished work; Keivan Razban Haghghi, Juusola lab). It would be particularly worthwhile to understand this limit for flying behaviour within the flight simulator system combined with the effect of distance.

Conclusions

The optomotor response of the fruit fly with differing stimuli distances strengthened when smaller patterns (2.4° and 4.8°) were presented closer to the eye. Close-small stimulus patterns elicit more robust optomotor responses at 25 mm than constantly sized patterns presented 50 mm from the fly's eyes. When presented with the larger spatial wavelengths (13° and 26°), which were presumably easier to detect due to their more prominent peak turning responses, distance did not affect the dynamic of the optomotor behaviour. When presented a stimulus pattern (6.6°) within the range reported for causing optomotor reversal, flies did indeed turn in the opposite direction when viewing both distances. However, as increasing rotational speeds and quasi-monocular vision demonstrate, this reversal can change to the typical syn-directional rotation associated with optomotor responses. This suggests that perceptual aliasing – initiated by the global dynamics of the photoreceptor microsaccades - rather than spatial aliasing (optics) is the cause of optomotor reversal. Taken together, this shows that pattern distance is an essential predictor of optomotor behaviour, specifically when testing high spatial frequencies associated with behavioural assessments of acuity.

Chapter 3

Small object detection and discrimination in fruit flies

Abstract

Flying insects must detect and classify visual objects in their environment to respond suitably. Historically, it had been thought that because the fruit fly (*Drosophila melanogaster*) possesses somewhat coarsely faceted compound eyes, it would have comparatively limited optical acuity to accomplish this task. However, recent work suggests that ultrafast photoreceptor microsaccades enhance their eyes' spatial resolution below their optical resolution limit. By measuring the perception of gratings, behavioural responses to patterns below the optical limit have been shown (see chapter 2), but little is known about the capacity for single target acuity. Furthermore, in certain stimulus conditions, small objects trigger innate aversion in fruit flies (especially when using LED-based panoramic flight arenas). However, it is unknown whether they respond differently to small and extremely small objects in more natural conditions. Here, I investigate whether fruit flies can detect singular dark visual cues smaller than the visual field of a single ommatidium. By performing behavioural experiments on tethered flying flies at the torque meter, I found that flies have an innate attraction to a single dark object (1°) placed amongst a background of gratings (2.3° horizontal), thus, suggesting that flies classify them differently from larger objects of the same shape. When presented with a tiny 3D object (2.7°) hidden within a 2D object (3.9°) with the same area and contrast of two other 2D objects, flies found the 3D target more salient. Further results show that flies can learn to orientate towards either the 2D or 3D target but fail to learn when one eye is occluded, suggesting that the input from both eyes is required for effective small object detection. Moreover, visual detection of objects is achieved with either photoreceptor channel (R1-R6 vs R7/R8) alone but with reduced proficiency. Taken together, I show that fruit flies can behaviourally respond to extremely small singular visual cues of different depths, an ability that suggests both high acuity and binocularity for close-range behaviour.

3.1 Introduction

Despite their presumed limited spatial acuity, insects can rapidly detect and categorise visual objects in their environment to act accordingly. For example, the fruit fly detects and responds to visual signals during courtship behaviour (Willmund and Ewing, 1982) and visually detects predators to produce defensive behaviours such as evasion (de la Flor *et al.*, 2017). One proposed mechanism to aid this is innate responses to particular shapes and sizes (Maimon, Straw and Dickinson, 2008). For example, as with many other insects, long vertical objects are attractive to *Drosophila* (Reichardt and Wenking, 1969; Wehner, 1972). In contrast, small dark objects, such as circular and square LED stimuli, trigger an innate aversion response in fruit flies (Maimon, Straw and Dickinson, 2008; Theobald, 2019; Palavalli-Nettimi and Theobald, 2020). However, little is known about whether flies detect and respond differently to tiny objects smaller than a single ommatidium's visual field.

The fruit fly is an unlikely model organism for the study of extreme acuity. It is of relatively tiny stature with few ommatidia (ca. 750 per eye) and a sizeable interommatidial angle of 4.5° (Gonzalez-Bellido, Wardill and Juusola, 2011). Such optic measurements imply little to no responses to visual objects much smaller. Nevertheless, recent work suggests that fruit flies possess enhanced acuity due to photomechanical photoreceptor microsaccades (Viollet, 2014; Colonnier *et al.*, 2015; Juusola *et al.*, 2017). Indeed, Keleş and Frye (2017) found that object detecting neurons in *Drosophila* show robust responses to an object only 2.2° in size, less than half the size predicted by the optical resolution limit for detection. This is similar to other species. For example, hoverfly neurons respond strongly to dark targets as small as 0.18° even though their optical resolution limit is approximately 1° (Nordström, Barnett and O'Carroll, 2006). This paper showed that hoverfly small target motion detectors (STMDs) respond to small moving targets even when presented against a moving background, whereas previous papers had only focussed on detecting the velocity differences between the target and background (Nordström, Barnett and O'Carroll, 2006). Additionally, a biomimetic model predicts the detection of moving targets in a visual clutter (Wiederman, Shoemaker and O'Carroll, 2008). More so, robber flies have been found to intercept targets considerably smaller than the acceptance angle (Wardill *et al.*, 2017). Wardill *et al.*, (2015) show how killer flies use a matched filter ratio of a targets angular subtense and angular velocity to aid hunting their prey which is smaller than the photoreceptor acceptance angle. Acceptance angles larger than the optimal target size as found in Wardill *et al.*, (2015) is likely preferred since larger

targets which cover several ommatidia cause lateral inhibition in STMDS (Nordström, 2012; Gonzalez-Bellido, Fabian and Nordström, 2016). It is therefore unsurprising that targets subtending the size of the optics are detectable to some animals and may be more common amongst other invertebrates.

Additionally, research has highlighted that fruit flies have the neuronal capacity to re-identify individual conspecifics (Schneider *et al.*, 2018), a possibly helpful feat during courtship behaviour. This visual task requires considerable resolving power, perhaps explaining the selection pressures placed on the fruit fly for high acuity. However, the distinct evolutionary advantage for this vision remains unclear, in contrast to aerial predators with a clear behavioural need (e.g. Wardill *et al.*, 2017).

Many insects use motion parallax to perceive depth (Sobel, 1990; Kral, 2003; Kim, Angelaki and DeAngelis, 2016). In contrast, only two invertebrates have been demonstrated to use stereopsis, the praying mantis and cuttlefish (Rossel, 2002; Nityananda, Tarawneh, *et al.*, 2016; Feord *et al.*, 2020). Nevertheless, continuing from Juusola and colleagues (2017), more recent work suggests that the left and right eyes' photoreceptor microsaccades sweep mirror-symmetrically from back to front, increasing their binocularity and providing depth information about nearby visual objects (Kemppainen *et al.*, 2022). This is possible as the frontal photoreceptors' receptive fields overlap at approximately 23.5° which may provide depth perception through the combination of retinal images from both eyes (Kemppainen *et al.*, 2022). Thus, fruit flies may use motion parallax as a source of depth information for further away objects (Carbrera and Theobald, 2013) and binocularity for depth perception during close-range visual tasks (Kemppainen *et al.*, 2022) Such nearby visual tasks may include courtship behaviour where for example females require sufficient visual stimulation (i.e. the red eye of the male) in order to become maximally sexually receptive (Willmund and Ewing, 1982).

Given the assumptions that photoreceptor microsaccades facilitate extreme acuity and binocularity for close-range behaviour, I hypothesise that fruit flies can detect small objects smaller than their optical limit and discriminate between objects of slightly different depths. On the other hand, if fruit flies cannot detect single objects of this size, this could indicate that single target acuity is not as high as grating acuity in fruit flies. In this work, I aimed to determine: **(1)** can fruit flies behaviourally respond to small ($1-4^\circ$) 2D and 3D singular objects? **(2)** do flies continue to find small dots aversive when this small? **(3)** does this require binocular

vision? (4) and are all photoreceptors contributing? I show that: (1) fruit flies do respond in the presence of a single target, changing their orientation from a predominantly arbitrary heading to a more biased direction, (2) this heading is towards the object, suggesting an attraction to the single most salient feature, (3) with one eye occluded the flies cannot discriminate between the 2D and 3D patterns in learning experiments, and (4) do not perform as well with either photoreceptor channel switched off, but still respond robustly to the stimuli.

3.2 Materials and Methods

3.2.1 Experimental animals

Wild type Berlin (WTB) *Drosophila* and visual mutants were prepared before the experiments, as described in Chapter 2. Adult females 3-10 days after eclosion were used in these experiments. Monocular flies were painted as previously described.

Mutant flies included Rh1-rescue *norpA*³⁶ flies (provided by Chi Hon Lee, Academia Sinica, Taiwan), which express blue-green-sensitive Rh1-rhodopsin which is present in the outer receptors only. These flies therefore sample with the outer retinula cells (R1-R6) but not with the inner cells (R7/8) to test how well the outer receptor channel alone enables the underlying hyperacuity observed by Juusola et al., (2017). In contrast, *ninaE*⁸ and Rh3-6 flies (provided by Chi Hon Lee) have functional R7/8 cells but not outer cells. R7 receptors express UV-sensitive Rh3 (R7 pale) or Rh4 (R7 yellow) while R8 cells express either blue sensitive Rh5 (R8 pale) or green sensitive Rh6 (R8 yellow) (Sharkey *et al.*, 2020). This is to test whether inner photoreceptor play a contributing role in hyperacute vision and so we inhibited input from the R1-R6 photoreceptor channel.

Two blind mutants were used as a control, *hdc*^{JK910} and *norpA*^{P24} rescue flies (provided by Roger Hardie, University of Cambridge). Blind *hdc*^{JK910} mutant photoreceptors have normal phototransduction but cannot synthesise histamine (their neurotransmitter), making them perceptually blind. Consequently, electroretinograms (ERGs) lack On- and Off-transients associated with synaptic information transfer to interneurons. Blind *norpA*^{P24} mutants have faulty phospholipase-C molecules, which halts phototransduction PIP₂ activation and therefore shows no electrical response to visible light. These blind mutants were used to test whether the results were due to vision, and validate that other cues such as olfaction were not influencing the results.

3.2.2 Single object detection in fruit flies

In the first experiment, I investigated whether *Drosophila* can perceive objects smaller than the interommatidial angle using negative contrast stimuli (dark stimuli on a bright background). Flies were presented a small black 2D dot (1°) placed amongst a panoramic stripe scene of dark and light gratings (2.3° horizontal) (Fig. 3.1A and B). Their yaw torque signals, indicating visual orientation behaviour, were recorded over 8 min of closed-loop flight, i.e. the fly controlled the arena position as its yaw torque was measured and feedback to the motor spinning the arena. In the first trial, the single target was placed centrally (vertically and horizontally) amongst a single light bar within the centre of the visual scene; this ensured a 180° distribution between the target and the paper-join (ends of the paper). To understand whether the paper-join was influencing orientation behaviour, I did additional stimuli moving the dot's location relative to the paper-join. In these trials, the single target was positioned either to the left or right of the centre by 90° . In addition, gratings with the dot absent were used as a control. Thus, there were four different visual stimuli presented to the animals: 'central dot' (0°), 'left dot' (-90°), 'right dot' (90°) and 'no dot' (control). The start position of the dot stimulus was randomised by 5 sec of open-loop bi-directional rotation at the initiation of the trial to ensure that all flies were not immediately facing the target. Each fly was presented the stimuli consecutively and in a randomised order.

3.2.3 Combining 3D with 2D visual cues

For experiment 2, to understand whether *Drosophila* can discriminate small objects with different depths, flies were presented with three black 2D dots (3.9°), one of which had a "camouflaged" 3D black pin (2.7°) placed within its centre. This dot size was chosen to provide sufficient coverage around the pin but remained below the optical resolution limit. The dots were visual features in an otherwise uniform white background (plain paper) (Fig. 3.1C and D). Flies were tested with the pin placed on either the central dot ('central pin', 0°), left dot ('left pin' -90°) or right dot ('right pin' 90°) to investigate whether flies responded differently to the 2D dot with the 3D pin. The pin was 4 mm long from the tapered tip to its base. Thus it was approximately 21 mm from an individual's fly's eyes to the pin tip, compared to the 25 mm to the 2D dots. Crucially, during the arena rotations generated by the fly, the pin continually pointed towards the arena centre (and fly). Thus, no subtended angles made the pin more visible to the fly, i.e. the pin was always viewed (relative to the fly) directly within the centre of the dot, even when its physical position moved rotationally. Thereby, if the fly can detect the presence of the 3D pin, it would have to use the increased binocularity due to the left

and right eye photoreceptor microsaccades. The experimental protocol was identical to Experiment 1. Individuals were recorded over 8 min of closed-loop unconditioned flight, with four different visual stimuli presented to the fly consecutively and presented in random order.

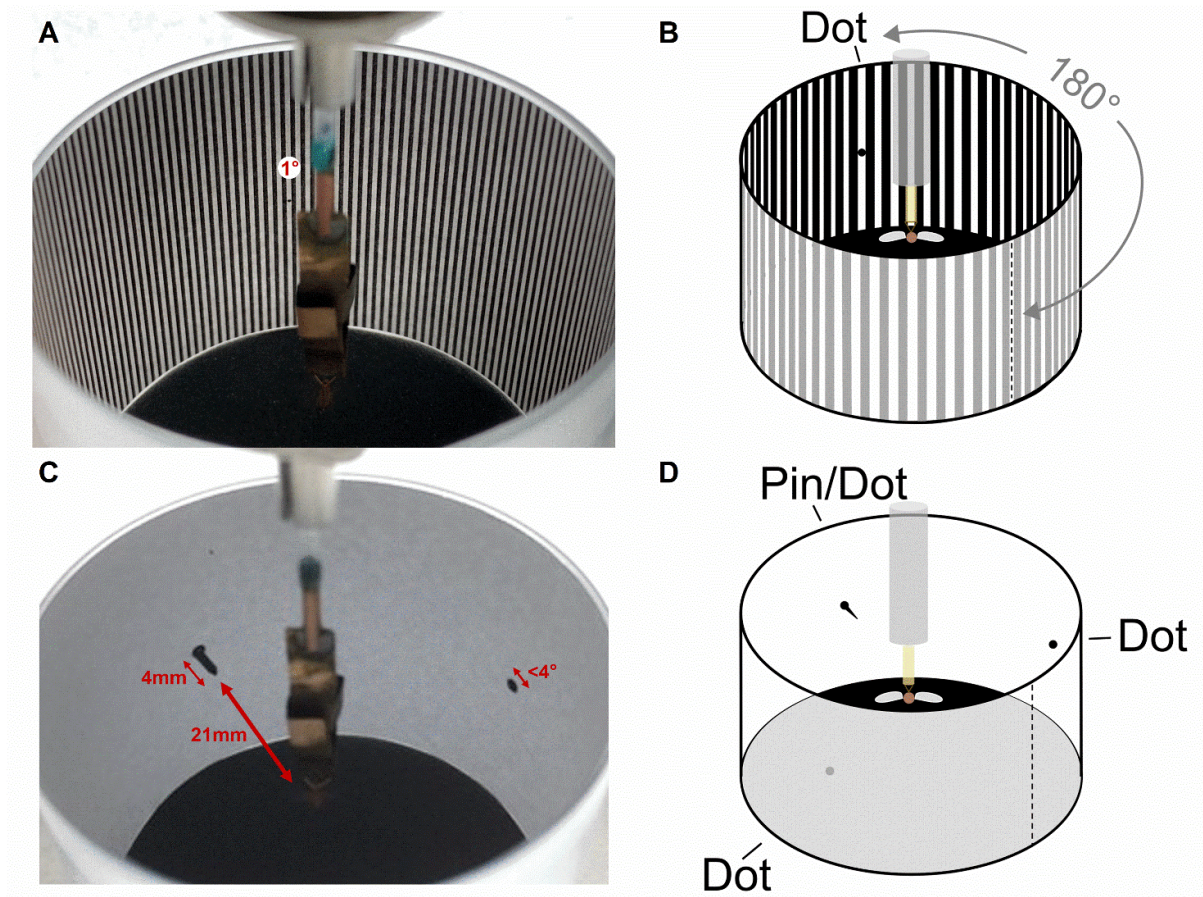


Fig. 3.1 Single object experiments.

(A, C) A fruit fly tethered at the torque meter within the flight simulator and (A) presented a small singular black dot (1°) placed centrally within a light bar amongst dark and light bars (2.3°). (C) A 4 mm black pin (2.7°) is placed centrally amongst one of three dots with a 90° distribution. (B, D) Schematic illustration of (B) the dot and (D) pin experiment.

3.2.4 Small pattern learning

This behavioural assay is based on previously described work investigating operant learning of *Drosophila* at the torque meter (Brembs, 2008). The test was an 18 min assay presenting a constant pattern over nine 2 min stages running sequentially. The fly's yaw torque is used to control the angular position of the patterns. The experiment delivers heat punishment

(unconditioned stimulus, US) with an laser to the fly's head when presented with the conditioned stimulus (CS). The laser was positioned 150 mm from the fly, placed 45° vertically and 25° horizontally to the left of the fly's centre. This was done in accordance with previous learning experiments (personal communication, Narendra Solanki). The laser delivers pulses (~200 msec pulse width at ~4 Hz) when the fly is within the quadrant of the CS, this intensity of the beam is reduced to ensure the fly can survive. In that case, the tested *Drosophila* should learn to orientate away from the conditioned stimulus associated with heat (CS+) and instead fly towards the "safe" stimulus (CS-).

During the pre-training (stages 1 and 2), the fly receives no reinforcement, and any naïve preference for one pattern can later be determined. During training (stages 3, 4, 6 and 7), the computer turns on the heat when one of the patterns is in the frontal visual field of the fly. During the test stages (stages 5, 8, 9), the fly receives no reinforcement, and we test the fly's pattern preference for the CS- following heat punishment. Between every 2 min stage, the scene is rotated bi-directionally for a random duration lasting 5 s overall. This manoeuvre randomises the starting position of the panorama for each stage relative to the fly's orientation.

I tested the learning performance index (PI) for three different visual stimuli (**Fig. 3.2**) presented in a random order, two hyperacute tests incorporating 3D and 2D objects and a 2D pattern control. The control was the classic 'T-shaped patterns', which have been well described for eliciting pattern learning (Wolf and Heisenberg, 1991; Dill, Wolf and Heisenberg, 1993, 1995; Dill and Heisenberg, 1995; Liu *et al.*, 1998, 1999, 2006). This pattern consists of four black T-shaped patterns measuring 40° vertically and 40° degrees horizontally; the bar width was 10° wide. There were two pairs of each type of pattern within the visual scene for each stimulus (i.e. two upright and two inverted). Therefore, identical patterns (i.e. both upright Ts) were placed in opposing quadrants at 180° apart (from the midline of the pattern), with a 90° separation between each pattern around the arena wall. For both hyperacute stimuli, I used the same 3D object as previously described in Chapter 3. First, four black 2D dots (3.9°) separated by 90°, two of the dots had the 3D object placed within them. So as with the alternating T-patterns, the dots alternated either with or without the 3D object. Second, an identical approach but now using vertical stripes (horizontal 3.9°, vertical 38°) with or without the 3D object present.

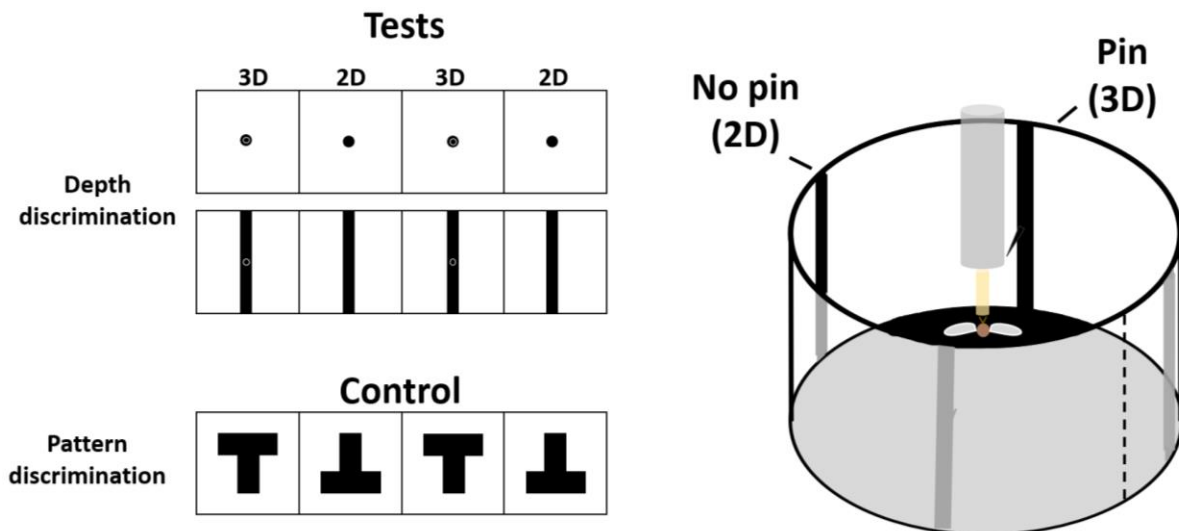


Fig. 3.2 Visual learning experiments.

(A, B) Schematic illustration of the (A) visual stimuli presented to the fruit flies, (top) test stimuli includes (upper) a dot stimulus (3.9°) and (lower) a stripe stimulus (horizontal width 3.9°). In each, four black patterns (90° separation) are presented to the fly with two pins (3D objects) placed within alternating quadrants (180° separation). (bottom) The control stimulus is the classic T-pattern with alternating upright and inverse T-shaped patterns. (B) A fly views the stripe stimulus with a pin, either present or absent.

Under software control, the scene was divided into four 90° quadrants aligned centrally with each physical pattern of the arena. The laser automatically turned on or off depending on which quadrant the CS+ was within. This switching occurred whenever the fly rotated the scene, crossed the invisible boundary from one quadrant, and entered another. Which pattern was the designated CS+ was randomised, although an effort was made to have both patterns the CS+ a broadly equal amount of times. The heat punishment was provided to the fly's head with a pulsating infrared laser (825 nm, 150 mW), guided using a piezo 3-axis micromanipulator (Sensapex, Finland), directed from above (degrees) and slightly off centre (degrees) from directly in front of the fly.

In contrast, traditionally, the heat punishment for this behavioural assay has been delivered from behind onto the head and thorax of the fly (Wolf and Heisenberg, 1991; Dill, Wolf and Heisenberg, 1993; Tang *et al.*, 2004). This approach provided a higher PI score when a few control flies were tested with this method (Fig. S8). This finding suggests that heat punishment from behind delivers a more potent unconditioned stimulus. Regardless, throughout the learning experiments, I delivered the punishment from ahead of the fly. This choice was due to

the rigid setup of the flight simulator system, meaning the best way to minimise additional visual cues, e.g. experimenter activity and external light sources surrounding the faraday cage, was to have a fly facing inwards i.e. towards the laser. Despite previous work showing higher PI scores, the comparison between groups within these experiments is valid since I use the same approach consistently.

3.2.5 Deep pseudopupil imaging

For Rh1-rescue *norpA*³⁶ flies, electroretinograms (ERGs) and deep pseudopupil imaging (performed by Joni Kemppainen) were undertaken immediately after the learning experiment. The deep pseudopupil imaging unexpectedly showed substantial variations in the photoreceptor microsaccade size of some individuals between their left and right eyes. This discovery highlighted that sometimes the mutants showed no lateral (sideways moving) photoreceptor microsaccades in one of their eyes (~10%). Of the 97 flies tested in the flight simulator (dots: 30; stripes: 30; t-patterns: 37), five escaped after behavioural assessment and before the eye could be imaged (stripes:1; t-patterns: 4), and a single fly (stripes) had no saccade movement in either eye. It is unclear why this fly had no saccade movement, yet it is likely due to development errors occurring in photoreceptor pivoting and anchoring for the Rh1-rescue *norpA*³⁶ genotype (Kemppainen *et al.*, 2022). Regardless, this phenomenon was helpful as it allowed me to categorise the flies into two additional subgroups (binosaccades and monosaccades) for analysis (see below).

3.2.6 Data analysis

All data collection and stimulus procedures were performed using custom-written MATLAB software. During the single object experiments, the panorama's position relative to the fly's fixed orientation was measured at 1 kHz and then given as the mean fixation probability. The optimal bin size was determined using Sturges' rule (Sturges, 1926) ($k = 1 + 3.22 \log(n)$) for visualisation of the distribution. This rule gave an optimal number of 15 bins, giving a bin width of 24°. I rounded down to 20° bin widths over 18 bins for visual clarity. The thin (hyperacute) paper-join seemed to affect fly behaviour with varying levels of attraction, which suggested it was an unexpected visual cue.

To compare whether flies preferred to fly towards the single dot or pin stimulus, I analysed each experiment in three $\pm 90^\circ$ bins from the object. These bins were the "left" section (-180° to 0°), the middle section (-90° to 90°) and the right section (0° to 180°). The mean probability within each bin was then compared to determine whether the section with the dot had a

statistically higher mean. For example, the central pin stimulus places the pin at 0° in the centre of the middle section (-90° to 90°). The two empty dots, meanwhile, are at -90° and 90° . Thus, they are placed within the centre of the left section (-180° to 0°) and right section (0° to 180°), respectively. I predicted the larger bin size (i.e. $\pm 90^\circ$) would be required to determine whether any preference was shown to the single object. Indeed, if the fly were to detect the visual cue, it is such a small cue that the behavioural response would likely not be sufficient with a smaller bin size, e.g. $\pm 25^\circ$. In contrast, I used $\pm 30^\circ$ bins to directly compare behaviour within a narrower range to compare the salience of the single dot or pin.

Each tethered fly had a combined flight time of 32 min when considering all four 8 min stimuli, so some experienced flying problems. These interruptions were easily observable and characteristic as a fly stopped flying and either dangled or erratically moved its legs. Struggling animals were encouraged to fly again with air blows while the trail was paused. Otherwise, the trial was stopped for the few that experienced reoccurring flying problems (i.e. stopped flying >5 times during a 2 min stage), and the fly was excluded from the dataset. Most typically, flies in the dataset experienced no flying problems during the experiments.

In learning experiments, I analysed the performance index (PI) for each of the 2 min stages. Performance indices were automated and recorded per millisecond in the computer storage. The performance index was calculated as the time the fly selected to orientate towards the CS+, minus the time the fly selected to orientate towards the CS-, divided by the total experiment time. Scores ranged from 1.0 (at all-times orientating towards the CS-) to -1.0 (at all-times orientating towards the CS+). Flies that spent an equal amount of time facing each pattern received a score close to 0. Which pattern was the designated CS+ was alternated for each new fly, thereby making each pattern the CS+ a broadly equal amount of times.

Theoretically, the fly should have no naïve preference to either pattern during the initial stages (pre-training). However, it has previously been shown that flies sometimes demonstrate a naïve preference for the inverted T pattern over the upright T (Dill and Heisenberg, 1995; Solanki, Wolf and Heisenberg, 2015). Consequently, since experiment 2 shows voluntary orientation towards the pin, a naïve preference may be shown during the pre-training phase, whereas, during training the fly should actively avoid the heat punishment and produce a robust positive PI. For stage 5, the initial test, it is expected that the fly should now produce a positive score, having experienced the first two phases of training. However, we found that performance for this stage varied immensely between subjects. If the fly can see the patterns as expected during

the test stage, we predict a positive learning score, though not as strong as during the training stages.

For the Rh1-rescue *norpA*³⁶ flies with varying photoreceptor microsaccades, the data is analysed first as the whole population of flies, whose microsaccade category was unknown at the time of behavioural experiments. Second, the ‘binocular microsaccade’ flies, with normal R1-R6 phototransduction and symmetrical microsaccades globally across both eyes. Finally, ‘monocular microsaccade’ flies with normal R1-R6 phototransduction but faulty microsaccades in one eye, producing asymmetrical monocular microsaccades. Therefore, a comparison could be drawn between normal or faulty microsaccadic movement and performance index during learning experiments.

3.2.7 Statistics

All statistical tests were performed using SPSS (IBM SPSS Statistics 26). Tests for normal distribution were performed using the Shapiro-Wilk test. To test whether the mean fixation within each section was statistically different during the single object experiments, I used either an independent samples t-test or a one-way ANOVA with Tukey’s post hoc test where appropriate.

In learning experiments, many flies exhibited varied and arbitrary preferences during the first test phase (stage 5) compared to the following phases (stages 8 and 9). To ensure that comparisons were made during the most reliable phase of the experiment as to whether a fly learnt or not, I focussed on Stage 8 alone for statistical evaluation as it was the first stage after all the training phases had been completed and before the performance would reduce due to waning memory in stage 9. Therefore, the performance of the fruit flies during a single performance index (Stage 8) was statistically compared against zero using a two-tailed one-sample t-test for each stimulus within the same group of flies.

To test whether the performance indices for the dot and stripe stimuli differed from the control stimulus within a group, I used a one-way ANOVA with Dunnett’s *post hoc* test. An independent samples t-test or a one-way ANOVA with Sidak’s *post hoc* test compared the performance indices between fly groups. I used a chi-square test to compare the number of flies with a performance index high than 0.1 in stage 8. During the initial phases (stages 1 and 2), many flies showed less than 0.1 or -0.1, i.e. equal preference. Thus, I designated a score higher than 0.1 to indicate a trained bias for the CS-.

3.3 Results

3.3.1 A small single visual cue

The yaw torque of the animals was recorded in the flight simulator to study the spatial resolving power of fruit flies in respect to a single tiny target (**Fig. 3.3**) when presented with a black dot within gratings as the only visual cue. This experiment builds on the relatively simple optomotor behaviour by exploring the visual perception of the fly. Many flies maintained a weak attraction for heading towards the stimulus without reinforcement. When presenting the dot 180° from the paper-join (central dot), the fruit flies kept attempting to centre the dot within the frontal visual field, as shown by the mean fixation (**Fig. 3.3B**). Indeed, when the middle region (-90° to 90°) is compared to the control, it differs significantly (Independent-sample t-test: $t(38) = 4.29$, $P \leq 0.001$; **Fig. 3.3G**). Typically, it was observed that flies continuously changed heading direction but would repeatedly return towards the small dot and perform small saccadic behaviour on either side of the stimulus. Saccadic behaviours (rapid high angular velocity turns) are a common feature of tethered flight at the torque meter, as flies do not hold the scene immobile or turn it smoothly (Brembs and Heisenberg, 2000). On the other hand, many flies would perform anti-fixation behaviour and fly towards the paper-join.

Next, to investigate whether fruit flies were biased by unknown visual cues or stimulus location within the system, the stimulus's position was shifted by 90° relative to the paper-join to the left (left dot) and right (right dot). Similar to the central dot, fruit flies often changed direction but would return to the dot stimulus located at the left (**Fig. 3.3A**) (Independent-sample t-test: $t(38) = 2.58$, $P = 0.014$; **Fig. 3.3F**). In contrast, the right dot stimulus (**Fig. 3.3C**) did not differ significantly from the control for the right section (0-180°) (Independent-sample t-test: $t(38) = 1.77$, $P = 0.084$; **Fig. 3.3H**). Nevertheless, flies predominantly kept an orientation to the right when the right dot was present (blue bar, **Fig. 3.3E**). Many flies maintained arbitrary headings throughout their flight when the singular visual cue was absent (no dot; **Fig. 3.3D**). However, it does show a peak between the paper-join and -90°. This finding suggests that the flies kept a chosen direction close to the paper-join when it was the only cue.

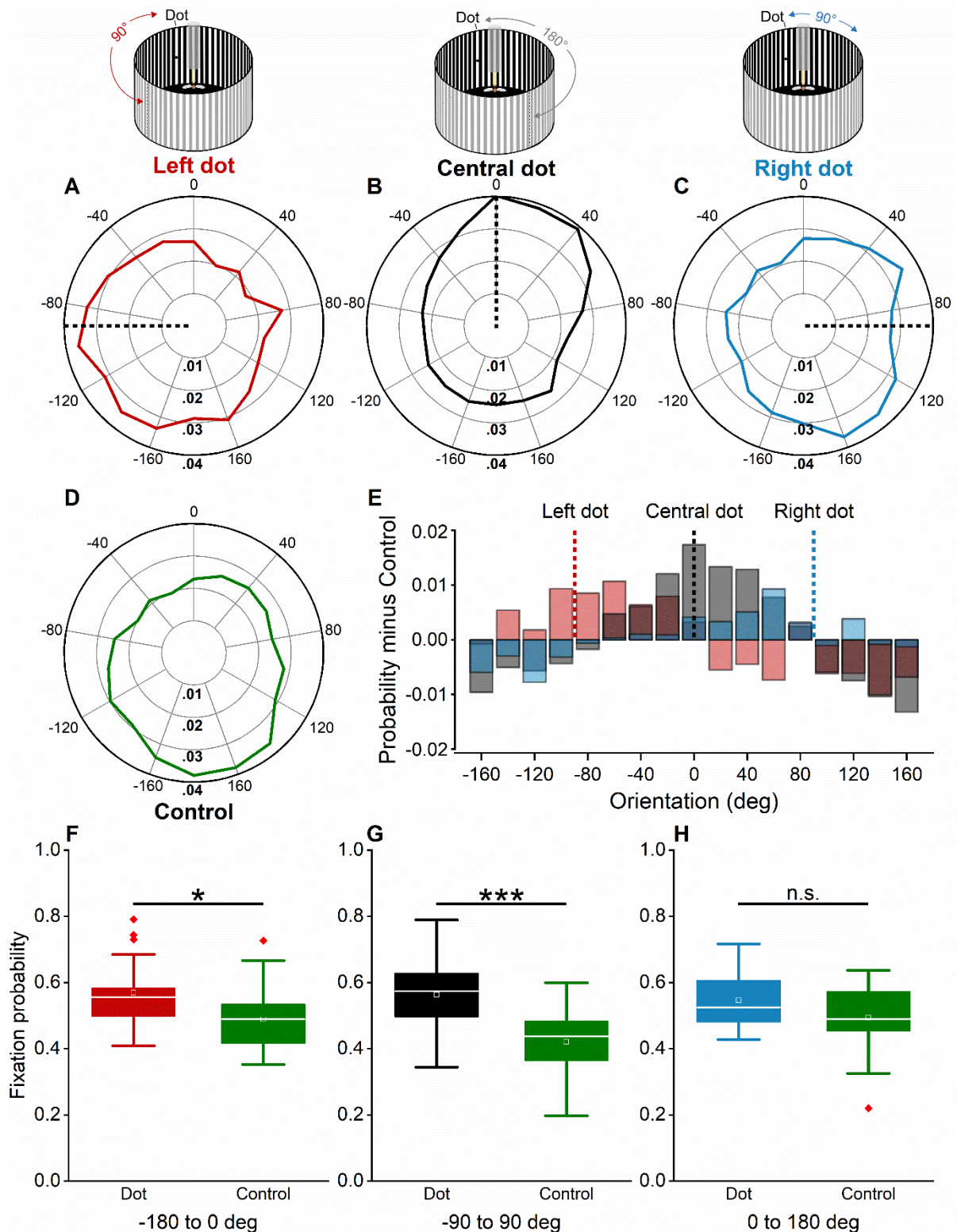


Fig. 3.3 Detecting and using a singular small visual cue to direct orientation.

The mean fixation probability of 8 min flights of tethered *Drosophila* ($n = 20$) presented with a small black dot (1°) placed centrally within the light bar of a panorama of gratings (2.3°), providing a singular visual cue in an otherwise homogeneous scene. **(A-C)** The flies' flight direction relative to the dot located at the **(A)** left, **(B)** central or **(C)** right position (relative to

the paper-join). The black dotted line shows the dot location. **(D)** The gratings are presented with the dot absent as a control. **(E)** The means of the left (red), central (black), and right (blue) dot locations have the mean of the control subtracted. The data shows that when the dot is present in a region, the flies prefer to orientate in that general direction. The coloured dotted lines represent the dot location for each stimulus. **(F-H)** Boxplots show that flies statistically prefer the left region (**F**, red box) and central region (**G**, black box) with the dot present, but this did not differ significantly for the right section (**H**, blue box). Boxes indicate the 25-75% interquartile range, the white line indicates the median, the white box is the mean, whiskers represent the entire data spread, and red diamonds represent outliers. Asterisks indicate the level of significance: * $P < 0.05$, ** $P < 0.01$, *** $P < 0.001$ and n.s. not significant. Means are calculated over 20° bins.

The slight preference for heading towards the dot stimulus suggests that fruit flies can detect single objects smaller than the optical resolution limit and find dots this small attractive. However, the behavioural response is not robust enough to suggest a strong attraction, as found for vertical stripes (Heisenberg and Wolf, 1979).

To investigate whether flies were changing direction regarding the dot stimulus being located in different arena sections (relative to the paper-join), I analysed the mean orientation for each section for each stimulus (**Fig. 3.4**). A two-way ANOVA revealed a significant interaction between stimulus position and arena section, $F(4, 171) = 12.49$, $P \leq 0.001$. The central dot stimulus was statistically different as shown by a Tukey *post hoc* test between the central region (with the dot) and left region ($P = 0.023$) but not with the centre and right regions ($P = 0.984$). When comparing the central section between all three stimuli, flies preferred to fly in this direction when the dot was present although this was not statistically different (Central dot vs left dot, $P = 0.096$; central dot vs right dot ($P = 0.071$); **Fig. 3.4 middle box of all plots**).

When the dot was located at the left region (i.e. left dot stimulus), i.e. -180° to 0° , the flies preferred to fly in the general direction of the dot. This was not significant against the middle section (Post-hoc Tukey: $P = 0.055$) but it was statistically different against the right section (Post-hoc Tukey: $P = \leq .001$). This finding was confirmed when comparing the left section for all three stimuli (**Fig. 3.4 left box of all plots**). There was a clear preference for the left section when the dot was present rather than absent (Post-hoc Tukey: left dot vs central dot ($P = 0.012$); left dot vs right dot ($P \leq 0.001$)).

Similar to what was observed with the left stimulus, *Drosophila* preferred to fly in the arena section with the dot for the right stimulus, though whether there a significant difference was inconsistent. There was no significant difference when comparing against the central region (Post-hoc Tukey: $P = 0.258$) but there was an effect when comparing against the left (Post-hoc Tukey: $P = 0.019$) regions. The right region of the right stimulus did not differ with statistical significance as shown by a tukey post hoc from the central dot ($P = 1.00$). However, there was a clear difference compared to the left stimulus ($P \leq 0.001$). **Fig. 3.4 right box of all plots**). These results confirm that (i) the flies can perceive the small visual cue and (ii) use that information for choosing a general flight direction in the flight simulator, possibly as it provides a reference point (or landmark) within the highly artificial environment.

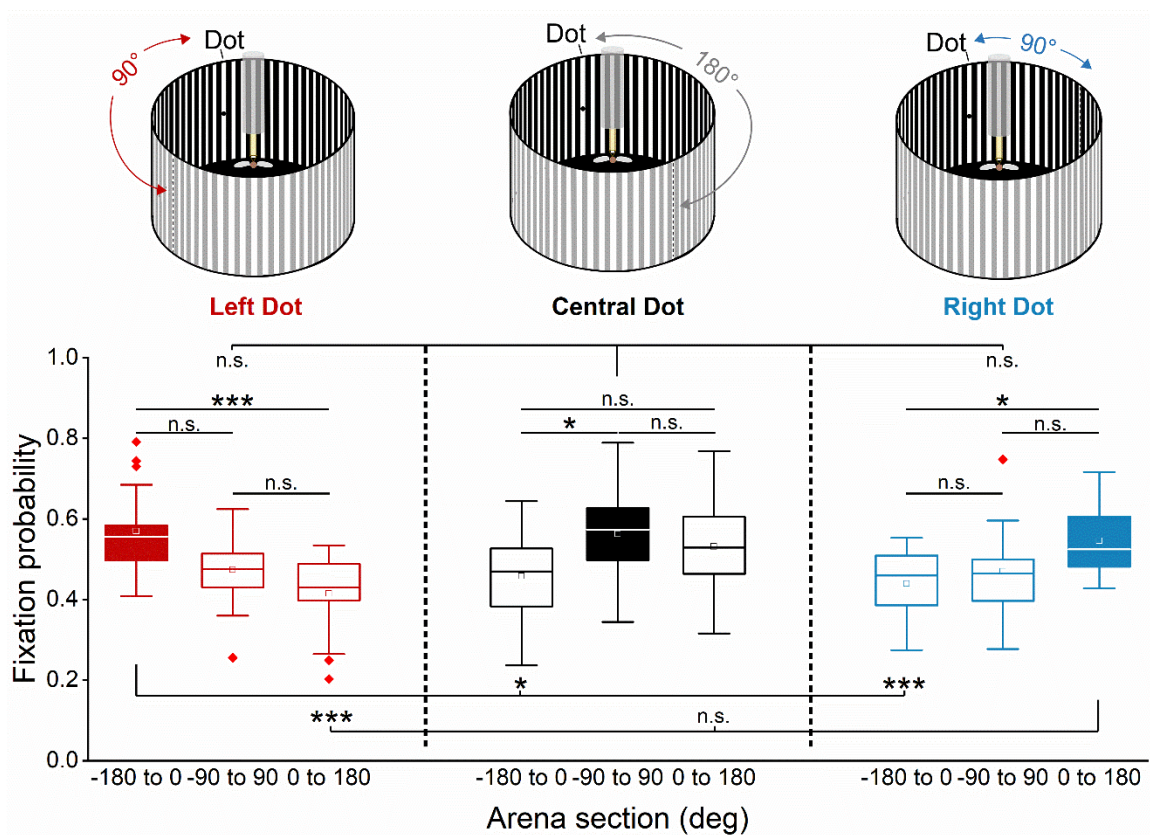


Fig. 3.4 Effect of dot position on orientation preference.

The fixation behaviour of fruit flies ($n = 20$) viewing a small dot indicates a bias towards the single object when presented towards the left (boxes outlined in red), central (boxes outlined in black) and right stimulus (boxes outlined in blue). Shaded boxes indicate the dot location in each stimulus (left, red box; centre, black box, right, blue box). Boxes indicate the 25-75% interquartile range, the red line indicates the median, whiskers represent the entire data spread, and red diamonds represent outliers. Asterisks indicate the level of significance: * $P < 0.05$, ** $P < 0.01$, *** $P < 0.001$, n.s. not significant. Shaded boxes are replotted from Figure 3.3 F, G and H. Means calculated over 180° bins.

3.3.2 The use of a small depth cue

The tested flies' mean fixation probability was investigated to analyse whether a single 3D object was detectable and more salient than multiple 2D objects (**Fig. 3.5**). When presenting the pin 180° from the paper join (central dot) within the middle dot, *Drosophila* kept attempting to centre the pin by repeatedly returning towards the pin and performing saccadic behaviour on either side of the 3D object (**Fig. 3.5B**). When the middle region (-90° to 90°) is compared to the control, it differs significantly (Independent-sample t-test: $t(38) = 4.89$, $P \leq 0.001$; **Fig. 3.5G**). Similar to the central pin, fruit flies often changed direction but would return to the pin's position when found at the left arena section (-180° to 0°) (**Fig. 3.5A**) (Independent-sample t-test: $t(38) = 2.33$, $P = 0.025$; **Fig. 3.5F**) as well as the right section (0° to 180°) (**Fig. 3.5C**) (Independent-sample t-test: $t(38) = 5.57$, $P \leq 0.001$; **Fig. 3.5H**).

A slight preference is shown for the single pin object as with the single dot. This finding suggests that they can detect the changing depth of the pin and find it more salient. A possible interpretation is that the fly's motivation is to attempt to escape the artificial environment and tether (Solanki, Wolf and Heisenberg, 2015). The pin perhaps is chosen as the best direction, viewing it as a landing site.

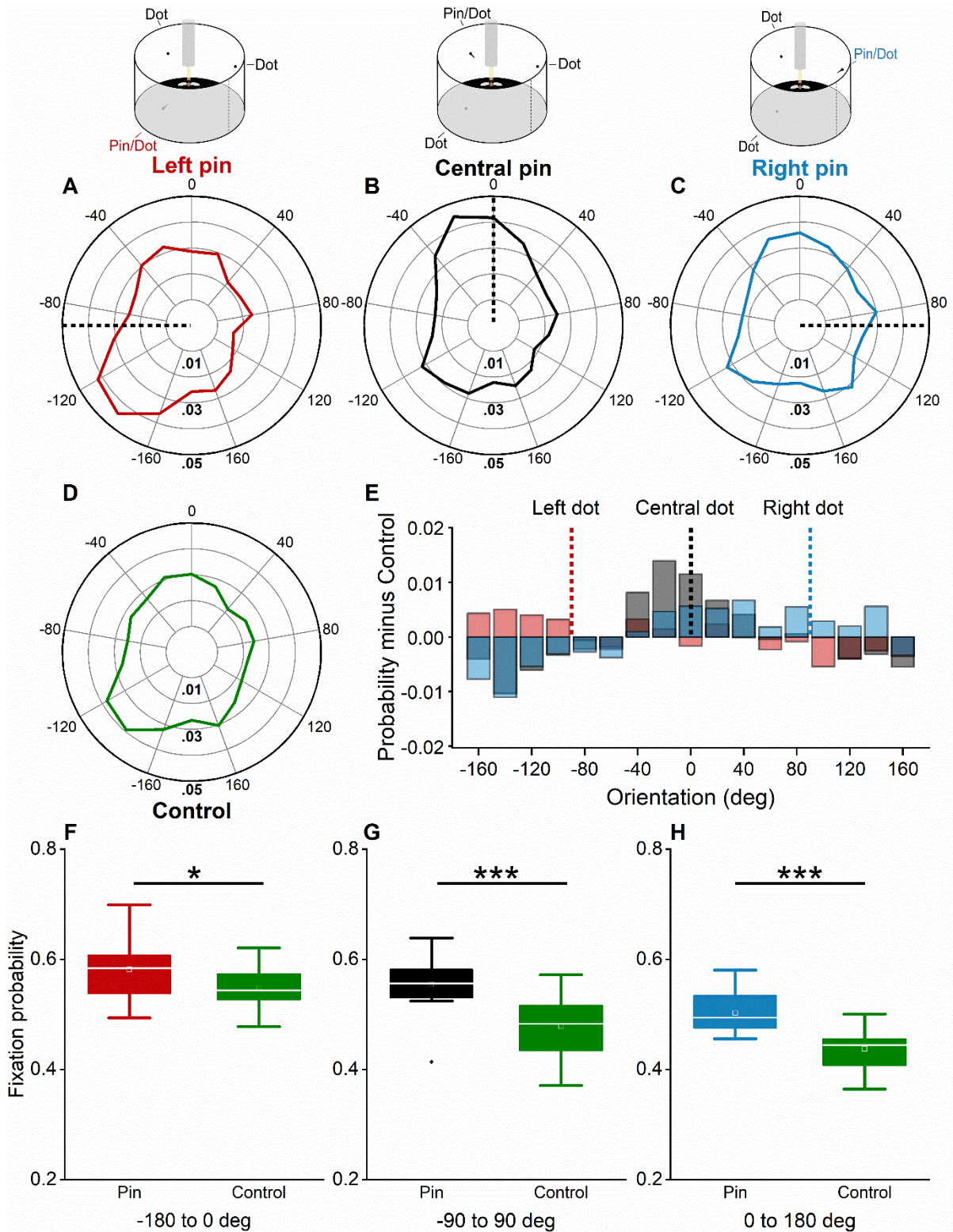


Fig. 3.5 Using a subtle depth cue within small objects for orientation.

The mean fixation probability of 8 min flights of tethered *Drosophila* ($n = 20$) presented with a 4mm black pin (2.7°) placed within the centre of one of three (90° separation) black 2D dots (3.9°). Presenting a singular depth cue amongst multiple visual cues. The flies' flight direction relative to the pin located at the (A) left, (B) central or (C) right position (relative to the paper-

join). The black dotted line shows the pin location. **(D)** No visual cues are presented as a control. **(E)** The means of the left (red), central (black), and right (blue) pin locations have the mean of the control subtracted. The data shows that when the pin is present in a region, the flies prefer to orient in that direction. The coloured dotted lines represent the pin location for each stimulus. **(F-H)** Boxplots show that flies statistically prefer the left **(F, red box)**, central **(G, black box)** and right region **(H, blue box)**. Boxes indicate the 25-75% interquartile range, the white line indicates the median, whiskers represent the entire data spread, and red diamonds represent outliers. Asterisks indicate the level of significance: * $P < 0.05$, ** $P < 0.01$, *** $P < 0.001$ and n.s. not significant. Means are calculated over 20° bins.

To compare the fruit flies' orientation preference between the changing pin positions, I analysed the mean fixation probability for each stimulus (**Fig. 3.6**). A two-way ANOVA revealed a significant interaction between stimulus position and arena section, $F(4, 171) = 20.43$, $P \leq 0.001$. The central dot stimulus was not statistically different as shown by a Tukey *post hoc* test between the central region (with the pin) and left region (dot only) ($P = 0.754$) but it was significant with the centre and right regions ($P \leq .001$). When comparing the central section between all three stimuli, flies preferred to fly in this direction when the dot was present, this was statistically different for the central dot vs left dot, $P \leq 0.001$ (Post-hoc Tukey) but not against the right dot (Post-hoc Tukey: $P = .354$). **Fig. 3.6 middle box of all plots**). These findings suggest that fruit flies favour the dot with the pin present, although often the flies show an arbitrary preference to the three dots, so the mean fixation preferring the pin is not robust.

When the pin is positioned to the left, i.e. -180° to 0° , the flies preferred to orient towards the left section compared to the central section (Post-hoc Tukey: $P \leq .001$) and right section (Post-hoc Tukey: $P \leq .001$). As with the left dot, this preference was reaffirmed when comparing the left section for all three stimuli (**Fig. 3.6 left box of all plots**). There was a clear preference for the left section when the dot was present rather than absent (left vs middle, Post-hoc Tukey: $P = .035$; left vs right, Post-hoc Tukey: $P \leq .001$).

In contrast, the right pin did not differ significantly between the sections (**Fig. 3.6 right plot**) when testing against the middle section (Post-hoc test: $P = .962$) and left section (Post-hoc test: $P = .997$). When comparing the right region with the pin present or absent, there was no statistical difference against the middle pin (Post-hoc test: $P = .208$) but there was against the left pin (Post-hoc test: $P \leq .001$) (**Fig. 3.6 right box of all plots**).

This finding indicates that while the right section did not attract the highest mean fixation during the right stimulus, it nevertheless had the highest fixation when comparing this section between the three different stimuli. Thus, this still suggests a preference to fixate the pin in all positions. As with the dot visual cue, this result suggests that it is the singular object that fruit flies generally choose to orientate towards, somehow deciding that this singular piece of visual information is more critical for choosing heading directions.

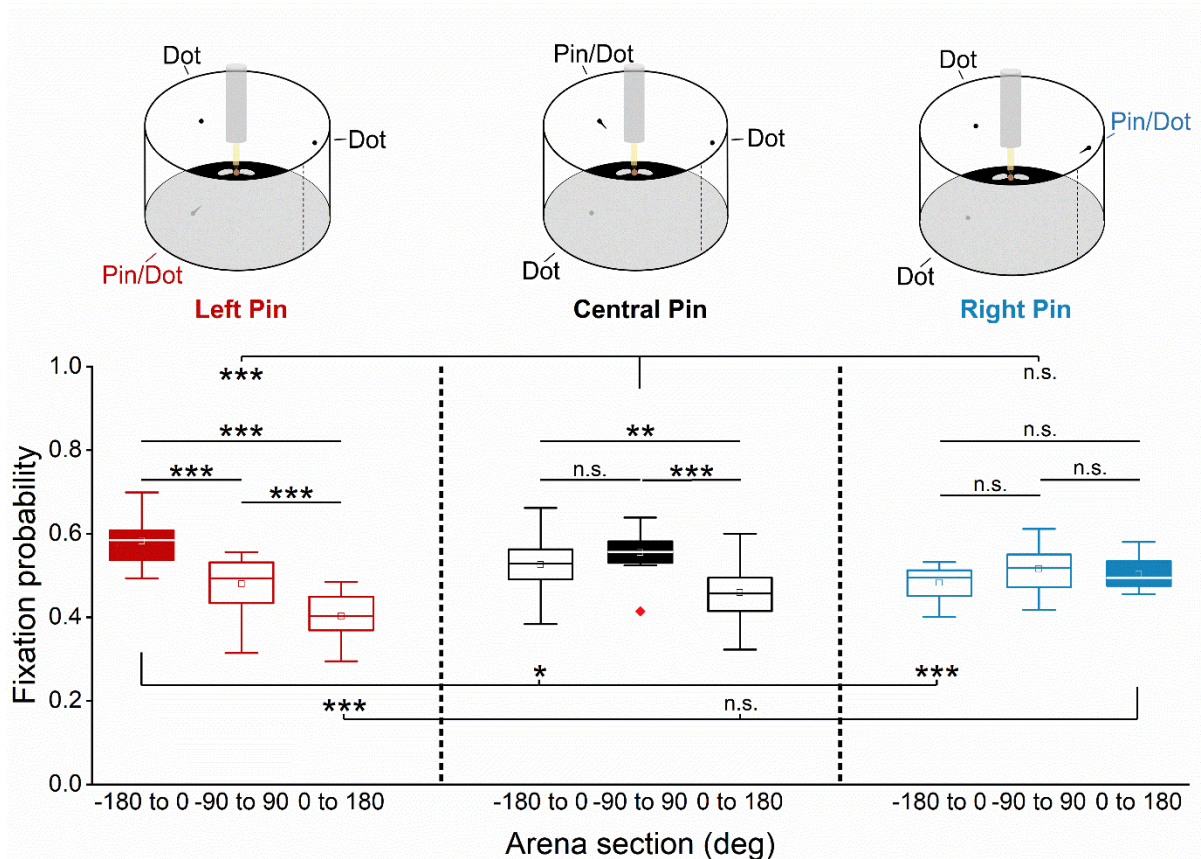


Fig. 3.6 Effect of pin position on orientation preference.

The fixation behaviour of fruit flies ($n = 20$) viewing a small pin and two dots indicates a bias towards the pin when presented towards the left (boxes outlined in red), central (boxes outlined in black) and right stimulus (boxes outlined in blue). Shaded boxes indicate the dot location in each stimulus (left, red box; centre, grey box, right, blue box). Boxes indicate the 25-75% interquartile range, the red line indicates the median, whiskers represent the entire data spread, and red diamonds represent outliers. Asterisks indicate the level of significance: * $P < 0.05$, ** $P < 0.01$, *** $P < 0.001$, n.s. not significant. Shaded boxes are replotted from Figure 3.5 F, G and H. Means calculated over 180° bins.

3.3.3 Preference for single 2D and 3D small visual cues

To characterise fixation performance in the presence of either the single dot cue or single pin cue, I compared the dot (**Fig. 3.3**) and pin (**Fig. 3.5**) data together to analyse the performance (**Fig. 3.7**). When plotted together (**Fig. 3.7A to F**), the traces suggest a robust similarity in the salience of the respective objects. Visually, the most striking difference is for the right stimulus (**Fig. 3.7A**), which show a peak in the central section for the pin stimulus (blue), which is absent in the dot stimulus (red). This is most likely due to the empty dot present within this section for the pin stimulus, which is absent for the dot stimulus.

The mean fixation probability does not significantly differ when the flies were presented with either visual cue for the left (Independent-sample t-test: $t(38) = 1.95$, $P = 0.06$; **Fig. 3.7G**), central (Independent-sample t-test: $t(38) = -0.88$, $P = 0.38$; **Fig. 3.7H**) and right stimulus (Independent-sample t-test: $t(38) = 1.43$, $P = 0.16$; **Fig. 3.7I**). This suggests that both cues are equally salient, indicating high acuity and binocularity in fruit flies.

3.3.4 Constant orientation throughout the flight

The mean fixation remained relatively constant when tested with dot stimuli throughout the flight time. This was indicated as there was no statistical difference for any of the four 2-min phases for the left dot (One-way ANOVA: $F(3, 76) = 0.17$, $P = 0.92$; **Fig. 3.8E**), central dot (One-way ANOVA: $F(3, 76) = 0.63$, $P = 0.6$; **Fig. 3.8F**), right dot (One-way ANOVA: $F(3, 76) = 0.42$, $P = 0.74$; **Fig. 3.8G**) or control (One-way ANOVA: $F(3, 76) = 1.57$, $P = 0.2$; **Fig. 3.8H**).

Similar to what is observed with the dot cue, fruit flies kept a relatively stable orientation preference throughout the entire 8 min experiment for the left pin (One-way ANOVA: $F(3, 76) = 0.39$, $P = 0.76$; **Fig. 3.9E**), central pin (One-way ANOVA: $F(3, 76) = 0.26$, $P = 0.85$; **Fig. 3.9F**), right pin (One-way ANOVA: $F(3, 76) = 2.59$, $P = 0.06$; **Fig. 3.9G**) and the control (One-way ANOVA: $F(3, 76) = 0.48$, $P = 0.7$; **Fig. 3.9H**). This suggests that the information fruit flies' place on the importance of the dot and pin stimulus remains stable over time within the flight simulator.

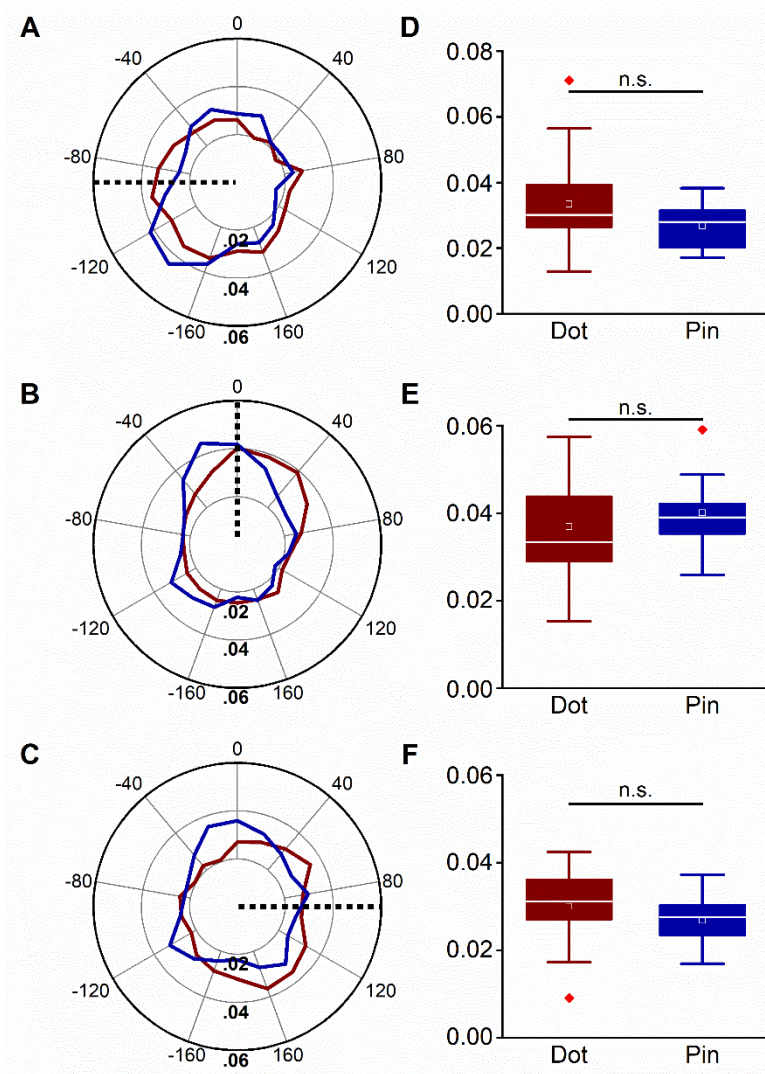


Fig. 3.7 Singular 2D or 3D objects, when tested separately, are equally salient.

The mean fixation behaviour of *Drosophila* ($n = 20$) of 8 min flight periods when presented with either the small black dot (red) or small black pin (blue). The flies' flight directions are relative to the singular landmark for the (A) left, (B) central and (C) right location. Means are calculated over 20° bins. Error bars indicate SEM. The black dotted line in A-F shows the dot and pin's combined location. (G-I) Boxplots show no significant difference in the mean fixation between the dot and pin. Boxplots are the same data as shown in Fig. 3.3 and Fig. 3.5 for dots and pins, respectively. Boxes show the interquartile range, the white line indicates the median, the white box is the mean, whiskers represent the entire data spread, and red diamonds represent outliers. n.s. not significant. D-F Means calculated over 30° bins.

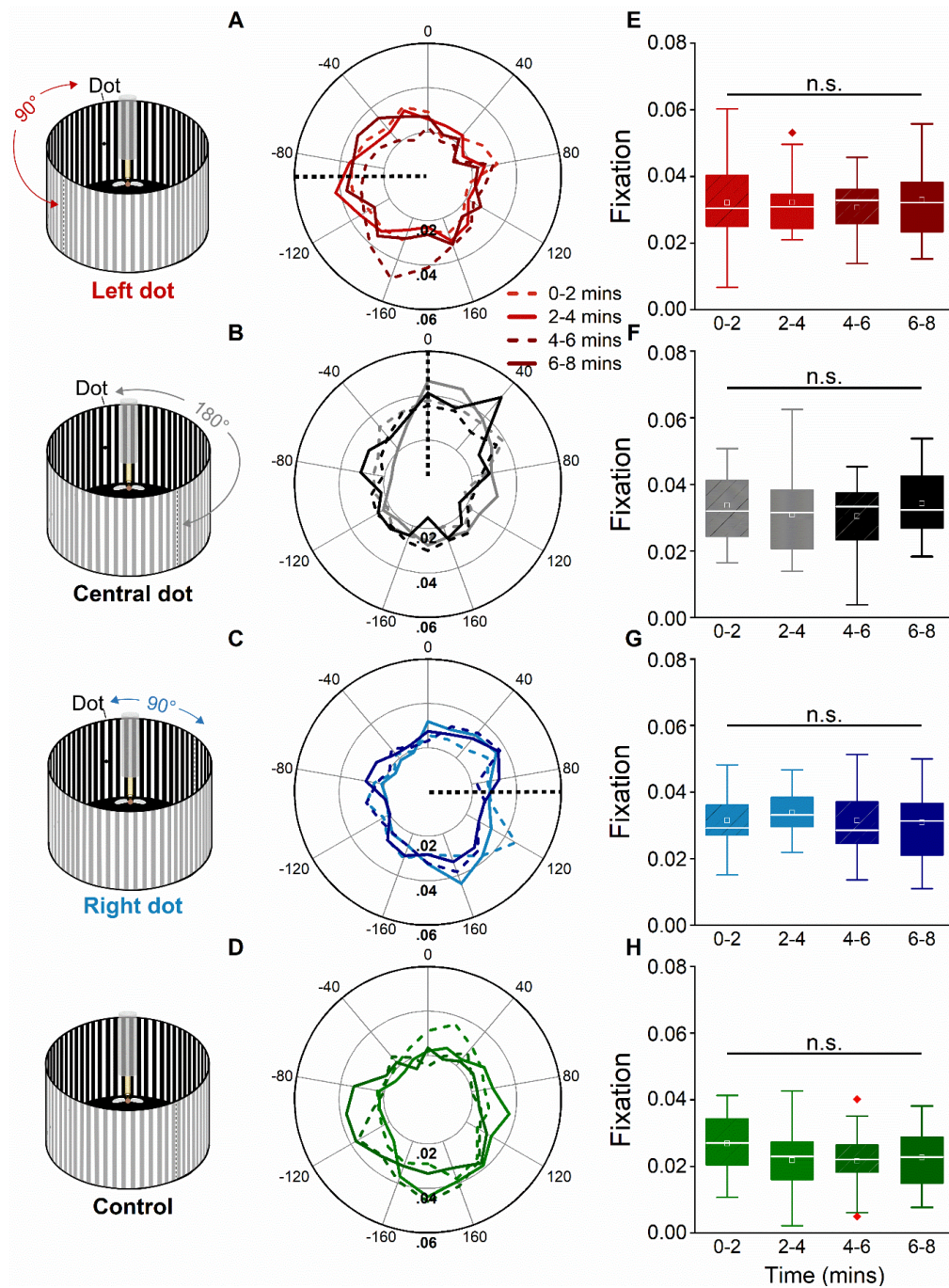


Fig. 3.8 Stable fixation in time when viewing a small single visual cue.

The mean fixation of flies ($n = 20$) shows similar orientation when viewing the dot stimulus during the first, second, third and fourth 2 min phase of the 8 min flight for the left (A), central (B), right (C) and control (D). This indicates that whether the dot is present or absent, fly behaviour is relatively constant with no apparent difference between each phase. The black dotted line in A-C shows the dot location. Means are calculated over 20° bins. (E-H) Boxplots confirm that there is no statistical difference between the 2 min phases. Boxes show the interquartile range, the white line indicates the median, the white box is the mean, whiskers represent the entire data spread, and red diamonds represent outliers. n.s. not significant.

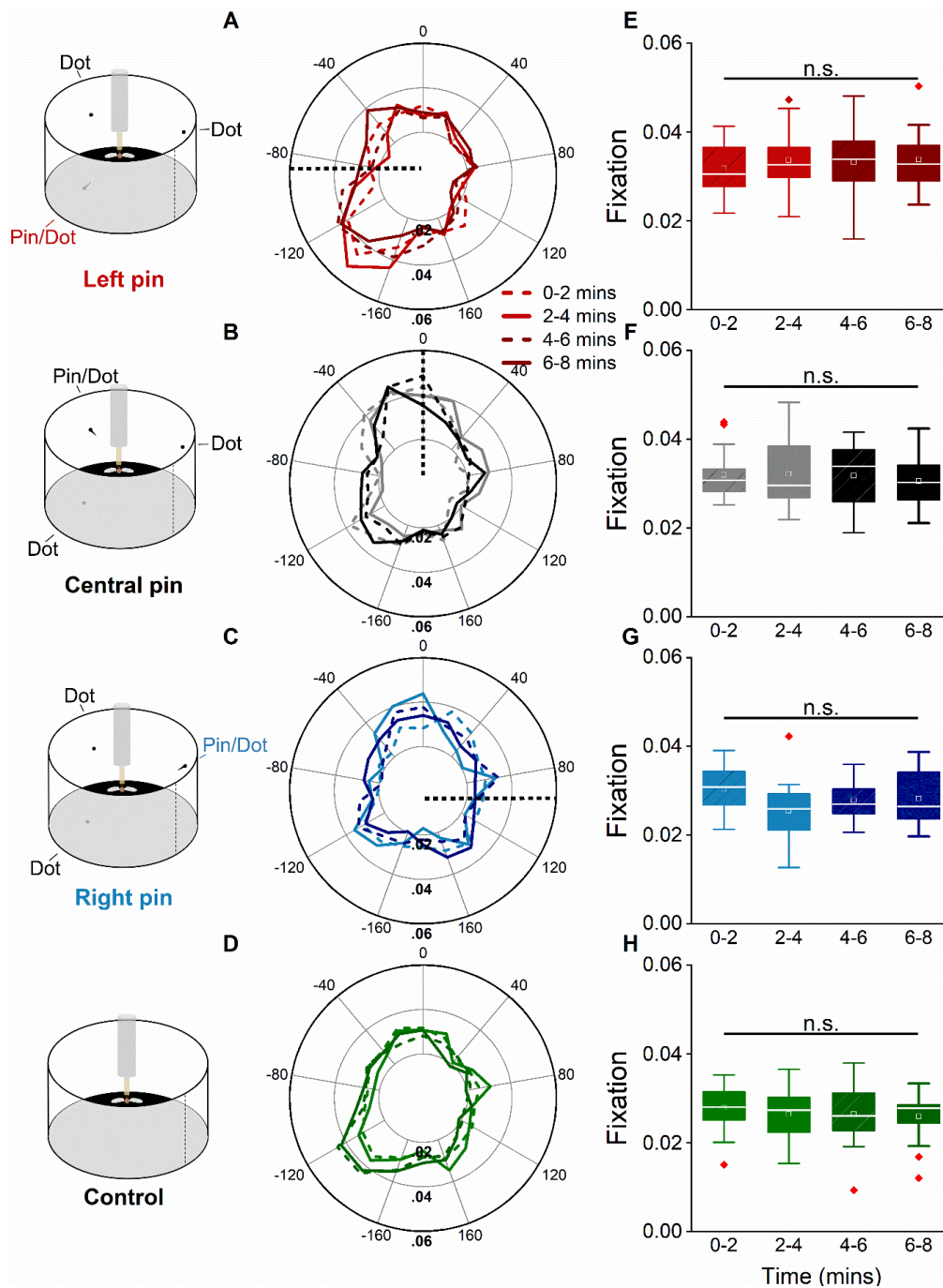


Fig. 3.9 Stable fixation in time when viewing a small single 3D object.

The mean fixation of flies ($n = 20$) shows similar orientation when viewing the pin stimulus during the first, second, third and fourth 2 min phase of the 8 min flight for the left (A), central (B), right (C) and control (D). This indicates that whether the dot is present or absent, fly behaviour is relatively constant with no apparent difference between each phase. The black dotted line in A-C shows the dot location. Means are calculated over 20° bins. (E-H) Boxplots confirm that there is no statistical difference between the 2 min phases. Boxes show the interquartile range, the white line indicates the median, the white box is the mean, whiskers represent the entire data spread, and red diamonds represent outliers. n.s. not significant.

3.3.5 Learning small visual cues requires both eyes in fruit flies

To study the visual learning of fruit flies concerning small 2D and 3D visual cues, the performance index of the animals was analysed at the torque meter when presented with dot or stripe stimuli with pins on alternating patterns. Associative learning at the torque meter has been described before for large 2D patterns (Wolf and Heisenberg, 1991, 1997; Brembs and Heisenberg, 2000). Many fruit flies, even though the visual cues were more challenging to distinguish than in T-patterns, learnt to avoid harmful stimuli and preferred heading directions towards the CS- (Fig. 3.10). When conditioned through heat punishment to either avoid or head towards the pin, binocular flies adjusted their orientation appropriately (Fig. 3.10A and B). On average, fruit flies had no naïve preference (stage 1 and 2, grey bar) towards either pattern for all stimuli (dot, -0.02 ± 0.18 ; stripe, -0.04 ± 0.3 ; control, 0 ± 0.28) ($M \pm SD$). In contrast, after all training stages the performance index during the first memory test (stage 8) increased significantly with respect to the dot stimulus (One-sample t-test: $t(19) = 4.28$, $P \leq 0.001$; Fig. 3.10A), stripe stimulus ($t(19) = 3.61$, $P \leq 0.001$; Fig. 3.10B) and control stimulus ($t(28) = 4.16$, $P \leq 0.001$; Fig. 3.10C). The performance index was similar in the dot, stripe and control, so no significant difference was found (One-way ANOVA: $F(2, 66) = 0.30$, $P = 0.74$; Fig. 3.10D). Example flies ($n = 2$) show exemplary associative learning (Fig. S4).

The majority of fruit flies could learn, though it is only a subpopulation of animals that ever show learning behaviour. Fifteen out of 20 flies (75%, Fig. 3.10E) showed a mean performance index greater than 0.1 when presented with the dot stimulus, while 14 out of 20 (70%, Fig. 3.10F) for the stripe stimulus, and 20 out of 29 fruit flies (69%, Fig. 3.10G) for the control. The remaining flies avoided the CS+ during training but failed to remember this association during the unconditioned test stage. This suggests an equal difficulty in discriminating between small and large cues in this flight simulator setup.

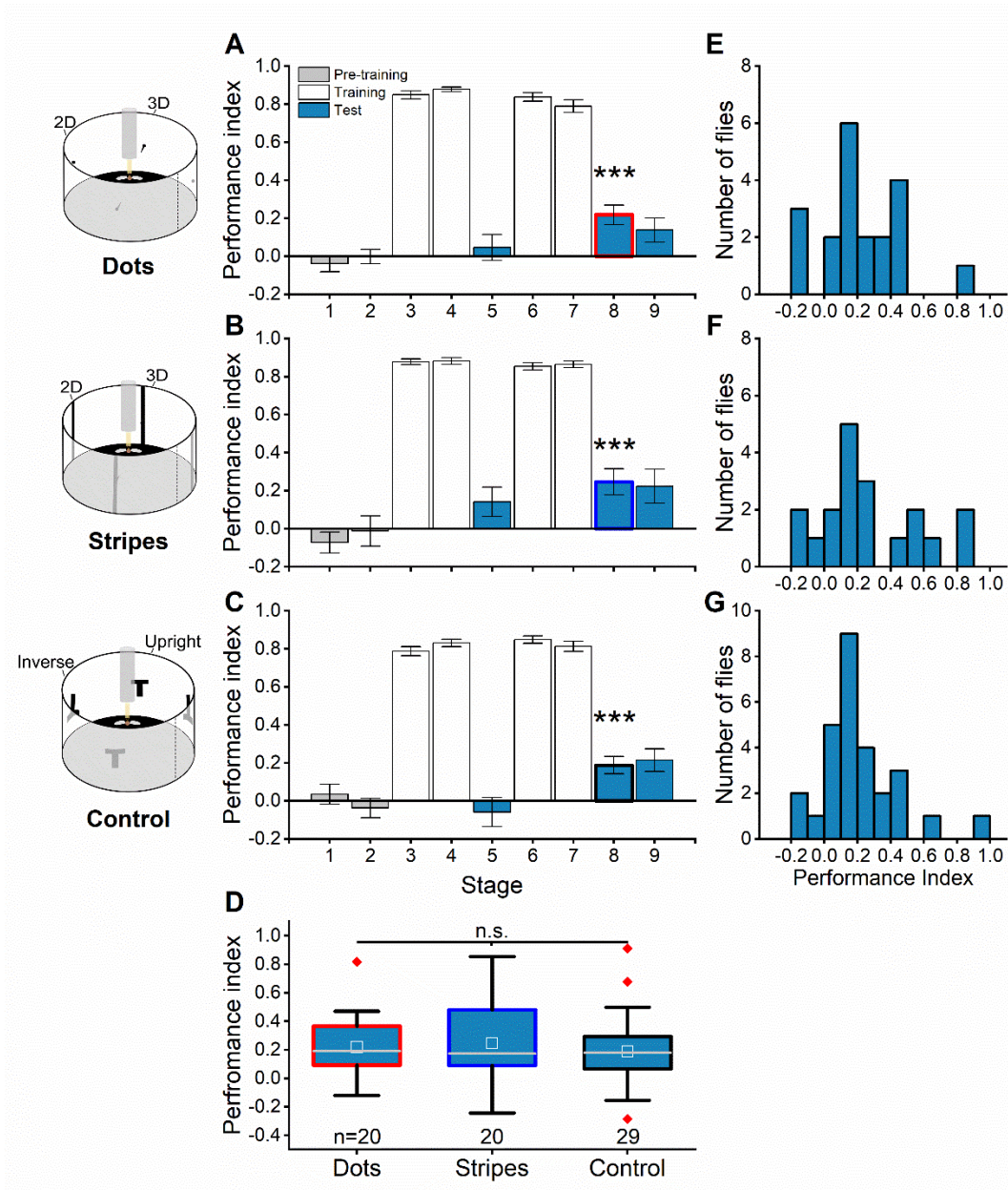


Fig. 3.10 Visual learning of fruit flies using small visual cues.

(A-C) Performance indices of fruit flies over nine 2 min stages for dots (A; n = 20), stripes (B; n = 20) and T-patterns (C; n = 29). Grey bar shows pre-training and no pattern preference. White bar shows training and a strong preference for the CS-. The blue bar shows the memory test and a learned preference for the CS- in stages 8 and 9 for all stimuli. Error bars indicate SEM. (D) Boxplots is the same data as shown in stage 8 of A-C, which did not differ significantly between the stimuli. Boxes show the interquartile range, the grey line indicates the median, the white box is the mean, whiskers represent the entire data spread, and red diamonds represent outliers. Asterisks indicate the level of significance: *P < 0.05, **P < 0.01, ***P < 0.001 and n.s. not significant. (E-G) Histogram of stage 8 performance indices of flies for the dot stimulus (E), stripe stimulus (F), and T-patterns (G).

To exclude any potential non-visual cues influencing the fruit flies' behaviour, two blind mutants were tested (**Fig. S5**). During training, the flies slightly bias their direction to the non-punishing pattern, although the means are lower than wild-type flies. This is as expected as visual input is not required for orientation (Wolf and Heisenberg, 1986). *hdc^{JK910}* mutants failed to direct their flight towards either pattern for all stimuli (Dots, One-sample t-test: $t(19) = -0.83$, $P = 0.42$; **Fig. S5A**; stripes, One-sample t-test: $t(19) = 0.49$, $P = 0.63$; **Fig. S5B**; control, One-sample t-test: $t(19) = -1.67$, $P = 0.11$; **Fig. S5C**) as well as *norpA^{P24}* mutants (Dots, One-sample t-test: $t(19) = -0.06$, $P = 0.95$; **Fig. S5D**; stripes, One-sample t-test: $t(19) = -0.7$, $P = 0.5$; **Fig. S5E**; control, One-sample t-test: $t(19) = -0.04$, $P = 0.97$; **Fig. S5F**). The mean score of stage 8 differed with statistical significance to the wild-type flies for the dot stimulus (Independent-sample t-test: $t(58) = 4.01$, $P \leq 0.001$; **Fig. S5G left plot**), stripe stimulus (Independent-sample t-test: $t(58) = -3.95$, $P \leq 0.001$; **Fig. S5G middle plot**), and control (Independent-sample t-test: $t(67) = 4.08$, $P \leq 0.001$; **Fig. S5G right plot**). Taken together, the bias to the non-punishing pattern by wild-type fruit flies after training show that this is visual learning as blind flies are incapable of learning the associations of the stimuli.

Next, to investigate whether fruit flies relied on the visual input from both eyes to learn associations with the small 3D and 2D cues, the fly's left or right eye was painted to block light. Unlike what was observed with normal (binocular) vision, fruit flies could not learn visual associations concerning the dot and stripe stimulus (**Fig. 3.11**). The orientation of the fruit flies shows no bias to the conditioned pattern for the dot stimulus (One-sample t-test: $t(19) = -0.17$, $P = 0.87$; **Fig. 3.11A**) as well as the stripe stimulus (One-sample t-test: $t(19) = -0.25$, $P = 0.81$; **Fig. 3.11B**). In contrast, the animal's mean performance index exceeded 0.1 for the control stimulus (One-sample t-test: $t(19) = 4.69$, $P \leq 0.001$; **Fig. 3.11C**). Compared to the binocular flies, there was a significant difference between stimuli (One-way ANOVA with Dunnett post hoc test: $F(2, 57) = 8.08$, $P = 0.001$; dot and control: $P \leq 0.002$, stripe and control: $P \leq 0.002$; **Fig. 3.11D**). Five out of 20 flies (25%, **Fig. 3.11E**) showed a mean performance index greater than 0.1 when presented with the dot stimulus, 7 out of 20 (35%, **Fig. 3.11F**) for the stripe and 14 out of 20 (70%, **Fig. 3.10G**) for the T-patterns.

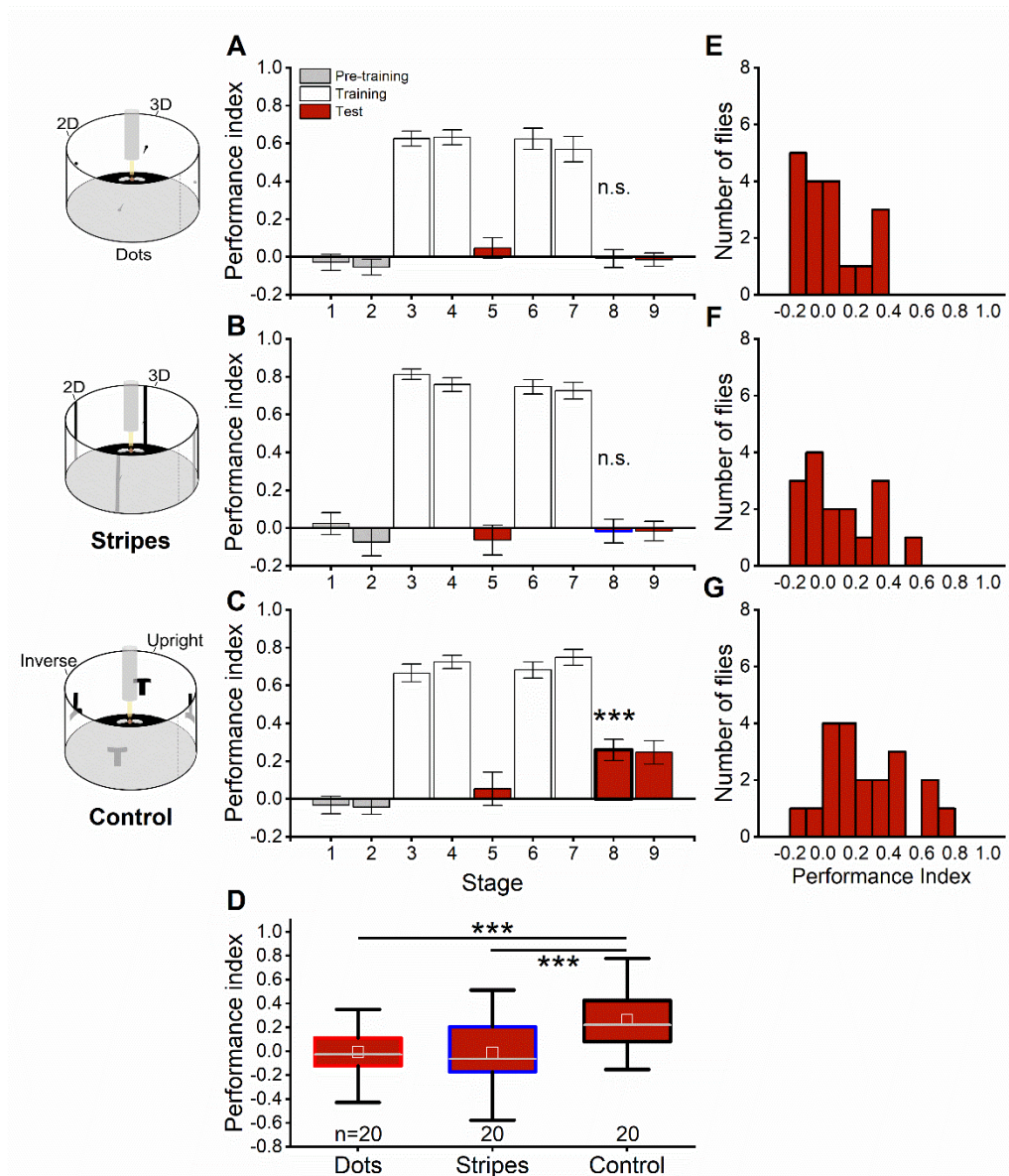


Fig. 3.11 Monocular vision inhibits visual learning of small cues.

(A-C) Performance index of fruit flies with one-eye painted over nine 2 min stages with respect to dots (A; n = 20), stripes (B; n = 20) and T-patterns (C; n = 20). Grey bar shows pre-training with no pattern preference. White bar shows training and a strong preference for the CS-. The red bar shows the memory test. Flies failed to learn dots stimulus (A) and stripe stimulus (B) but learned the control (C). Error bars indicate SEM. (D) Boxplots is the same data as shown in stage 8 of A-C, which differ significantly between the control and test stimuli. Boxes show the interquartile range, the grey line indicates the median, the white box is the mean, whiskers represent the entire data spread, and red diamonds represent outliers. Asterisks indicate the level of significance: *P < 0.05, **P < 0.01, ***P < 0.001 and n.s. not significant. (E-G) Histogram of stage 8 performance indices of flies for the dot stimulus (E), stripe stimulus (F), and T-patterns (G).

Next, the learning performance was compared between the binocular and monocular experiments. The score of the binocular flies tended to be higher during the training stages (3,4,6,7) (Fig. 3.12A to C). During the test, there was a significant difference for dots (Independent-sample t-test: $t(38) = 3.25$, $P = 0.002$; Fig. 3.12D) and stripes (Independent-sample t-test: $t(38) = 2.84$, $P = 0.007$; Fig. 3.12E). In contrast, the mean performance index of binocular and monocular flies was similar during stage 8 (Fig. 3.12F), associated with large cues still being perceived with one eye painted. There was no significant difference between their mean performances (Independent-sample t-test: $t(47) = -1.01$, $P = 0.32$). In summary, the data shown in Fig. 3.12 show that fruit fly learning of small visual cues is affected by removing the visual input from one eye. This result suggests that *Drosophila* use the retinal images from both eyes for object detection at close distance, whether this remains constant when tested at greater distances from the eye remains to be investigated.

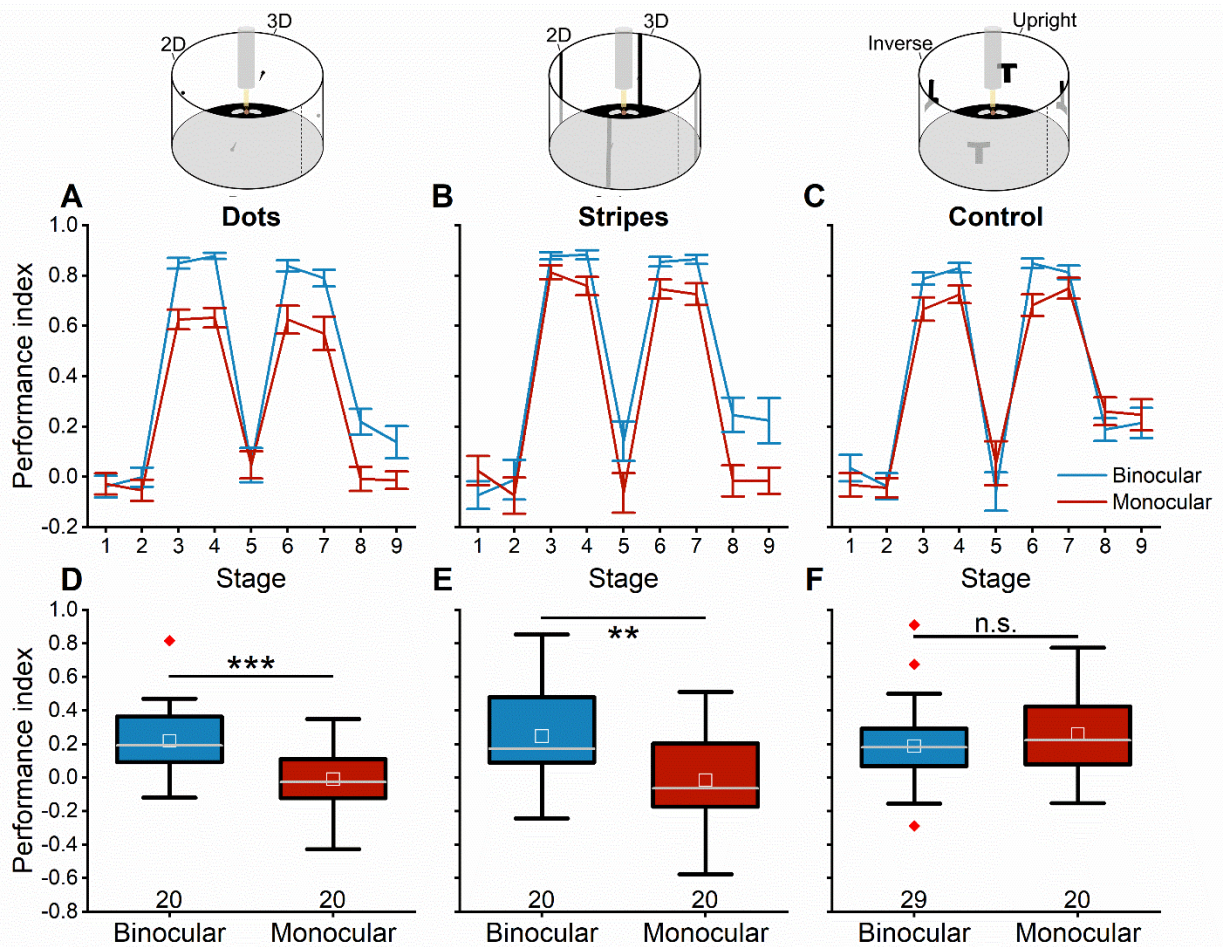


Fig. 3.12 Fruit flies use both eyes for learning small visual cues.

(A, C) Performance index of binocular (blue) and monocular (red) fruit flies show decreased performance indices during training and test stages for monocular flies with respect to dots (A) (n = 20, binocular; n = 20 monocular) and stripes (B) (n = 20, binocular; n = 20 monocular). Similar scores are shown in the test stage for the T-patterns (C) (n = 29, binocular; n = 20 monocular). Error bars indicate SEM. (D-F) The learning ability differed significantly for the small visual cues (D, E) but did not differ for the T-patterns (F). Boxes show the interquartile range, the grey line indicates the median, the white box is the mean, whiskers represent the entire data spread, and red diamonds represent 3D outliers. Asterisks indicate the level of significance: *P < 0.05, **P < 0.01, ***P < 0.001. n.s. not significant. All binocular data as shown in Fig. 3.10, monocular data from Fig. 3.11.

Traditionally, visual learning experiments at the torque meter have delivered the heat punishment from behind the fly, while here, the flies are hit by the laser from above and ahead due to the system setup. Therefore, an experiment was performed in which flies were presented the dot and control stimulus but were conditioned using the traditional method from behind Fig. S8. Subsequently, any different characteristics over the entire 18-min experiment can be

explored. This preliminary data suggests that flies perform better when hit from behind (**Fig. S8F**), yet there is no statistical difference (Dots, Independent-sample t-test: $t(21) = -0.17$, $P = 0.87$; **Fig. S8C**; control (Independent-sample t-test: $t(37) = -1.85$, $P = 0.07$; **Fig. S4F**) likely due to the low sample size (dots, $n = 3$; control, $n = 10$) which limits the ability to interpret the data. Interestingly, the training stages have a lower performance index and greater variation during the behind method than the ahead method (**Fig. S8D and E**).

3.3.6 Faulty microsaccades disrupt learning

To investigate how each photoreceptor channel contributes to learning small visual cues, mutants with either the outer (R1-R6) or inner (R7/8) photoreceptors functional were tested. Surprisingly, *Rh1-norpA rescue* mutants tested for their functional R1-R6 photoreceptors sometimes show faulty or disrupted photoreceptor movements as found by deep pseudopupil recordings and ERGs. Consequently, *Rh1-norpA mutants* were subdivided into two groups. All flies with “normal” binocular mirror-symmetric lateral photoreceptor microsaccades (**Fig. 3.13**) flies with normal phototransduction but monocular asymmetric lateral photoreceptor microsaccades (**Fig. 3.14**) with a comparison of two subtypes (**Fig. 3.15**). It is worth noting that since a separate investigator performed the imaging after the behavioural experiments, it was not known which group a fly would be placed in throughout the behavioural experiments.

To quantify how microsaccades function affects visual learning, the flies tested with normal microsaccades were grouped for each stimulus (**Fig. 3.13**). The data of the mean performance index show that flies could visually learn to a statistical difference for the dot stimulus ($n = 20$, One-sample t-test: $t(19) = 3.20$, $P = 0.005$; **Fig. 3.13A**) and T-patterns ($n = 20$, One-sample t-test: $t(19) = 3.12$, $P = 0.006$; **Fig. 3.13C**). The data for the stripe stimulus shows that although there was a bias for the CS-, which suggests visual learning, there was no statistical difference ($n = 20$, One-sample t-test: $t(19) = 1.52$, $P = 0.15$; **Fig. 3.13B**). Importantly, presenting different stimuli did not significantly change the learning performance (One-way ANOVA: $F(2, 57) = 0.13$, $P = 0.88$; **Fig. 3.13D**). Indicating robust learning for small and large visual cues. Fourteen out of 20 flies (70%, **Fig. 3.13E**) showed a mean performance index greater than 0.1 when presented with the dot stimulus, while 9 out of 20 (45%, **Fig. 3.13F**) for the stripe stimulus, and 13 out of 20 flies (65%, **Fig. 3.13G**) for the control.

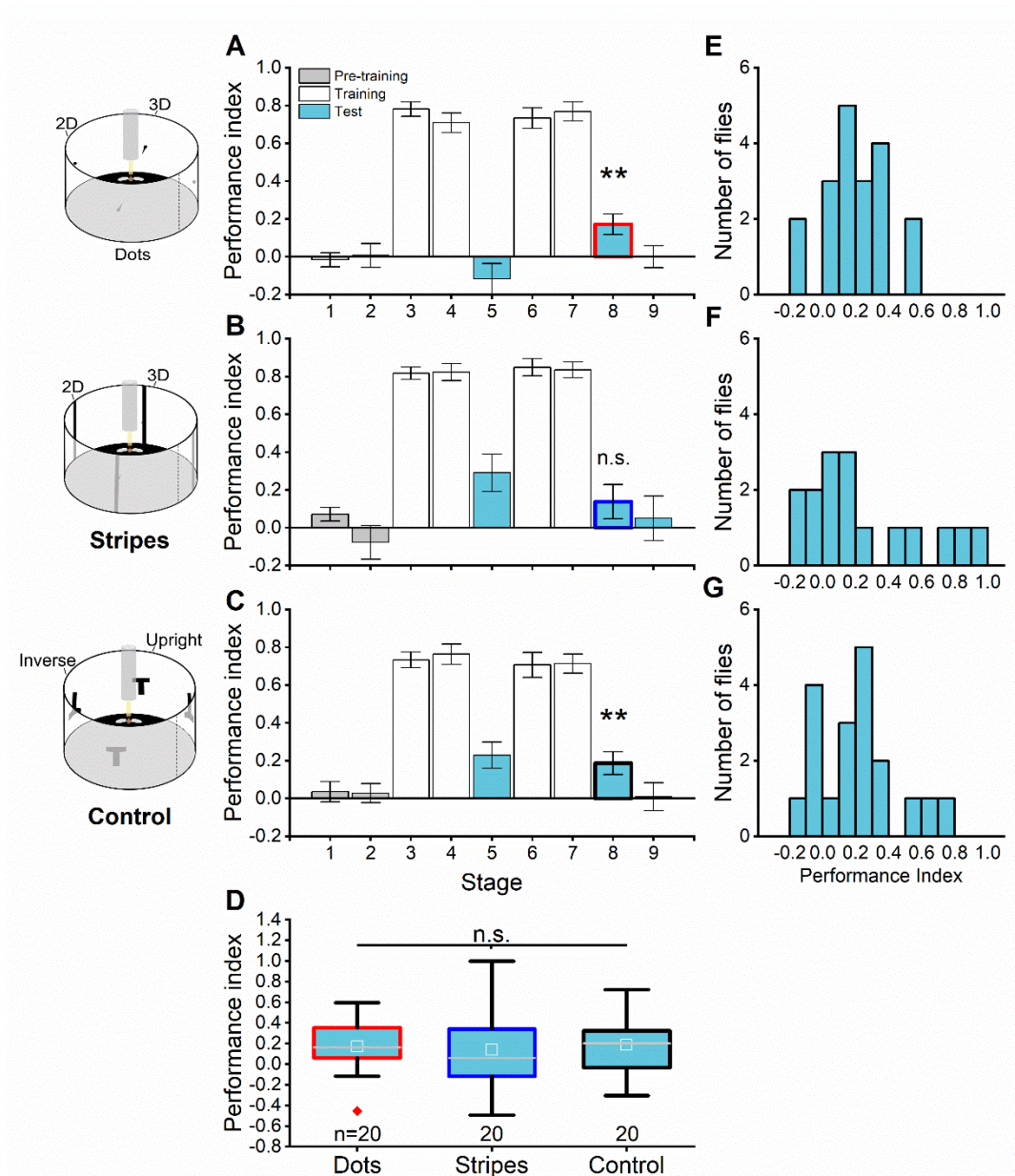


Fig. 3.13 Fruit flies require photoreceptor microsaccades to learn small visual cues.

(A-C) Performance index of *Rh1-norpA* rescue mutants with functional microsaccades in both eyes over nine 2 min stages for dots (A; n = 20), stripes (B; n = 20) and T-patterns (C; n = 20). Grey bar shows pre-training with no pattern preference. White bar shows training and a strong preference for the CS-. The light blue bar shows the memory test and a learned preference for the CS- in stage 8 for all stimuli. Error bars indicate SEM. (D) Boxplots is the same data as shown in stage 8 of A-C, which did not differ significantly between the stimuli. Boxes show the interquartile range, the grey line indicates the median, the white box is the mean, whiskers represent the entire data spread, and red diamonds represent outliers. Asterisks indicate the level of significance: *P < 0.05, **P < 0.01, ***P < 0.001 and n.s. not significant. (E-G) Histogram of stage 8 performance indices of flies for the dot stimulus (E), stripe stimulus (F), and T-patterns (G).

Next, to investigate whether faulty microsaccades in one eye inhibited learning, the flies were grouped for each stimulus (**Fig. 3.14**). Fruit fly orientation showed no bias for the conditioned stimulus associated with heat punishment for the dots (One-sample t-test: $t(9) = -0.68$, $P = 0.52$; **Fig. 3.14A**), stripes (One-sample t-test: $t(8) = 1.01$, $P = 0.34$; **Fig. 3.14B**) and control (One-sample t-test: $t(11) = -0.93$, $P = 0.37$; **Fig. 3.14C**). Therefore, there is no statistical difference between stimuli (One-way ANOVA: $F(2, 28) = 0.59$, $P = 0.562$; **Fig. 3.14D**). Only 3 out of 10 flies (30%, **Fig. 3.14E**) showed a mean performance index greater than 0.1 when presented with the dot stimulus, 4 out of 9 (44%, **Fig. 3.14F**) for the stripe and 4 out of 12 (33%, **Fig. 3.14G**) for the T-patterns.

Strikingly, even though flies with painted eyes still learnt the T-patterns (**Fig. 3.11C**), flies with faulty microsaccades showed much less ability to learn large visual cues in addition to small cues. Indeed, there is a significant difference between ‘painted’ and ‘faulty flies (Independent-sample t-test: $t(30) = 3.24$, $P = 0.003$; **Fig. S6 right plot**). Yet, there is no statistical difference for the dots (Independent-sample t-test: $t(28) = 0.69$, $P = 0.5$; **Fig. S6 left plot**) and stripes (Independent-sample t-test: $t(27) = -0.66$, $P = 0.51$; **Fig. S6 middle plot**). This therefore suggests that the issue with the microsaccades may be a larger problem for the eye limiting there ability to learn even very large stimuli.

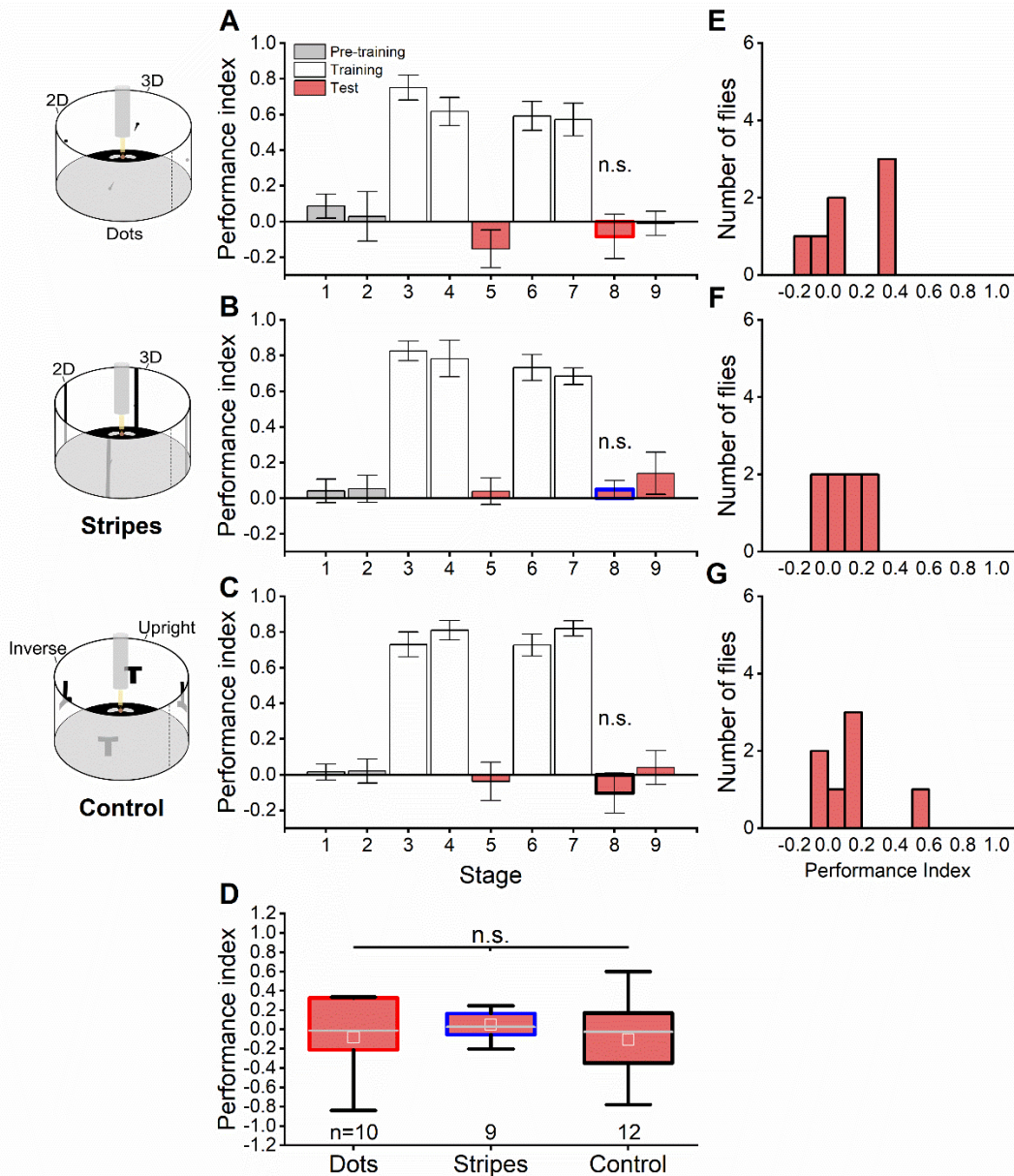


Fig. 3.14 Faulty photoreceptor microsaccades inhibit visual learning.

(A-C) Performance index of *Rh1-norpA* rescue mutants with faulty non-functional microsaccades in one eye, over nine 2 min stages concerning the dots (A; n = 10), stripes (B; n = 9) and T-patterns (C; n = 12). Grey bar shows pre-training with no pattern preference. White bar shows training and a strong preference for the CS-. The pink bar shows the memory test and a learned preference for the CS- in stages 8 and 9 for all stimuli. Error bars indicate SEM. (D) Boxplots is the same data as shown in stage 8 of A-C, which did not differ significantly between the stimuli. Boxes show the interquartile range. The grey line indicates the median. The white box is the mean. Whiskers represent the entire data spread. n.s. not significant. (E-G) Histogram of stage 8 performance indices of flies for the dot stimulus (E), stripe stimulus (F), and T-patterns (G).

To explore this in further detail, the mean performance index of both groups were compared. The data shows that with fully functioning microsaccades, the orientation of the flies is strongly biased to the non-punishing pattern, unlike the monocular flies, for both the dots (Independent-sample t-test: $t(28) = 2.22$, $P = 0.04$; **Fig. 3.15D**) and T-Patterns (Independent-sample t-test: $t(30) = 2.51$, $P = 0.02$; **Fig. 3.15F**). On the other hand, there was no significant effect for the stripe stimulus (Independent-sample t-test: $t(27) = 0.63$, $P = 0.54$; **Fig. 3.15E**) due to its lower performance index.

Taken together, these results suggest that the photomechanical photoreceptor microsaccades facilitate the detection and visual learning of small visual cues and that when the microsaccades are missing or faulty, flies visual ability is greatly diminished as they find large visual cues challenging to distinguish.

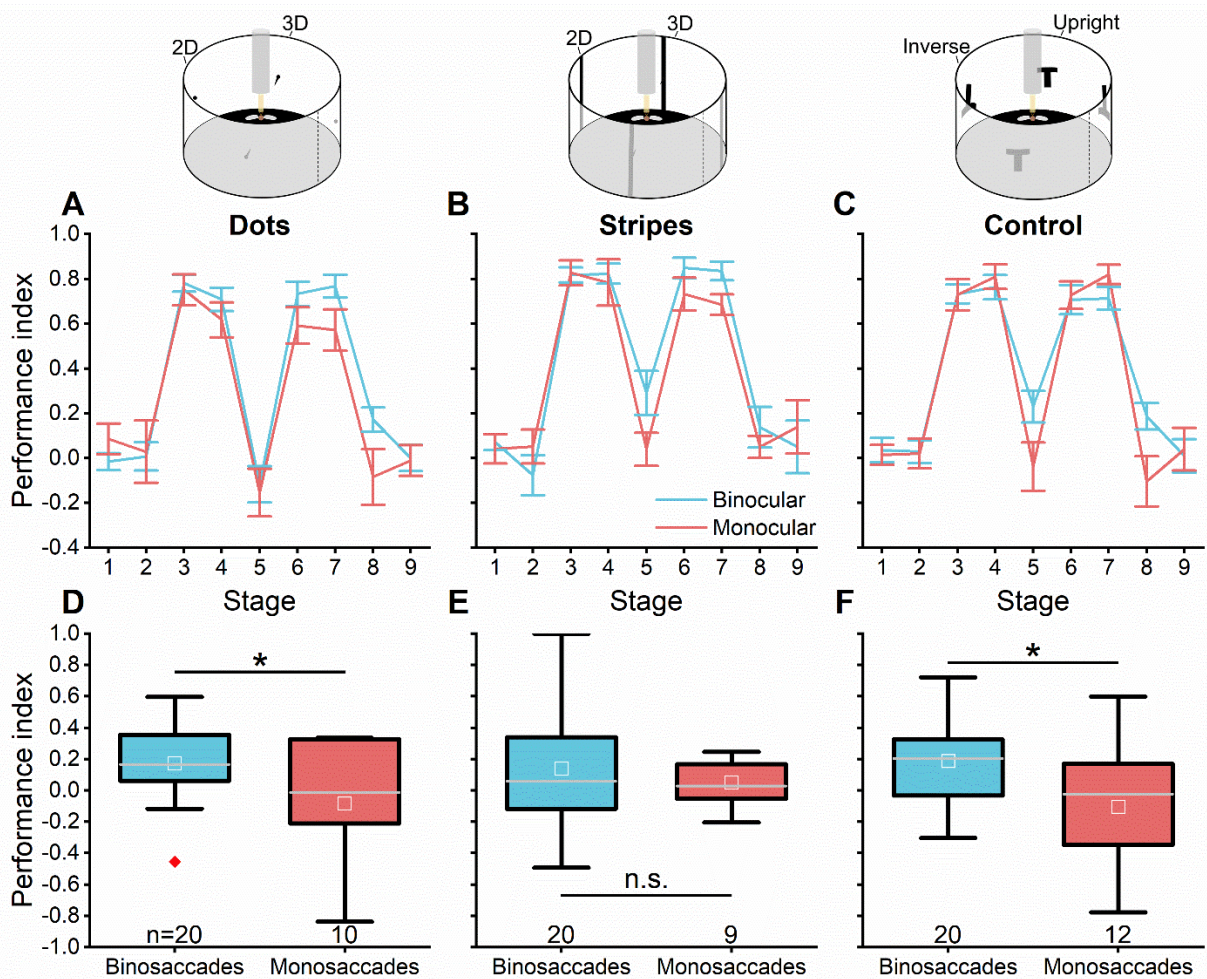


Fig. 3.15 Visual learning is dependent on functional microsaccades.

(A, C) Performance index of 'binosaccades' (light blue) and 'monosaccades' (pink) fruit flies show similar means during training and stage 9. Stage 8 is higher for binocular flies in dots (A) ($n = 20$, binosaccades; $n = 10$ monosaccades) and T-patterns (C) ($n = 20$, binosaccades; $n = 12$ monosaccades) but not for stripes (B) ($n = 20$, binosaccades; $n = 9$ monosaccades). Error bars indicate SEM. (D-F) Boxplots is the same data as shown in stage 8 of A-C, this highlights the difference for stage 8 for the dot (D) and control (F), but there is no statistical difference for the stripes (E). Boxes show the interquartile range, the grey line indicates the median, the white box is the mean, whiskers represent the entire data spread, and red diamonds represent outliers. Asterisks indicate the level of significance: * $P < 0.05$, ** $P < 0.01$, *** $P < 0.001$ and n.s. not significant. All binocular data as shown in Fig. 3.13, monocular data from Fig. 3.14.

3.3.7 Combination of inner and outer photoreceptors

To determine whether the flies ability to see hyperacute objects is facilitated by the R1-R6 receptors exclusively (Juusola *et al.*, 2017) or whether the R7/8 receptors also contribute to the hyperacute vision, we tested flies with only either function R1-R6 receptors (motion vision channel) or R7/8 receptors (colour vision channel). To test the isolated contribution of the R1-R6 photoreceptors, we used Rh1-rescue *norpA*³⁶ flies, as Rh1 is present in the outer photoreceptors this allows them to function whilst isolating the inner photoreceptors. The R1-R6 group was the same flies from the previous section (3.3.6), (i.e. combining both binosaccade and monosaccade flies). Additionally, a single fly with no microsaccades in either eye was in the dataset (stripes: n = 1) as well as 5 flies which escaped after the behavioural assessment but before the deep pseudopupil could be imaged.

The animals developed a slight bias for headings for the dot stimulus (One-sample t-test: $t(29) = 3.19$, $P = 0.003$; **Fig. 3.16A**). When presented the stripe stimulus and control, the tested animals kept a heading slightly directed towards the CS-, though in both conditions there was not a significant effect (Stripes, One-sample t-test: $t(29) = 1.90$, $P = 0.07$, **Fig. 3.16B**; control, One-sample t-test: $t(36) = 1.79$, $P = 0.08$, **Fig. 3.16C**). Nonetheless, the mean performance index of all stimuli was not statistically different (One-way ANOVA: $F(2, 94) = 0.09$, $P = 0.91$; **Fig. 3.16D**), suggesting that overall animals were learning a bias for one pattern over the other. When analysing the frequency of learning, 17 out of 30 flies (57%, **Fig. 3.16E**) showed a mean performance index greater than 0.1 when presented with the dot stimulus, 14 out of 30 (47%, **Fig. 3.16F**) for the stripe and 20 out of 37 (54%, **Fig. 3.16G**) for the T-patterns. This suggests that the population consisted of approximately half very good learners and half bad learners. This may be explained by both the subpopulation of monocular flies and the expected small subpopulation of flies that do not learn.

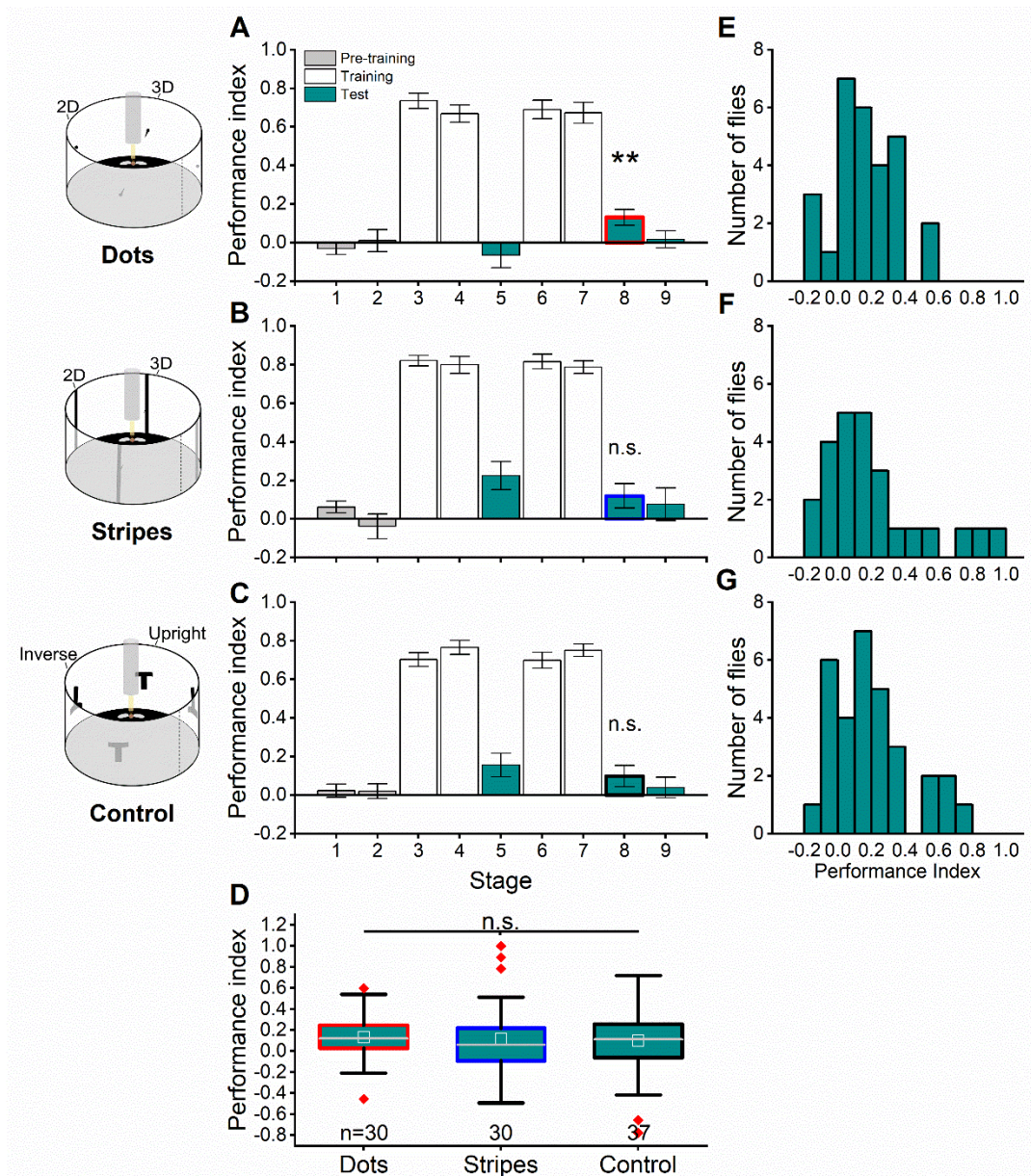


Fig. 3.16 Outer (R1-R6) photoreceptors elicit learning.

(A-C) Performance index of Rh1-rescue *norpA*³⁶ flies over nine 2-min stages with respect to dots (A; n = 30), stripes (B; n = 30) and T-patterns (C; n = 37). Grey bar shows pre-training with no pattern preference. White bar shows training and a strong preference for the CS-. The blue bar shows the memory test and a slight preference for the CS- in stage 8 for all stimuli. This was statistically significant for the dot stimulus (A) but not the dot (B) or control (C). Error bars indicate SEM. (D) Boxplots is the same data as shown in stage 8 of A-C, which did not differ significantly between the stimuli. Boxes show the interquartile range, the grey line indicates the median, the white box is the mean, whiskers represent the entire data spread, and red diamonds represent outliers. Asterisks indicate the level of significance: *P < 0.05, **P < 0.01, ***P < 0.001 and n.s. not significant. (E-G) Histogram of stage 8 performance indices of flies for the dot stimulus (E), stripe stimulus (F), and T-patterns (G).

Next, the stimuli were presented to two mutant flies (*ninaE*⁸ and Rh3-6 flies) with only functional inner photoreceptors. To test whether the R7/R8 photoreceptors had an important role, we used two mutants with rescued R7/8 photoreceptor channels but inhibited outer photoreceptors (R1-R6). To see how each mutant performed separately, their mean performance was compared (**Fig. 3.17**) before being pooled (**Fig. 3.18**) to then make comparisons with the R1-R6 data (**Fig. 3.19**). In general, fruit flies did change their direction after training and have a small bias in flight direction. In both mutants, there was a statistical difference for the stripe stimulus (*ninaE*⁸, One-sample t-test: $t(14) = 3.29$, $P = 0.005$; **Fig. 3.17B**; Rh3-6, One-sample t-test: $t(15) = 3.24$, $P = 0.006$; **Fig. 3.17E**). Though this significance was not observed for the dot stimulus (*ninaE*⁸, One-sample t-test: $t(14) = 1.89$, $P = 0.079$; **Fig. 3.17A**; Rh3-6, One-sample t-test: $t(15) = 2.01$, $P = 0.06$; **Fig. 3.17D**). Interestingly, for the T-pattern stimulus *ninaE*⁸ mutants performed less well (One-sample t-test: $t(14) = 1.43$, $P = 0.18$; **Fig. 3.17C**), while Rh3-6 mutants did learn the control but not as high as with the stripes (One-sample t-test: $t(14) = 2.13$, $P = 0.05$; **Fig. 3.17F**). The inconsistencies in this dataset open up the possibility that the inner photoreceptors might not contribute as much to small target detection, so the responses are not as robust in all conditions. Nevertheless, the data show for the first time that the inner photoreceptors in addition to the outer (Juusola *et al.*, 2017), elicit behavioural responses to hyperacute visual cues. Furthermore, between mutant comparisons show that their mean performance indices are similar, and so there is some level of robustness in their response (Dots: Independent-sample t-test: $t(29) = -1.18$, $P = 0.86$; **Fig. 3.17G left plot**; stripes: Independent-sample t-test: $t(29) = -0.42$, $P = 0.68$; **Fig. 3.17G middle plot**; control: Independent-sample t-test: $t(28) = -0.63$, $P = 0.53$; **Fig. 3.17G right plot**).

Next, as the two mutants did not significantly differ from each other, their datasets were pooled together to analyse their precise contribution to visual learning. The mean performance index was greater than 0.1 for all stimuli (Dots, One-sample t-test: $t(30) = 2.81$, $P = 0.009$; **Fig. 3.18A**; stripes, One-sample t-test: $t(30) = 4.63$, $P \leq 0.001$; **Fig. 3.18B**; control, One-sample t-test: $t(29) = 2.57$, $P = 0.02$; **Fig. 3.18C**) and so did not differ significantly (One-way ANOVA: $F(2, 89) = 0.80$, $P = 0.45$; **Fig. 3.18D**). Seventeen out of 31 (55%, **Fig. 3.18D**) for the dots, 14 out of 31 (45%, **Fig. 3.18E**) and 18 out of 30 (60%, **Fig. 3.18D**).

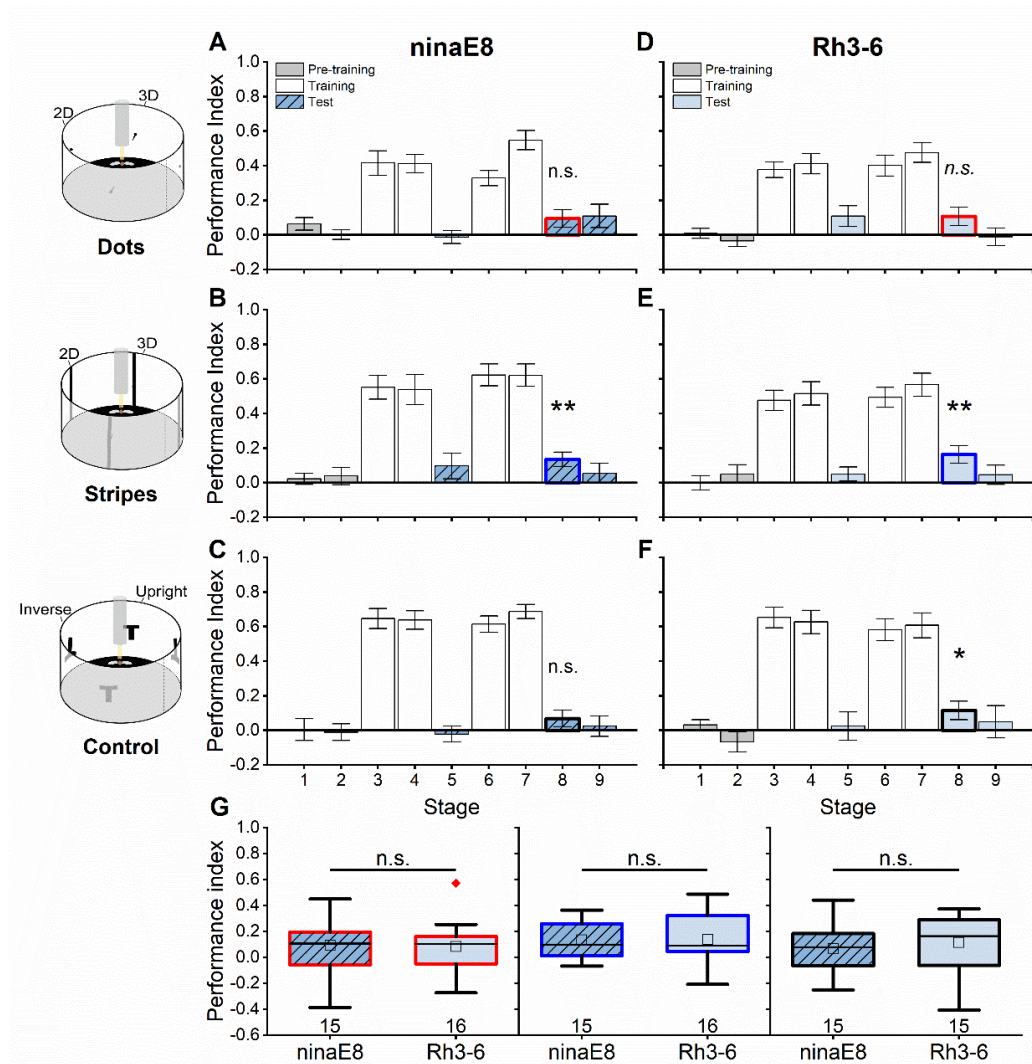


Fig. 3.17 Inner (R7/8) photoreceptors elicit learning.

The performance index of mutant flies (A-C) *ninaE⁸* (striped blue) and (D-F) Rh3-6 (light blue) that view a dot stimulus (A, D) ($n = 15$, *ninaE⁸*; $n = 16$, Rh3-6), a stripe stimulus (B, E) ($n = 15$, *ninaE⁸*; $n = 16$, Rh3-6), and T-pattern control (C, F) ($n = 15$, *ninaE⁸*; $n = 15$, Rh3-6), over nine 2 min sections. The grey bar shows the pre-training indicating the fly has no preference for either pattern. The white bars show the training and a general preference for the CS-. The memory test shows a trend but no statistically different performance index for the dot stimulus and (A, D). Both learn for the stripe stimulus (B, E), but *ninaE⁸* learn the control (C) while Rh3-6 do not (F). Error bars indicate SEM. G is the same data as shown in stage 8 of A-F. The mean performance index of both mutants shows that there was no statistical difference in each mutants ability to learn the dot (left plot), stripe (middle plot) and T-pattern (right plot) stimuli. Boxes show the interquartile range, the black line indicates the median, the black box is the mean, whiskers represent the entire data spread, and red diamonds represent outliers. Asterisks indicate the level of significance: * $P < 0.05$, ** $P < 0.01$, *** $P < 0.001$ and n.s. not significant.

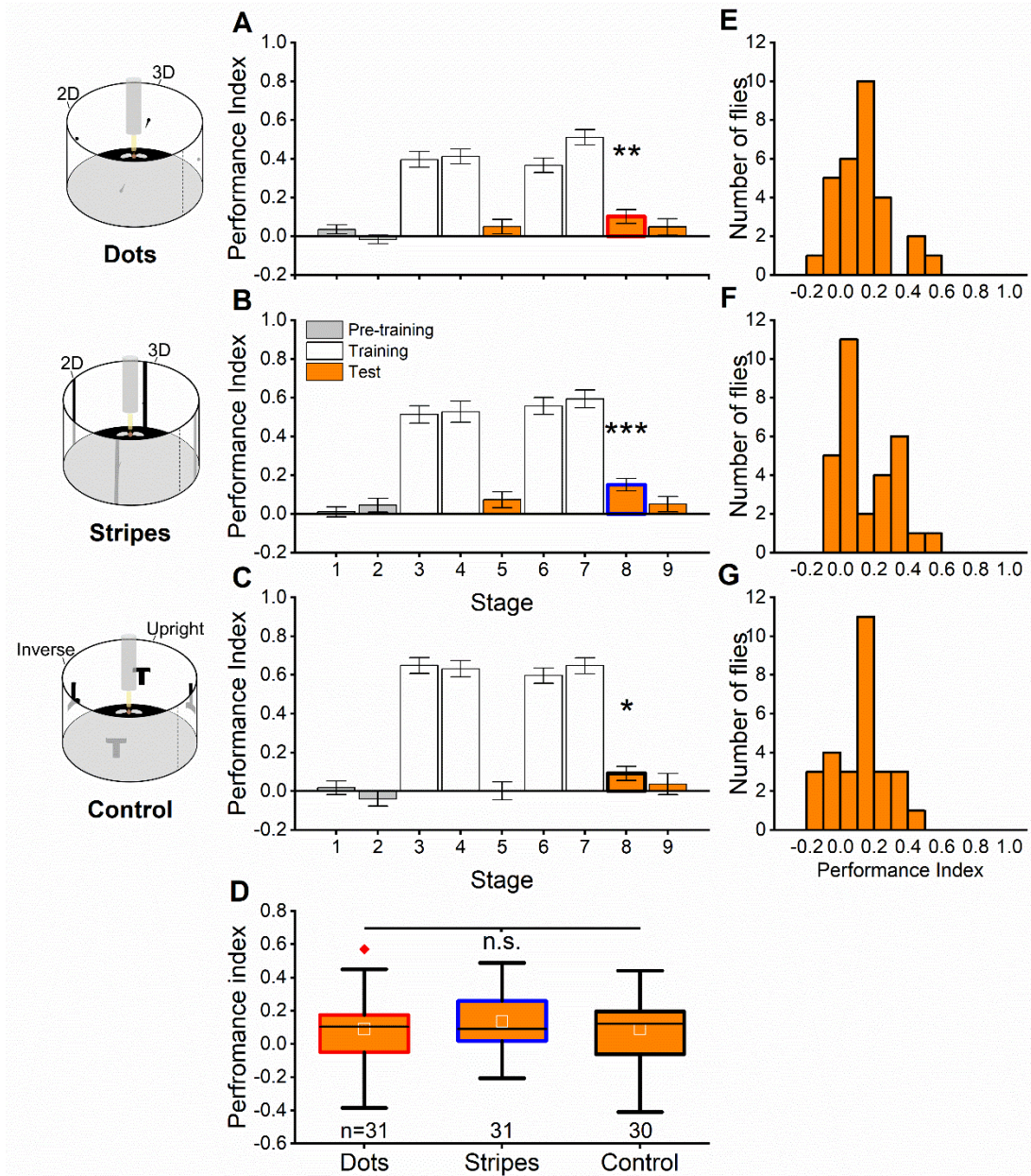


Fig. 3.18 Pooled scores of mutants with inner (R7/8) photoreceptors.

(A-C) Performance index of both R7/8 mutant flies over nine 2 min stages to dots (A; n = 31), stripes (B; n = 31) and T-patterns (C; n = 30). Grey bar shows pre-training with no pattern preference. White bar shows training and a strong preference for the CS-. The light blue bar shows the memory test and a learned preference for the CS- in stage 8 for all stimuli. Error bars indicate SEM. (D) Boxplots is the same data as shown in stage 8 of A-C, which did not differ significantly between the stimuli. Boxes show the interquartile range, the grey line indicates the median, the white box is the mean, whiskers represent the entire data spread, and red diamonds represent outliers. Asterisks indicate the level of significance: *P < 0.05, **P < 0.01, ***P < 0.001. n.s. not significant. (E-G) Histogram of stage 8 performance indices of flies for the dot stimulus (E), stripe stimulus (F), and T-patterns (G).

To characterise visual learning in the presence of all or limited photoreceptor contribution, the mean performance index of each experiment was directly compared (**Fig. 3.19C**). The performance of flies did not show any significant differences for each stimulus (Dots, One-way ANOVA: $F(2, 78) = 1.83$, $P = 0.17$; **Fig. 3.19D**; stripes (One-way ANOVA: $F(2, 78) = 1.27$, $P = 0.29$; **Fig. 3.19E**; control (One-way ANOVA: $F(2, 93) = 1.189$, $P = 0.31$; **Fig. 3.19F**).

Nevertheless, there is clear robustness in the response of all treatment groups. All photoreceptors functional produces consistently better learning performance. Interestingly, with the R7/8 mutants pooled, both the performance indices and learning frequency look similar to the R1-R6 data. This is in contrast to when the R7/8 mutants were analysed individually and seemed inconsistent. Instead, it suggests that both photoreceptor channels contribute more or less equally. Thus, producing the higher learning scores observed in wild-type flies. In summary, these results suggest that flies detect small visual cues combining the visual information acquired from all photoreceptors.

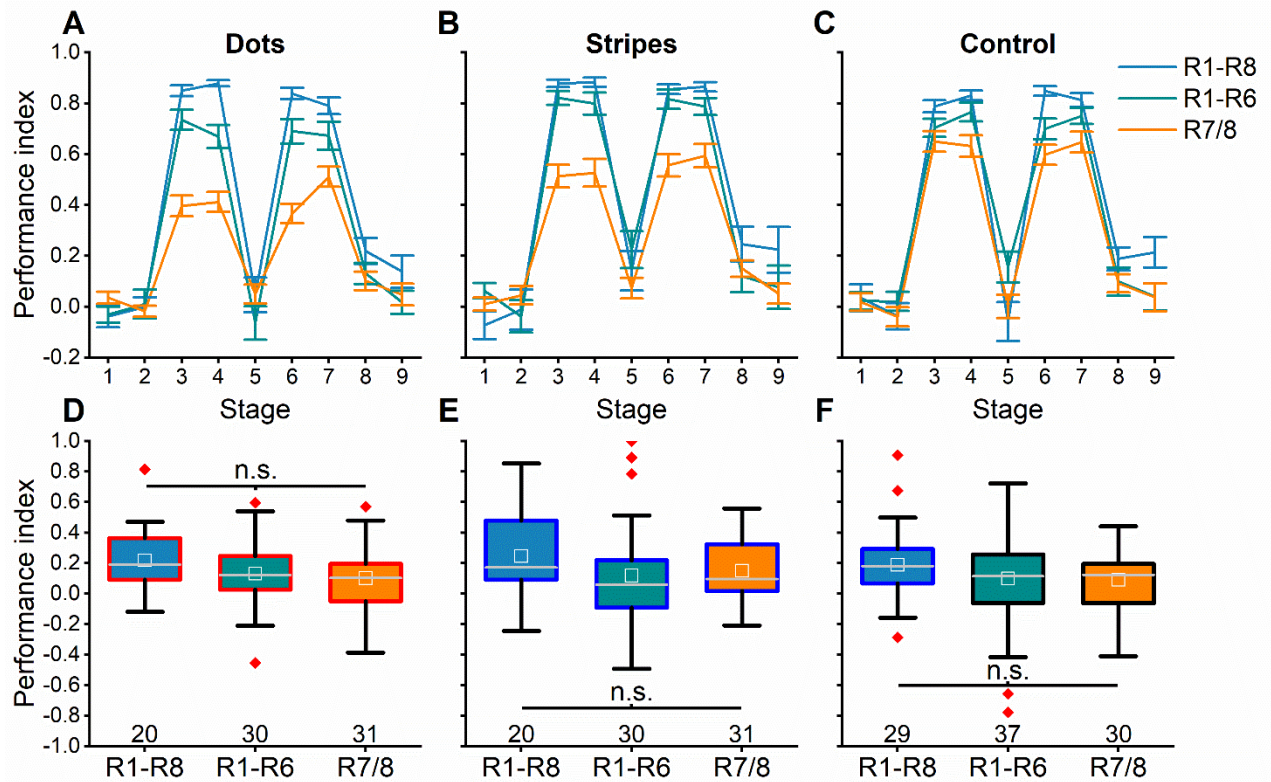


Fig. 3.19 Combined photoreceptor channels enhance the learning of small visual cues in fruit flies.

(A, C) Performance index of wild-type flies (R1-R8), mutants with only functional outer photoreceptors (R1-R6) and inner photoreceptors (R7/8). (A-C) Mean scores of flies during training and test stages shows a decrease in scores in respect to wild-type, outer and inner function. Error bars indicate SEM. (D-F) The learning ability shows a slight trend for a small reduction in performance, but this does not differ with statistical significance for dots (D) (R1-R8, n =20; R1-R6, n = 30; R7/8, n = 31), stripes (E) (R1-R8, n =20; R1-R6, n = 30; R7/8, n = 31), and the control (F) (R1-R8, n =29; R1-R6, n = 37; R7/8, n = 30). Boxes show the interquartile range, the grey line indicates the median, the white box is the mean, whiskers represent the entire data spread, and red diamonds represent outliers. n.s. not significant. Shaded boxes are replotted from Figure 3.10 (blue boxes), figure 3.16 (green boxes) and figure 3.18 (orange boxes).

3.4 Discussion

Single object detection

The results show that fruit flies – even with an interommatidial angle of 4.5° - detect and bias their heading choices towards a singular small visual cue (1°) in a virtual environment. This further supports that the optical resolution limit does not restrict the spatial resolution in flies (Gonzalez-Bellido, Wardill and Juusola, 2011; Juusola *et al.*, 2017). Thus, optical measurements alone cannot predict single object resolution (Spaethe and Chittka, 2003). Whether the minimum single object threshold goes beyond 1° in fruit flies, as found in other flying insects such as the killer fly and robber fly (Wardill *et al.*, 2015, 2017), remains to be investigated.

The experiment shows that fruit flies are biased to choose a general flight direction towards the small dark dot (**Fig. 3.3**), although often flies choose arbitrary headings or fail to “follow” the dot location when shifted to the left or right. The former is similar to the finding with vertical stripes that also elicit fixation behaviour (Reichardt and Wenking, 1969; Wehner, 1972), although the headings towards the small dot in **Fig. 3.3** are less robust than the stripes, possibly resulting from the reduced ease of detecting and fixating such a small visual cue. Furthermore, in previous experiments, a small dark dot (10° - 30°) as seen in a coarse LED matrix is innately aversive (Maimon, Straw and Dickinson, 2008; Theobald, 2019; Palavalli-Nettimi and Theobald, 2020), whereas in these experiments, the same dot shape only much smaller (1°) led to either chosen headings in the general direction of the dot or arbitrary headings with a minimal preference for any direction. Altogether, this suggests that object shape alone does not predict the innate response elicited from the animal observer. Next, it will be interesting to present increasingly larger dots to the fruit flies to test at which size the fruit flies’ begin to find the stimulus aversive.

Anti-fixation behaviour, i.e. flying 180° from dot, does occur, consistent with that observed in stripes (Heisenberg and Wolf, 1984), which suggests aversive behaviour. However, this often occurs during the central dot but not for either the left or right. Additionally, this anti-fixation behaviour occurs concurrently with fixation behaviour during a trial rather than replacing it. Thus, this indicates that the paper-join is the cue affecting their behaviour at this scene region and not anti-fixation in response to the dot cue. The paper-join may be perceived as a long vertical bar, which flies have been shown to have a strong attraction for (Maimon, Straw and Dickinson, 2008; Cheng, Colbath and Frye, 2019). Thus, it is not an aversion for the dot but an

attraction to a second slight visual cue. Interestingly, since the visual cue of the paper-join is a nominally broader dark or light bar, this difference is smaller than 1° . Therefore this also suggests high acuity.

Small objects are more salient with depth cues

The first experiment provided new insight into the behavioural response to a tiny single target, yet I also wanted to explore whether a 3D object, still smaller than the interommatidial angle, would be distinguished from 2D objects of the same area and contrast. Each of the three dots is smaller than the interommatidial angle, so detecting the depth of the pin within a dot would not be possible as predicted by the optical resolution limit, as each target would subtend an angle smaller than a 'pixel'. Thus, each target would appear identical, with no dot being more salient than the other.

The results show that flies presented with a small 3D object protruding from one of three dots showed increased attraction to the singular object (**Fig. 3.5**). This suggests that depth changes in small nearby objects can convey different messages of significance. Therefore, it has to keep a catalogue of the significance of each object for every pattern in the visual field. When presented with a 3D object in the middle, the fly shows a strong attraction to the object over the 2D dots. Similarly, when the pin is shifted to either the left or right dot, the fly fixates between the dot and paper join, seemingly using both as landmarks. However, as with the dot experiment, the right object does not show equally strong fixation behaviour (discussed further below). However, overall it suggests that both eyes are being used to detect the pin's depth, as monocular cues would not distinguish it from the black dot behind.

Given the pins small size, it falls within the corresponding receptive fields of a single photoreceptor from each eye. However, the sweeping nature of the corresponding left and right eye photoreceptors swinging back to front mirror-symmetrically creates disparity. As the pin moves side to side, corresponding with the fly's yaw torque during saccadic turning behaviour, the pin moves in the same direction as the receptive field from one eye but the opposing direction of the receptive field in the other eye. Such movement would elicit phasic differences in the photoreceptor voltage responses (Song *et al.*, 2012; Juusola *et al.*, 2017). Fruit flies can then determine depth using the disparities of the neural image (Kemppainen *et al.*, 2022).

The mean fixation for the singular object is similar in both the dot and pin experiments (**Fig. 3.7**), thus suggesting an equal salience under such artificial conditions for a singularly unique

object. Indicating that flies showed an innate tendency to orient towards the more salient object and were able to discriminate between the objects (Sareen, Wolf and Heisenberg, 2011).

Contrast and hyperacute vision

According to the theory before Juusola *et al.*, (2017) a fly would not be able to detect the small (0.98°) black dot placed amongst a single light bar of 1.2° gratings as it would perceive a uniform grey colour (Fig. 6G, Kemppainen *et al.*, 2022). Even though the object may fall within the field of view of a single ommatidium, that does not mean the proposed hyperacuity in fruit flies is the reason why flies responded behaviourally to its presence as the retinal image, or 'pixel' where the dot is located would have a slight contrast change even if it is considerably less than the original contrast of the object (for clarity see Fig 3. O'Carroll and Wiederman, (2014)). An alternative explanation for the results is therefore that the flies were detected contrast changes and it was not the result of hyperacuity.

It does make the dot stimulus used in these experiments more akin to a point source than an extended source stimuli (Warrant and McIntyre, 1993). A point source is a stimulus which subtends an angle much smaller than the interommatidial angle while an extended source is larger, such as a grating. So in effect I am testing a point source placed within an extended source stimulus.

The pin experiment shows that with a similar contrast (black pin hidden on the black dot), the fly performs very consistent behaviour to that with the single pin (Fig. 3.7). This lends support to the theory that the behaviour observed is in relation to *Drosophila*'s hyperacute vision. Were the results of the dot experiment due to contrast differences, then it seems unusual that the behaviour would have been comparable across both experiments. Nevertheless, future work could attempt to control the contrast of the dot to exclude this explanation. For example, a much weaker starting contrast (e.g. grey dot) would then have almost no contrast change when it is approximately 1° as the object's luminance is predicted to change to be limited to approximately 36% of its original luminance (O'Carroll and Wiederman, 2014). In addition, using different coloured objects with various *Drosophila* mutants may demonstrate whether hyperacuity is needed to detect the small object. This would be useful as when the contrast between an object and its background decreases it becomes more challenging to distinguish which in these experiments would require hyperacute vision for the fruit flies to respond behaviourally to them.

Visual acuity of gratings and single objects

It may be assumed that grating acuity is a reliable predictor of single target acuity. Therefore, it may be expected that because of the optomotor responses to bars smaller than an individual sampling unit (Juusola *et al.*, 2017), single objects this small would also be resolved by fruit flies. However, different physical and neurophysiological mechanisms may determine how well an animal can resolve a fine bar compared to a small object. More so, different visual behaviours will extract different information, not necessarily requiring the highest resolution (Land, 1997). The limitation to resolving bars has historically been linked to retinal sampling density, while contrast sensitivity limits the detection of single small targets (O’Carroll and Wiederman, 2014). Consequently, objects smaller than the interommatidial angle are still detectable with high contrast. This is the exact scenario of the dot stimulus presented to the flies in this experiment. Thus, one possible explanation for the slight fixation towards the dot may be the high contrast of the object and its edges compared to the background of the light bar, as opposed to the fruit flies resolving the fine spatial detail. However, the relatively stable fixation levels (albeit somewhat low) shown for the pin stimulus would contradict this interpretation. Indeed since the pin stimulus hides the object within a dot of the same contrast, there are no contrast cues in this experiment, and therefore, there should have been no preference for the pin. Consequently, it seems highly unlikely that high contrast elicited the fixation behaviour alone. Detailed mathematical modelling further supports this conclusion (Kemppainen *et al.*, 2022). Nevertheless, it would be useful in future studies to test the response to varying dot parameters.

Object size and attraction

In previous experiments, flies have shown an innate aversion to small visual objects (Maimon, Straw and Dickinson, 2008; Cheng, Colbath and Frye, 2019; Tanaka and Clark, 2020). It is worth highlighting that an apparent, strong repulsion was exhibited in this prior work by the flies, which is a fundamentally different response to the weak attraction exhibited in the current experiments. So next, it is important to not only investigate *if* the flies can see the dot but instead to understand *why* the flies are slightly attracted to it? What is its identifiable function in the flight simulator, and what is the fly’s motivational state?

The most apparent difference between this study and the previous findings is the actual size considered to be a “small” target and their use of LED arenas while I used paper stimuli. The pulse-width modulation present in LEDs may be affecting the fly behaviour. Here I tested a tiny dot at approximately one degree of a fly’s visual field, and previous studies tested object’s

at 5°-10° (Maimon, Straw and Dickinson, 2008), 10° (Tanaka and Clark, 2020) and 30° (Cheng, Colbath and Frye, 2019). While the reasoning for opposing responses to vertical stripes and large dots is reasonably clear, the varied responses to large dots and small dots are less clear. The fly has an object classification system that recognises stripes as a source of vegetation or landing/feeding sites and is advantageous for the fly to head towards (Maimon, Straw and Dickinson, 2008). On the other hand, large dots may indicate a head-on collision with another insect or an aerial predator, so innate aversion is beneficial. Alternatively, the used LED matrix stimuli may appear highly unnatural and scary to *Drosophila*. The setup used in this thesis with paper stimuli is no less artificial to the fly, however, differences between the stimuli may still yield different behavioural outputs. These findings show that fruit flies show a weak attraction to a tiny dot smaller than the receptive field of a single sampling unit. This suggests that stimulus size is critical in decision-making and not just shape.

So, if flies think a large dot is representative of a predator, small dots may provoke attraction as it is likely to be a conspecific or unharmed insect. A conspecific is a potential mate or rival, so orientating towards it is beneficial, which in the simulator, it is observed as fixation or gaze stabilisation behaviour. Furthermore, if it were a predator, it would indicate that it was large and far away and not an immediate threat. However, since Chapter 2 indicates that more spatial detail will be discerned for physically closer objects, it is likely the fruit fly can immediately classify it as a small-close object instead of a large-far object, hence why there is still attraction behaviour instead of aversion. Further behavioural experiments could investigate the relationship between object size and the behavioural responses of attraction or avoidance. It will next be interesting to investigate when increased object size switches from attraction to aversion behaviour in fruit flies.

It is difficult to interpret from a virtual environment what the visual behaviour indicates, and how once removed from a highly artificial environment and observed in its natural setting, this behaviour would function as. Indeed, unlike the exhaustive knowledge of wild honeybee behaviour (Srinivasan, 2010), we know very little about the wild behaviour of *Drosophila* to draw interpretations from their behaviour in a laboratory setting. Nevertheless, most likely fixation behaviour at the torque meter can be considered a short-range behavioural reflex to head in the direction of close objects. In the wild, this behaviour would rapidly progress into either obstacle avoidance or landing behaviour (Sareen, Wolf and Heisenberg, 2011). On the other hand, one explanation is that fruit flies are attempting to escape the highly artificial

scenario of being tethered at the torque meter (Guo *et al.*, 1996) and should exhibit evasive behaviour by flying towards a salient object. For this, the fly has to arrive at its own “theory” of the current situation and the object’s significance (Heisenberg and Wolf, 1984). This is why flies may orientate towards the dot and why, given a choice between a singular pin and dots, favour the pin.

However, regardless of how we interpret the fly’s goal, it will always be unattainable for the fly under such experimental conditions, so it is difficult to understand its motivational state. Furthermore, the flight simulator makes it challenging to distinguish between a stabilised course occurring regardless of any visual cues, and a chosen heading maintained by the fly in response to visual cues which are used as landmarks to guide orientation. Therefore, it is more challenging to study *Drosophila* orientation by measuring the spontaneous preferences for simple visual stimuli as in experiments 1 and 2. Stimuli as simple as this are less likely to elicit consistent behaviour unless flies are tested with either a more complex (naturalistic) scene or conditioned as in experiment 3.

Less fixation for the ‘right section’

There was less fixation behaviour towards the ‘right dot’ in contrast to the other stimuli (Fig. 3.3C). This is particularly worth noting as the same trend occurred in the pin experiment (Fig. 3.5C). Therefore, a possible explanation is that an artefact within the system was a common restrictive factor for this particular region across all experiments. It is likely due to a mechanical fault with the stepping motor attached to the arena base and rotating the drum. Post-analysis, I explored the flight simulator raw data because of this different result. This highlighted regular smooth arena rotation throughout, except for a tiny position (1°). Subsequently, the rotation would suddenly jump forward (approximately 15°) in a continuous direction of movement. Surprisingly, this issue varied and was not always present. Regardless, a small sub-section of the scene was passed by but not due to the fly’s choice. Consequently, it is the most likely reason why fixation behaviour was lower in this section. However, this was not a visible issue during testing as it appears identical to a torque spike of the fly and simply normal saccadic movement of the arena in response to the fly.

Nevertheless, despite this likely mechanical issue, when comparing this specific right section between all stimuli, the mean fixation was higher when the dot (and pin) were present (right stimulus) rather than absent (left and central stimulus) for this region (Fig. 3.3E and 3.4). This indicates that the fly is still attempting to be in this section more frequently, despite this issue

limiting its ability to do so. It would be worthwhile in future studies with this bespoke flight simulator to resolve any mechanical fault and repeat or apply a similar experimental design to validate an equal preference for the right section.

Possible limitation of head restriction

Fixing the flies head rigid is the standard procedure when testing flies at the torque meter (Brembs, 2008). However, independent head movements help stabilise flight control (Cellini and Mongeau, 2020). Therefore, better performances may occur if the head remains unrestricted. Indeed, it has been shown that head movements maximise gaze stability in freely walking *Drosophila* presented with dots both smaller (1° and 2.5°) and larger (5° and 10°) than the interommatidial angle (Cruz, Pérez and Chiappe, 2021). However, the larger dots elicited better gaze stabilisation performances. This work supports my finding that flies can detect dots as small as 1° , but that performance becomes worse with decreasing size as the task becomes more difficult for the flies. Visual cues so small have not been tested before in the flight simulator. Therefore, in the flight simulator, continuing the method of head restriction likely put the flies at a disadvantage for such a challenging visual task. Fox and Frye (2014) found that head fixation impairs the ability to fixate an object (3.75° vertical bar which is comparable in size horizontally to the dots and almost identical the stripe stimuli used here) if there is also ground motion. This is also the case in the flight simulator as the arena floor rotates along with the rest of the arena. Consequently, it would have been helpful to compare head-free and head-fixed flies at the onset of experiments. If better performances were to be shown by independent head movement, future experiments on *Drosophila* acuity within a flight simulator should adopt this head-free approach.

Effect of time on attraction

To investigate whether the fruit flies varied their chosen headings over the entire 8 min flight, I analysed their orientation on a finer temporal scale by looking at each 2 min phase of the flight for both the dot (Fig. 3.8) and pin experiments (Fig. 3.9). Numerous scenarios may have occurred. For example, in the first 2 min stage, when the fly was still naïve and adjusting to the simulator, either arbitrary and strong erratic flight occurred, or the flies may have chosen a fixed heading regardless of a visual cue. Furthermore, the fly may have detected the single object early on (e.g. 0-2 and 2-4 min), seemingly achieves no goal and ceases to fixate on it during the latter half of the flight (e.g. 4-6 and 6-8 min). In contrast, with erratic movement at first, it may take longer for the fly to notice the cues and slowly begin to choose a heading direction towards the object given time. Indeed, all the above scenarios seemingly occurred (as

can be best interpreted) as I observed individual flies in the simulator. However, as a population taken together, the results show that overall, fruit flies kept a relatively stable orientation throughout their tethered flight.

Two eyes permit learning small visual cues

I have also investigated operant visual learning of fruit flies in the virtual environment of the flight simulator using hyperacute depth cues. Using a well-established method (Brembs, 2008), heat punishment trains the fly to avoid one pair of patterns in favour of another. Traditionally, this approach has been explored for pattern discrimination (Dill, Wolf and Heisenberg, 1995), colour discrimination (Wolf and Heisenberg, 1997), combined pattern and colour (Brembs and Heisenberg, 2001) and yaw torque learning (Brembs and Heisenberg, 2000). However, to the best of my knowledge, neither hyperacute pattern learning nor depth discrimination has been investigated at the torque meter. Indeed, hyperacute patterns combined with depth discrimination has not been undertaken.

The results show that fruit flies with normal binocular vision can be conditioned to discriminate hyperacute visual stimuli (**Fig. 3.10A** and **B**). On the other hand, visual learning was confirmed as visually impaired mutants failed to avoid the punishing patterns (**Fig. S5**). Furthermore, as reported previously in *Drosophila*, we found that flies can develop associations after training for large 2D objects (Dill, Wolf and Heisenberg, 1993) (**Fig. 3.10C**), which was used as a control to compare learning performance (**Fig. 3.10D**). However, flies could still learn the T-patterns with one eye occluded (**Fig. 3.11C**). This result is consistent with the translation invariance shown at the torque meter (Tang *et al.*, 2004). Here, flies could recognize visual patterns (e.g. T patterns) with one eye during a learning assay.

In contrast, compared to normal binocular vision, flies cannot learn after training for either test stimuli with monocular vision (**Fig. 3.11A** and **B**). As in many learning paradigms, responses are highly variable. Some animals seemingly learnt having positive learning scores, while others lost all ability to learn without binocular cues. Consequently, as most flies seemed to be affected by the absence of binocular vision for the test stimuli, it suggests that both eyes are required to see small objects.

A possible explanation is that the smaller stimuli were a more challenging task to discriminate with one eye occluded, resulting in most flies failing to learn. Nevertheless, monocular vision should have made it a more challenging task and presumably should have performed worst

even for the T-pattern. However, monocular flies surprisingly performed slightly better for the T-patterns than binocular flies. Though this did not differ significantly, it indicates robust learning for either vision type. This is supportive of previous work on monocularly deprived flies. For example, when testing the walking behaviour of monocular flies, most flies would turn to the side with the eye covered by paint, but within a few seconds, the fly would adjust and walk straight (Heisenberg and Wolf, 1984). This indicates that the visual guidance is imbalanced and requires time and practise to equilibrate it. Nevertheless, the flies can acquire this experience rapidly and seemingly compensate for the defect. Thus, this suggests that painting the eye is not overly disruptive to the flies ability for operant visual learning.

Learning with normal or defective photoreceptor movements

As the photomechanical photoreceptor microsaccades are proposed to be the mechanism giving rise to high acuity and binocularity, painting over the eye to remove their contribution seems a rather crude technique. Therefore, it was fortunate and beneficial to discover the variation in the microsaccades of Rh1-*norpA* rescue flies being tested due to the R1-R6 functioning alone. The length of movements of the photoreceptor cells varied considerably within and between eyes, as shown by deep pseudopupil imaging (Kemppainen *et al.*, 2022). As such, some flies appeared to have no movements in one eye but normal (as best we currently interpret “normal”) movement in the other eye. The reason for this remains to be investigated. However, it is likely a developmental error for this mutant as it was not observed in wild-type flies.

Flies with normal symmetrical microsaccades were able to learn all stimuli (Fig. 3.13) as expected because of the performance of wild type binocular flies. Conversely, the flies with monocular asymmetrical microsaccades did not learn (Fig. 3.14). This is consistent with simulations from Kemppainen *et al.* (2022), which predicts any asymmetry in the sampling of the photoreceptors would restrict binocularity. In contrast to the T-patterns painted flies, monocular microsaccade flies could not learn (Fig. 3.15F). Whatever cause the faulty microsaccades one eye, such as a developmental problem, must be an inherently larger problem for the individual when tested in visually guided behaviours. Future work may be better excluding this mutant in visual experiments either completely or until this issue is better understood. It is worth highlighting that this occurrence has not yet been observed in wild-type flies and so suggests a specific problem for this mutant. In summary, these results suggest that normal binocular photoreceptor microsaccades are required for operant visual learning of hyperacute 2D and 3D stimuli.

Both photoreceptor channels contribute to hyperacute vision

Drosophila genetics were utilised to investigate the contribution of each photoreceptor subtype for this vision. Various mutants were used with specific subtypes switched off. Two visual mutants (*norpA^{P24}* and *ninaE⁸*) with only R7/8 photoreceptors were tested to confirm the robustness of learning scores. Importantly, this showed for the first time that the inner photoreceptor cells and the outer cells tested by Juusola and colleagues (2017) were able to detect hyperacute stimuli. This finding establishes that while R1-R6 input alone facilitates such vision, R7/8 input must be contributing. As expected this was less robust than in wild-type flies, since we already knew the outer photoreceptor played a role in hyperacute vision (Juusola *et al.*, 2017) than if the inner photoreceptors were also contributing than it must be with less ability, which we observed in both the training and test stages (Fig. 3.17). The two mutants were consistent in their performance and did not differ from one another. Hence they were pooled together to make comparisons against wild-type and R1-R6 mutants.

In reality, however, wild-type flies' R1-R6 and R7/8 photoreceptors likely contribute more alone than determined by the visual mutants. In wild-type flies, the inner and outer photoreceptors move and contract in unison and simultaneously amplify each other, enhancing the microsaccade amplitude (Kemppainen *et al.*, 2022). This is likely another reason why wild type flies with all photoreceptors performed better in the learning experiment (Fig. 3.19). It could be expected that the stripe stimulus would elicit better learning scores than the dot stimulus. This is because the stripes cover a much larger visual area (vertically) and may evoke stronger microsaccades than the smaller dot stimulus. However, the learning score for each stimulus is seemingly inconsistent, with no apparent trends for any fly group. Taken together, this establishes that both the outer and inner photoreceptors affect the fly's ability for hyperacute stereopsis. However, the performance has reduced proficiency.

The use of real object depth

These studies used three-dimensional objects with real object depth to investigate *Drosophila* depth perception during single object and learning experiments. This is in contrast to typical binocularity studies, which have used either glass prisms or coloured filters to only give the impression of changing depth (Collett, 1996; Nityananda, Tarawneh, *et al.*, 2016; Feord *et al.*, 2020). Indeed, this approach is common since using tangible objects to measure depth perception increases the likelihood of detecting unintended cues (not limited to visual cues), inadvertently contributing to behavioural performance. Therefore, a possible interpretation is that the other cues - such as motion parallax, chemosensory and anemotaxis - provided

information to the fruit flies to influence their heading direction and explain their seeming ability to discriminate between the 2D and 3D objects.

As discussed above, head restriction potentially reduced the performance of flies to stabilise gaze on the small object. Nevertheless, by having the head-fixed, fruit flies could not use motion parallax cues to perceive depth, thereby ensuring that the fly could not utilise translational or rotational motion parallax to detect the 3D pin or perceive monocular cues to construct a neural image of the 3D object. Therefore, theoretically, the only movement is from the photoreceptor microsaccades to discriminate the pin.

Furthermore, the pin's rotational movements' air currents could provide a non-visual cue. In that case, though, were anemotaxis to have any contributing factor to the learning performance, blind mutants would not have performed so poorly (**Fig. S5**). Additionally, differences in the chemosensory content of the paint (pins) and ink (dots) may have provided a cue. However, this possibility can also be excluded due to the performance of the blind mutants. Nevertheless, future experiments with similar stimuli could cover all patterns (both paint and ink) with a uniform outer shell (e.g. clear nail polish) to control any chemosensory differences. Shadows from the pin were also not providing a cue as the ring-shaped light tube provides uniform illumination of the stimuli without generating shadows. Alternatively, it is possible the pins were reflecting polarised or UV light which aided object detection. Polarised light is doubtful as all skylight was blocked out of the experimental room. Additionally, although also unlikely as effort was made to black out all light around the setup with a roller curtain, it is possible that there was UV reflection upon the 3D objects. Future studies could use UV flies as a control as they only express Rh3 rhodopsin (UV) and see UV but not green, learning scores could then be compared to wild-type flies to see any influence from UV reflection.

Another possibility is that flies detected the 3D object because it was not camouflaged amongst the black pattern (dot or stripe). This could arise due to the manual preparation of the 3D object compared to a virtual stimulus, which is that the pin's positioning is not perfect. Therefore, as it rotated, the fly may have seen the side of the object when it should have been hidden. However, the pin's placement amongst a dot or stripe was inspected under magnification to ensure perfectly central placement and angular positioning. Furthermore, the stripe stimulus with full vertical coverage of the paper scene alleviates this concern as the pin is more easily placed amongst the dark background of the stripe. Nevertheless, future experiments could use larger dots with the pin to ensure the pin is convincingly obscured within the dot.

A behavioural need for high acuity and binocularity

The most fundamental question is why fruit flies require high acuity and binocularity? Unlike other flying insects, it does not perform a vast repertoire of complex visual tasks such as aerial prey capture (Wardill *et al.*, 2013). It has a tiny brain and eyes, even by insect standards. Besides, unlike the praying mantis, the only insect to conclusively have been shown to use stereopsis for prey capture (Nityananda, Tarawneh, *et al.*, 2016), there is no specific task or apparent selection pressures that would have driven this adaptation in fruit flies.

During flight, fruit flies rely on many sensory modalities for navigation (Currier and Nagel, 2020), where close-range spatial details may not be as important. This may be true during walking behaviours, though it seems more likely that binocularity and high acuity may be most beneficial when performing walking behaviours. For example, walking is when flies perform their most complex visual behaviours (Heisenberg and Wolf, 1984). It seems likely that such behaviours are where selection pressures arose for enhanced resolvability. Therefore, it seems more prudent for any future stereopsis investigations to focus on the walking behaviours of the fruit fly rather than on flight.

Furthermore, this finding raises an interesting question: how would males perform compared to females? Males arguably perform the more sophisticated visual behaviours, such as fighting during courtship behaviour (Heisenberg and Wolf, 1984). Females were used in this thesis as their larger size elicits better performance at the torque meter. Nevertheless, future work could attempt to investigate the performance of male fruit flies.

These flight simulator experiments suggest that fruit flies use stereopsis to discriminate the pin stimulus. Nevertheless, more conclusive behavioural evidence would be required to make such a claim definitive. A possible series of experiments to strengthen the case would be an attempt to use the ‘anaglyph glasses’ as reported for the mantis and cuttlefish (Nityananda, Tarawneh, *et al.*, 2016; Feord *et al.*, 2020). However, very few behaviours can be elicited from the fly to make the glasses/filters a useful tool. However, if the fly performs more robust optomotor responses to physically closer fine gratings as the results in chapter 2 suggest, then attempts to test their optomotor behaviour may be suitable. For example, if the fly were fitted with glasses and the disparity altered so that the proximity of high spatial frequency gratings appeared to change on a virtual screen, the fly would produce stronger and weaker responses consistent with the results from the different sized arenas in the flight simulator.

Conclusions

Fly responses to small visual cues within the flight simulator reveal that small patterns are detected and innately attractive to the fly when it is the most salient feature in the virtual environment. This is different from previously published work on larger (but still small) dots. This expands the potential role of shapes in the wild, demonstrating that size is an essential predictor for appropriate responses. The current chapter also suggests that binocularity enables the perception of small patterns of slightly different depths in fruit flies. Thus, fruit flies use motion parallax for further away objects and binocularity for close-range objects. Based on the findings of the previous and current chapter, it would appear that the proximity of the environment affects spatial resolving power and that different mechanisms contribute to depth perception.

Chapter 4

Concluding remarks

In conclusion, the results assembled in this thesis contribute to a better understanding of the visual performances of fruit flies in a virtual reality system. Alongside other results, I show that the optical resolution limit does not determine the minimum threshold for a behavioural response in the fruit fly. The findings show that the viewing range over which fruit flies respond to hyperacute gratings does influence the behavioural response. The flies appear to see patterns smaller than the interommatidial angle more clearly when viewed from a closer distance ([chapter 2](#)). This ability allows fruit flies to detect close-small objects with better clarity than large-far objects.

In single object experiments, fruit flies maintain slight preferences to choose heading directions towards the singular most salient object ([chapter 3: experiments 1 and 2](#)). However, in the literature, they find larger objects of similar shapes innately aversive. Fruit flies thus categorise objects according to the relative size and not only to shape.

Furthermore, I show that fruit flies can be conditioned to avoid hyperacute 2D or 3D objects with binocular vision, but the fly cannot learn when one eye is covered ([chapter 3: experiments 3](#)). Fruit flies likely use the disparity from photoreceptor microsaccades in each eye to detect and discriminate the small objects. Both the outer (R1-R6) and inner (R7/8) photoreceptors contribute to this ability but do so with less aptitude.

The data I present in Chapter 3 may not provide any answers to the newly theorised stereopsis in regards to its neural mechanisms in fruit flies, but it does show behaviourally that *Drosophila* respond in a way that suggests stereo vision. Taken together, the results compiled in this thesis show that flies possess high acuity. They also suggest that flies are using binocularity for close-range depth perception. However, more conclusive evidence would be required utilising both behaviour and neural approaches. Nevertheless, it is a first step providing a basis for future investigations.

Future directions

The investigation of hyperacute stereopsis in *Drosophila* requires the development of behavioural experiments, especially in a lab where the research questions had to be developed around an existing piece of apparatus, the flight simulator. Unfortunately, this relatively old system was not initially developed with such ideas (3D stimuli) under consideration. The work from my PhD has established a visual stimulation setup and utilised recognised but effective behavioural paradigms and analyses to tackle new questions. Providing the foundation for future work attempting to characterise behavioural responses of *Drosophila* to small 2D or 3D patterns.

One of the reasons I chose to measure optomotor behaviour at two different distances was because of the absence of any obvious stimuli problems associated with using a 3D pin (discussed below). I hoped to find differences in optomotor responses between two clearly different-sized arenas to serve as guidance for a more selective approach afterwards. I also intended to establish response properties to multiple spatial wavelengths smaller than the interommatidial angle rather than a single wavelength (2.4°) as this would highlight a much clearer dynamic of the detectability of small gratings. Issues arose with the construction of different-sized arenas due to inconsistencies with the existing small arena, thus time constraints left me unable to solve this and ultimately unable to measure different spatial wavelengths with the two different sized arenas I had available. Thus, future work should include a systematic analysis of the optomotor behaviour to numerous distances with an emphasise on sub-interommatidial angle wavelengths.

Our system utilises paper stimuli which may not be well suited to investigations into hyperacuity but is less convenient for studies into stereopsis. But it would be entirely possible to design systems that could be a modification of the existing techniques to test 3D vision. Methods commonly employed in mantis stereo research, such as the projection of stimuli to be perceived by the animal to be at different distances (Nityananda *et al.*, 2018, 2019) are more challenging to apply to fruit flies due to a lack of effective behaviours that can be evoked. Enhanced control of the 3D test, such as 3D glasses and perceived depth rather than real-world 3D objects, is required. With this setup, a screen or panel can be presented to the animal and rule out any of the possible cues and problems associated with using a real object (e.g. shadow, UV reflection). An ideal experiment would use the concept of chapter two to measure the optomotor response to changing depths.

Our understanding of invertebrate stereopsis is almost exclusively based on the work with mantids utilising glass prisms (Collett, 1996) and ‘anaglyph’ glasses (Nityananda, Tarawneh, *et al.*, 2016) in behavioural studies as well as in neuronal studies (Rosner *et al.*, 2019). It is interesting to consider how a relatively expensive neural process such as stereoscopic vision may be present in an unlikely species like the fruit fly. The recent studies by Juusola *et al.*, (2017) and Kempainen *et al.*, (2022) demonstrated the possibility that fruit flies perceive the nearby world in high resolution and use both eyes for enhancing depth perception, exemplifying the uncertainty of stereopsis being present in any other invertebrate. Furthermore, very little is known about the characteristics of photomechanical photoreceptor microsaccades and their existence in any other invertebrate species. Highlighting the need to expand the research of Kempainen and colleagues (2022) using different techniques and developing new behavioural assays in *Drosophila*, as well as branching into new species to determine whether we can attribute photoreceptor contractions to any other invertebrate.

Impact in the field

The overall importance of this research is emphasised by the growing evidence of *Drosophila* experiments investigating visually guided behaviour. Specifically, they respond to stimuli far smaller than their optics have traditionally predicted. Many in the field will view the results of this thesis and Kempainen *et al.*, (2022) with scepticism due to the chosen model organism. In the same vein as other invertebrate species, this should not be surprising as several species such as the robber fly and black fly have been shown to have acuity which surpasses their optics. However, to explore both hyperacute vision and stereo vision, the fly with its genetic toolbox may very well be a more advantageous model species. Gaining knowledge of a visual process such as stereo in a new species is essential to understanding the selection pressures which drive such a neural process. Thus, visual studies in fruit flies can go on to provide many novel insights into the field of vision research and neuroethology.

Supplement figures

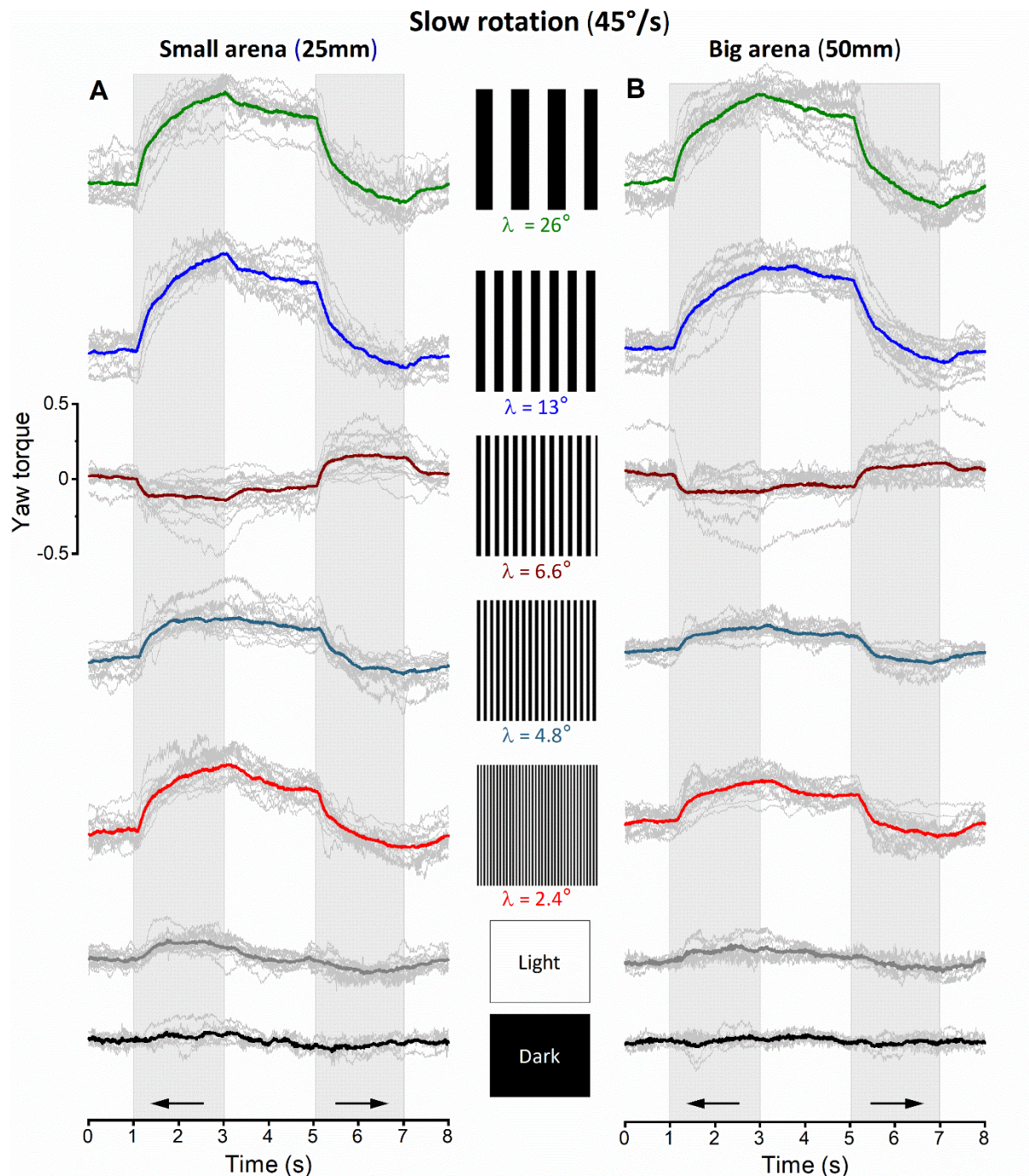


Fig. S1 *Optomotor* responses of fruit flies presented gratings with different wavelengths at two distances under slow rotational velocity (45°/s).

Each fly was presented with gratings of five different wavelengths and two control stimuli (light and dark) tested at either 25 mm (**A**; $n = 15$) or 50 mm (**B**; $n = 15$). Individuals were presented with each stimulus multiple times. Thin traces show the pooled optomotor responses of each fly. Thick traces show the population mean. Grey shading indicates the rotational period. Black arrows show the direction of rotation as viewed by the fly.

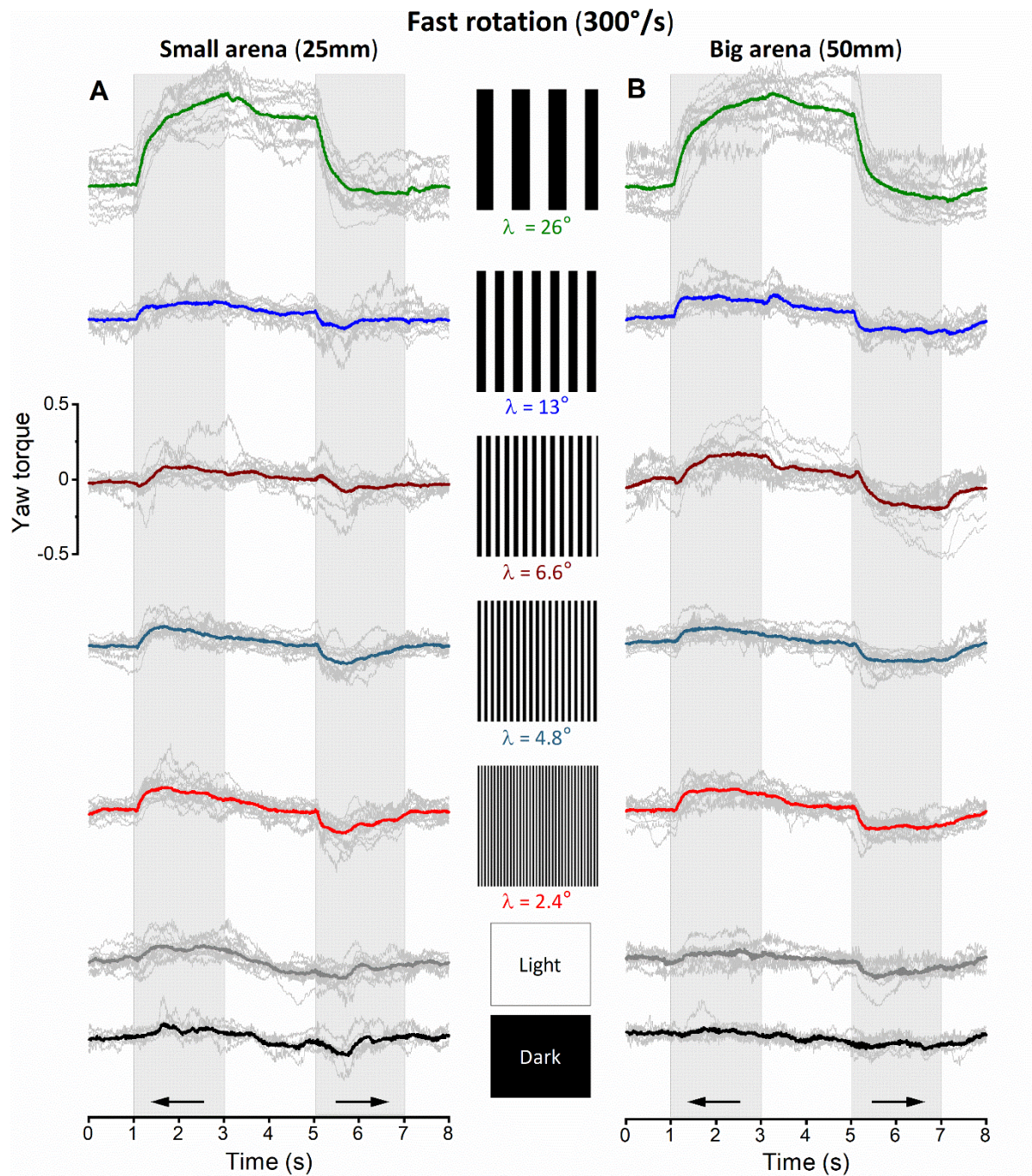


Fig. S2 Optomotor responses of fruit flies presented gratings with different wavelengths at two distances under fast rotational velocity (300°/s).

Each fly was presented with gratings of five different wavelengths and two control stimuli (light and dark) tested at either 25 mm (**A**; $n = 15$) or 50 mm (**B**; $n = 15$). Individuals were presented with each stimulus multiple times. Thin traces show the pooled optomotor responses of each fly. Thick traces show the population mean. Grey shading indicates the rotational period. Black arrows show the direction of rotation as viewed by the fly.

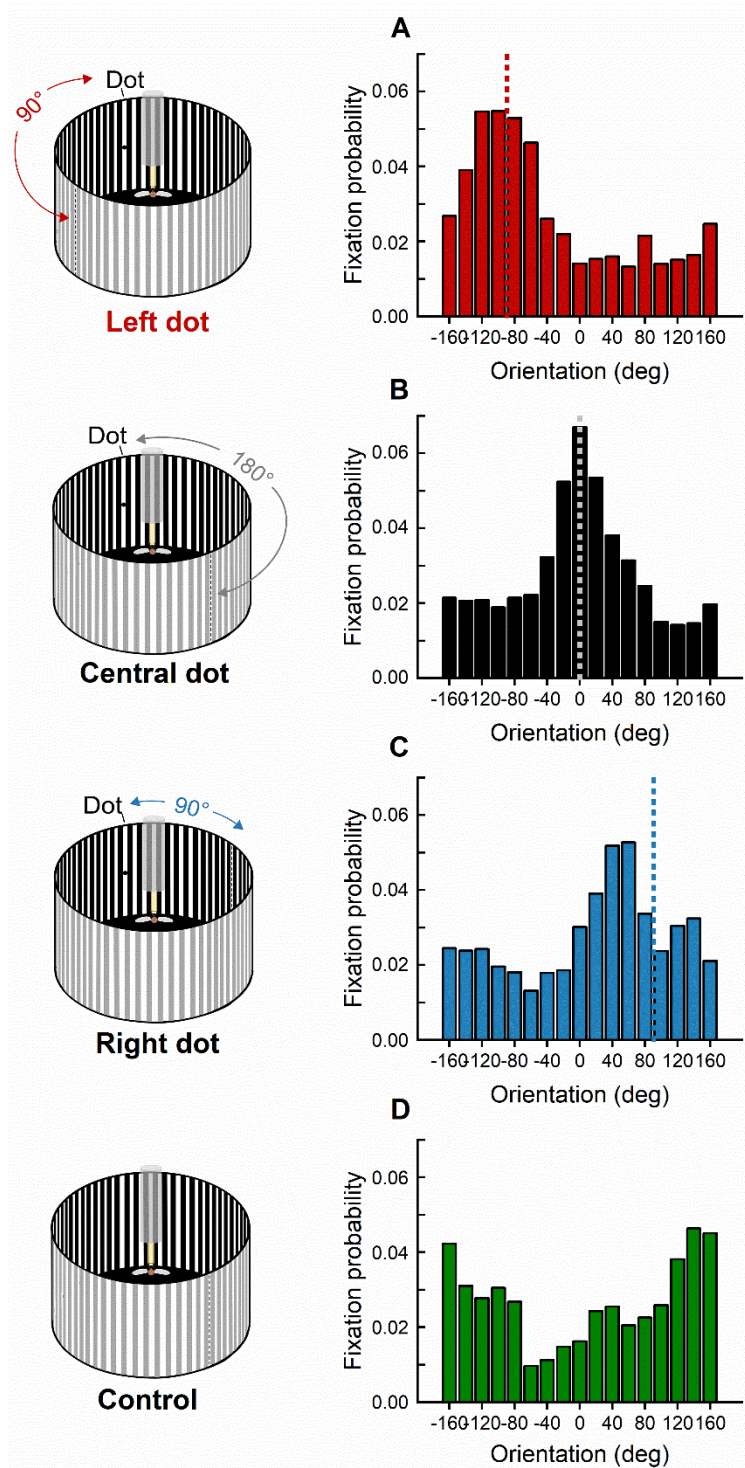


Fig. S3 Example flies show a strong bias towards the small dot.

Best performing individuals ($n = 3$) show an evident change in direction when accordingly presented with the dot to the left (A, E), centre (B, F) and right (C, G). (D, H) The flies show no fixation peak except near the paper-join for the control.

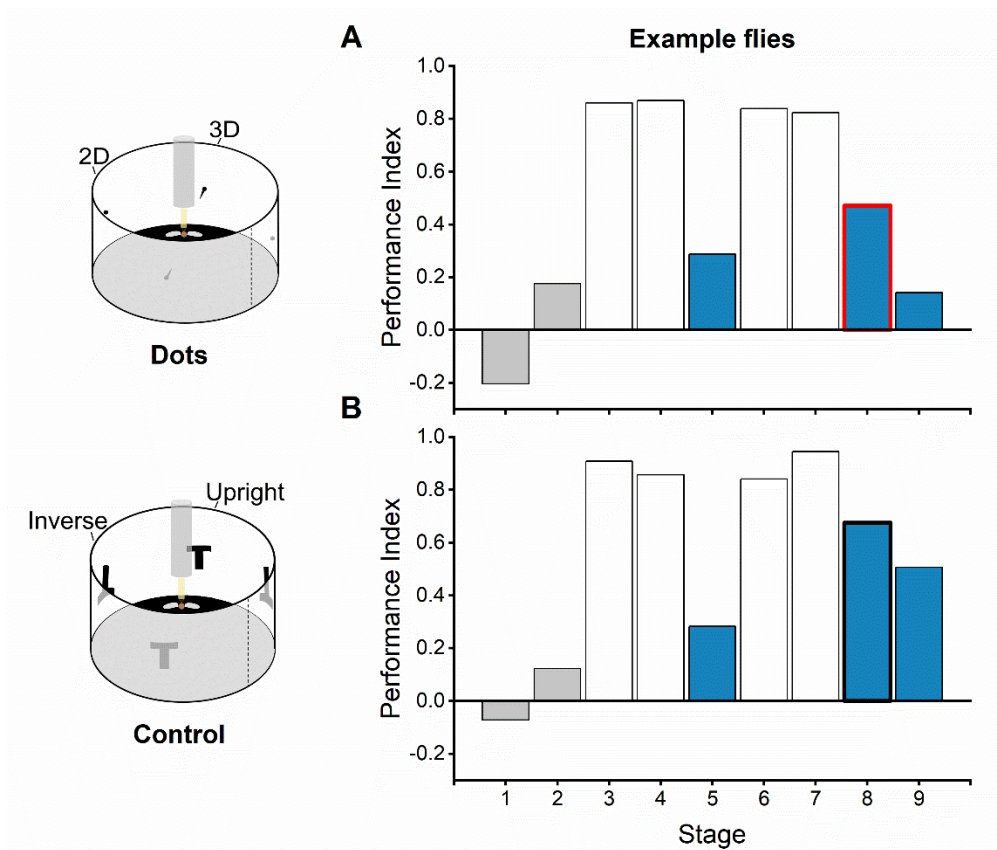


Fig. S4 Example flies of visual learning.

(**A**, **B**) Performance indices of exemplary fruit flies for visual learning of the dot stimulus (**A**; $n = 1$) and control stimulus (**B**; $n = 1$). Grey bar shows no pattern preference during pre-training. White bar shows training and a strong preference for the CS-. The blue bar shows the memory test and a learned preference for the CS- in stage 8.

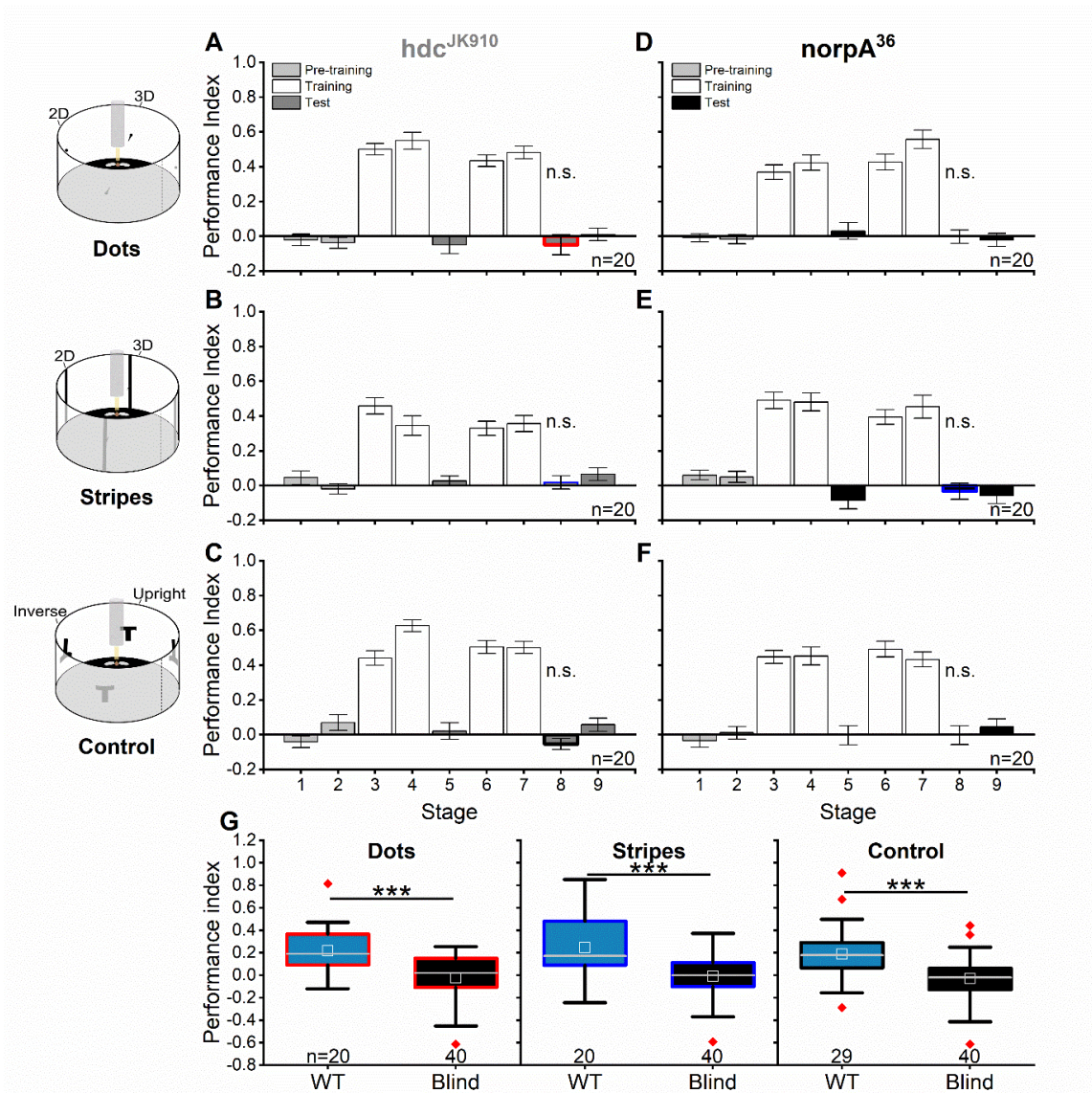


Fig. S5 Blind mutants confirm visual learning in fruit flies.

The performance index of mutant flies (**A-C**) *hdck^{JK910}* (dark grey, n = 20 for each stimulus) and (**D-F**) *norpA^{P24}* (black, n = 40 for each stimulus) that view (**A, B**) a dot stimulus, (**C, D**) a stripe stimulus, and (**E, F**) a control of T-patterns over nine 2-min sections. The grey bar shows the pre-training indicating the fly has no preference for either pattern, the white bars show the training and a general preference for the CS-, the memory test (dark grey and black) shows no learning in both mutants viewing all stimuli. Error bars indicate SEM. **G** is the same data as shown in stage 8 of **A-F**. The mean performance index of wild-type and blind mutants differed significantly for the dot stimulus (left plot), stripe stimulus (middle plot), and T-patterns (right plot). Boxes show the interquartile range, the grey line indicates the median, the white box is the mean, whiskers represent the entire data spread, and red diamonds represent outliers. Asterisks indicate the level of significance: *P<0.05, **P<0.01, ***P<0.001 and n.s. not significant.

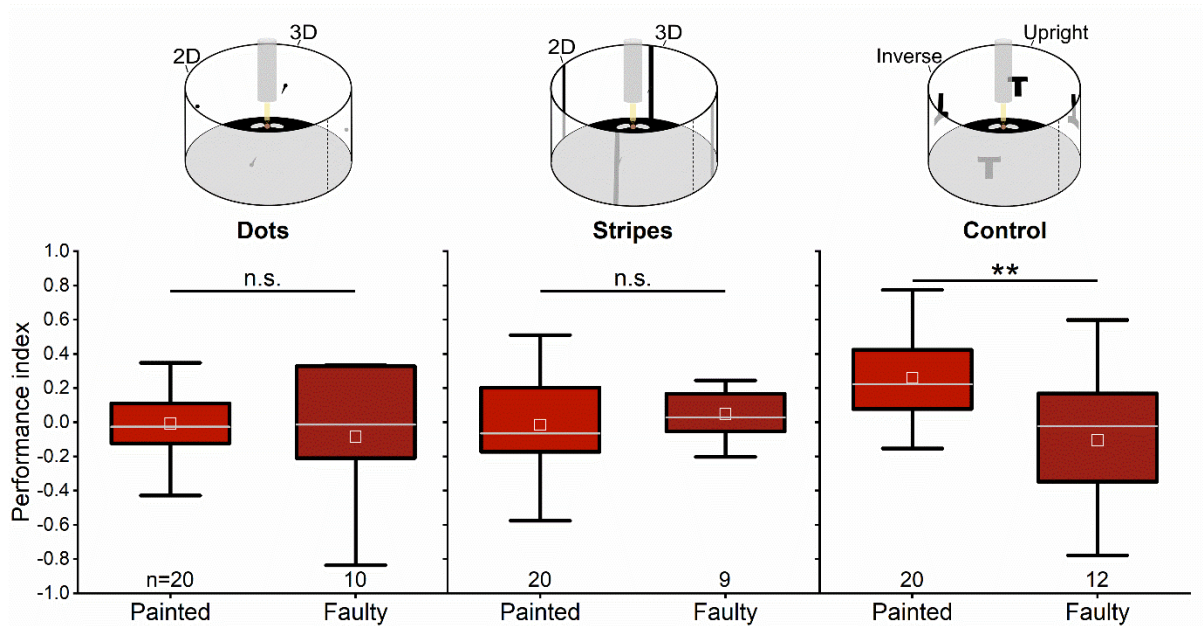


Fig. S6 Monocular vision type and learning performance.

The performance index of flies with different types of monocular vision. Either a painted eye (red) or faulty microsaccades in one eye (dark red) viewing the dot stimulus (left plot) ($n = 20$ painted; $n = 10$, faulty), stripe stimulus (middle plot) ($n = 20$ painted; $n = 9$, faulty), and t-patterns (right plot) ($n = 20$ painted; $n = 12$, faulty). Painted fly data is the same shown in stage 8 of Fig. 3.11, faulty fly data is from Fig. 3.14. The mean performance index of stage 8 shows no statistically significant difference for the dot stimulus and stripe stimulus. There is a significant difference between painted and faulty flies viewing the T-patterns. This shows that flies need both eyes to learn associations with the small visual stimuli. For large stimuli, painted flies still learn, but faulty flies do not. This indicates that disruption to the photoreceptor saccades strongly influences small object detection. Boxes show the interquartile range, the grey line indicates the median, the white box is the mean, whiskers represent the entire data spread. Asterisks indicate the level of significance: * $P < 0.05$, ** $P < 0.01$, *** $P < 0.001$ and n.s. not significant.

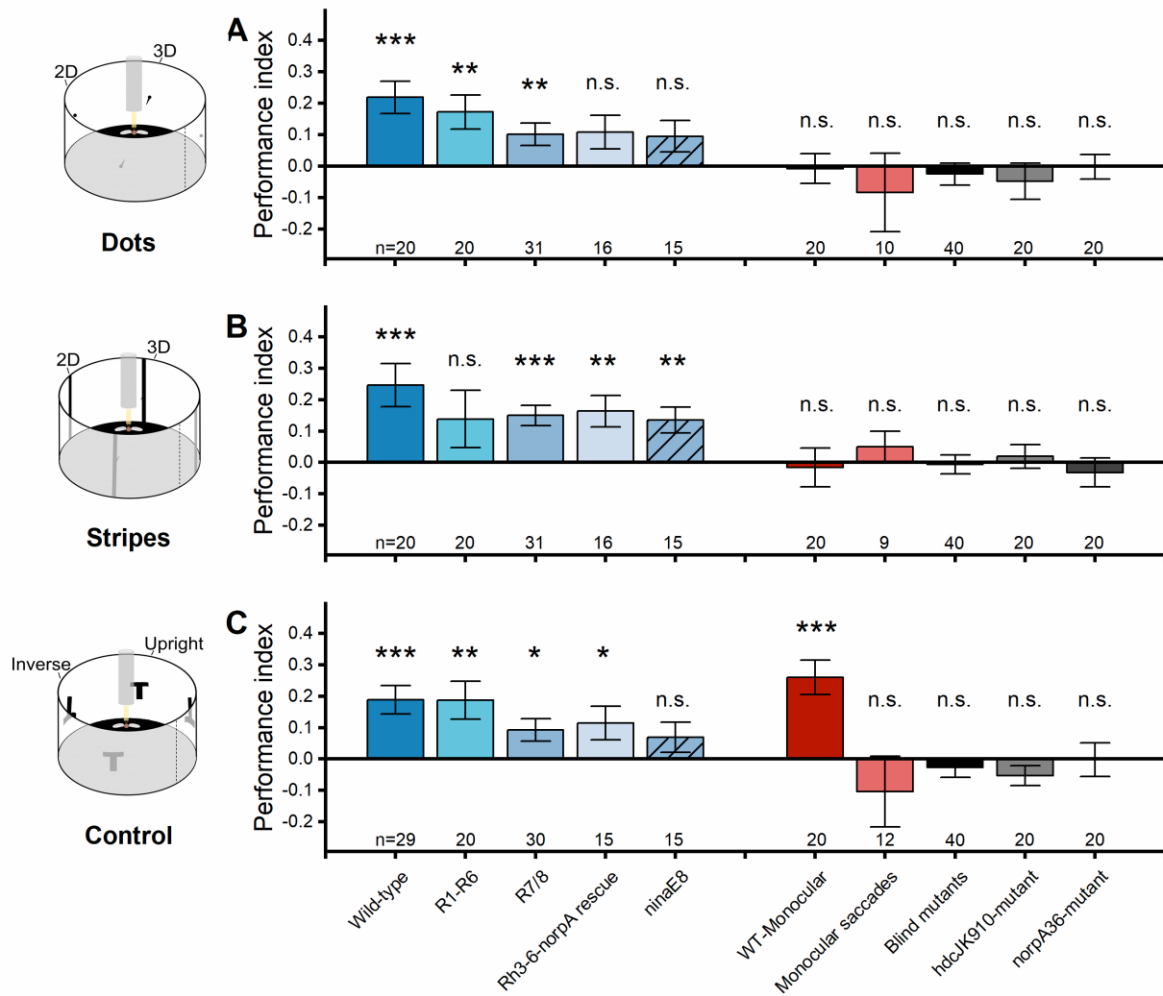


Fig. S7 Learning scores for all fly groups.

Comparison of each fly genotype and phenotype performance during stage 8 for the dot (A), stripe (B) and control (C). Asterisks indicate the level of significance: * $P < 0.05$, ** $P < 0.01$, *** $P < 0.001$ and n.s. not significant.

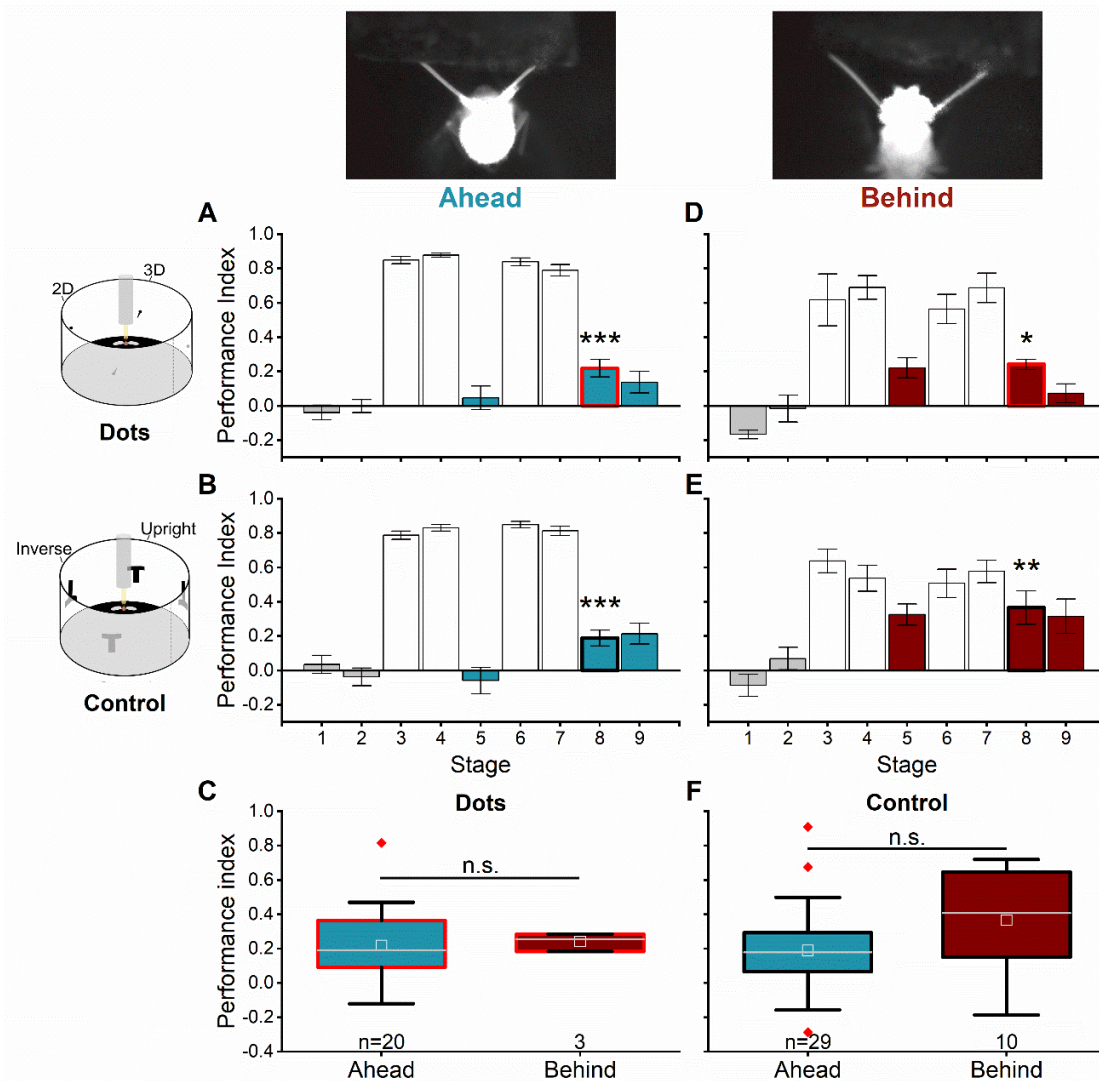


Fig. S8 Direction of heat punishment effects visual learning.

Comparison of the learning score of fruit flies conditioned with the laser directed from ahead (current method, blue) or behind (classic method, red). Grey bar shows no pattern preference during pre-training. Mean performance index suggests robust learning for the ahead method (A, B) for dots ($n = 20$) and t-patterns ($n = 29$). Lower sample sizes in the behind method for dots ($n = 3$) and t-patterns ($n = 10$) suggest the flies can learn but with no statistical difference to the ahead method. White bar shows training and a strong preference for the CS-. Blue and red bars show the memory test and a learned preference for the CS- in stage 8. Error bars indicate SEM. **C** and **F** is the same data as shown in stage 8 (**A-D**). The mean performance index of ahead and behind method flies did not differ significantly for the dot stimulus (**C**) and T-patterns (**F**). Boxes show the interquartile range, the grey line indicates the median, the white box is the mean, whiskers represent the entire data spread, and red diamonds represent outliers. Asterisks indicate the level of significance: * $P < 0.05$, ** $P < 0.01$, *** $P < 0.001$. n.s. not significant.

References

- Au, W. W. L. and Simmons, J. A. (2007) 'Echolocation in dolphins and bats', *Physics Today*, 60(9), p. 40. doi: 10.1063/1.2784683.
- Banks, M. S. *et al.* (2016) '3D Displays', *Annual review of vision science*. doi: 10.1146/annurev-vision-082114-035800.
- Barlow, H. B. and Levick, W. R. (1965) 'The mechanism of directionally selective units in rabbit's retina.', *The Journal of Physiology*, 178(3). doi: 10.1113/jphysiol.1965.sp007638.
- Barnett, P. D., Nordström, K. and O'Carroll, D. C. C. (2007) 'Retinotopic organization of small-field-target-detecting neurons in the insect visual system', *Current Biology*, 17(7), pp. 569–578. doi: 10.1016/j.cub.2007.02.039.
- Behnia, R. and Desplan, C. (2015) 'Visual circuits in flies: beginning to see the whole picture', *Current Opinion in Neurobiology*, 34, pp. 125–132. doi: 10.1016/j.conb.2015.03.010.
- De Belle, J. S. and Heisenberg, M. (1994) 'Associative odor learning in *Drosophila* abolished by chemical ablation of mushroom bodies', *Science*, 263(5147). doi: 10.1126/science.8303280.
- Blondeau, J. and Heisenberg, M. (1982) 'The three-dimensional optomotor torque system of *Drosophila melanogaster*', *Journal of comparative physiology*, 145(3), pp. 321–329. doi: 10.1007/BF00619336.
- Borst, A. (2000) 'Models of motion detection', *Nature Neuroscience*, 3(11s). doi: 10.1038/81435.
- Borst, A. (2009) 'Drosophila's view on insect vision', *Current Biology*, 19(1), pp. R36–R47. doi: 10.1016/j.cub.2008.11.001.
- Borst, A. and Egelhaaf, M. (1989) 'Principles of visual motion detection', *Trends in Neurosciences*. doi: 10.1016/0166-2236(89)90010-6.
- Borst, A. and Helmstaedter, M. (2015) 'Common circuit design in fly and mammalian motion vision', *Nature Neuroscience*. doi: 10.1038/nn.4050.

- Braitenberg, V. (1967) 'Patterns of projection in the visual system of the fly. I. Retina-lamina projections', *Experimental Brain Research*, 3(3), pp. 271–298. doi: 10.1007/BF00235589.
- Brembs, B. (2008) 'Operant learning of *Drosophila* at the torque meter', *JoVE (Journal of visualized experiments)*, (16), pp. 12–14. doi: 10.3791/731.
- Brembs, B. and Heisenberg, M. (2000) 'The operant and the classical in conditioned orientation of *Drosophila melanogaster* at the flight simulator', *Learning & Memory*, 7(2), pp. 104–115. doi: 10.1101/lm.7.2.104.
- Brembs, B. and Heisenberg, M. (2001) 'Conditioning with compound stimuli in *Drosophila melanogaster* in the flight simulator', *Journal of Experimental Biology*, 204(16), pp. 2849–2859.
- Brembs, B. and Hempel De Ibarra, N. (2006) 'Different parameters support generalization and discrimination learning in *Drosophila* at the flight simulator', *Learning & Memory*, 13(5), pp. 629–637. doi: 10.1101/lm.319406.
- Brembs, B. and Wiener, J. (2006) 'Context and occasion setting in *Drosophila* visual learning', *Learning & Memory*, 13(5), pp. 618–628. doi: 10.1101/lm.318606.
- Briscoe, A. D. and Chittka, L. (2001) 'The evolution of color vision in insects', *Annual Review of Entomology*, 46(1), pp. 471–510. doi: 10.1146/annurev.ento.46.1.471.
- Brogie, L. de (1924) 'XXXV. A tentative theory of light quanta', *The London, Edinburgh, and Dublin Philosophical Magazine and Journal of Science*, 47(278), pp. 446–458. doi: 10.1080/14786442408634378.
- Buchner, E. (1971) *Dunkelanregung des stationaeren Flugs der Fruchtfliege Drosophila*. Julius-Maximilians-Universität, Würzburg, Germany.
- Buchner, E. (1976) 'Elementary movement detectors in an insect visual system', *Biological Cybernetics*, 24(2), pp. 85–101. doi: 10.1007/BF00360648.
- Buschbeck, E. K. and Friedrich, M. (2008) 'Evolution of insect eyes: tales of ancient heritage, deconstruction, reconstruction, remodeling, and recycling', *Evolution: Education and Outreach*, 1(4), pp. 448–462. doi: 10.1007/s12052-008-0086-z.

- Carbrera, S. and Theobald, J. (2013) ‘Flying fruit flies correct for visual sideslip depending on relative speed of forward optic flow’, *Frontiers in Behavioral Neuroscience*, 7, p. 76. doi: 10.3389/fnbeh.2013.00076.
- Carroll, D. O. (1993) ‘Feature-detecting neurons in dragonflies’, *Nature*, 362(6420), pp. 541–543.
- Cartwright, B. A. and Collett, T. S. (1979) ‘How honey–bees know their distance from a nearby visual landmark’, *Journal of Experimental Biology*, 82(1), pp. 367–372.
- Cellini, B. and Mongeau, J. M. (2020) ‘Active vision shapes and coordinates flight motor responses in flies’, *Proceedings of the National Academy of Sciences*, 117(37), pp. 23085–23095. doi: 10.1073/pnas.1920846117.
- Cheng, K. Y., Colbath, R. A. and Frye, M. A. (2019) ‘Olfactory and neuromodulatory signals reverse visual object avoidance to approach in *Drosophila*’, *Current Biology*, 29(12), pp. 2058–2065. doi: 10.1016/j.cub.2019.05.010.
- Chittka, L. (1996) ‘Optimal sets of color receptors and color opponent systems for coding of natural objects in insect vision’, *Journal of Theoretical Biology*, 181(2), pp. 179–196. doi: 10.1006/JTBI.1996.0124.
- Chouinard-Thuly, L. *et al.* (2017) ‘Technical and conceptual considerations for using animated stimuli in studies of animal behavior’, *Current Zoology*, 63(1), pp. 5–19. doi: 10.1093/cz/zow104.
- Collett, T. S. (1996) ‘Vision: simple stereopsis’, *Current Biology*, 6(11), pp. 1392–1395.
- Collett, T. S. and Land, M. F. (1975) ‘Visual control of flight behaviour in the hoverfly *Syritta pipiens* L.’, *Journal of Comparative Physiology ■ A*, 99(1), pp. 1–66. doi: 10.1007/BF01464710.
- Colonnier, F. *et al.* (2015) ‘A small-scale hyperacute compound eye featuring active eye tremor: application to visual stabilization, target tracking, and short-range odometry’, *Bioinspiration and Biomimetics*, pp. 1–18. doi: 10.1088/1748-3190/10/2/026002.
- Combes, S. A. *et al.* (2012) ‘Linking biomechanics and ecology through predator-prey interactions: Flight performance of dragonflies and their prey’, in *Journal of Experimental*

Biology, pp. 903–913. doi: 10.1242/jeb.059394.

Cronin, T. W. *et al.* (eds) (2014) *Visual ecology*. Princeton University Press.

Cruz, T. L., Pérez, S. M. and Chiappe, M. E. (2021) ‘Fast tuning of posture control by visual feedback underlies gaze stabilization in walking *Drosophila*’, *Current Biology*, 31(20), pp. 4596–4607. doi: 10.1016/j.cub.2021.08.041.

Currea, J. P., Smith, J. L. and Theobald, J. C. (2018) ‘Small fruit flies sacrifice temporal acuity to maintain contrast sensitivity’, *Vision Research*, 149, pp. 1–8. doi: 10.1016/j.visres.2018.05.007.

Currier, T. A. and Nagel, K. I. (2020) ‘Multisensory control of navigation in the fruit fly’, *Current Opinion in Neurobiology*, pp. 10–16. doi: 10.1016/j.conb.2019.11.017.

Dacke, M. *et al.* (2013) ‘Dung beetles use the Milky Way for orientation’, *Current Biology*, 23(4), pp. 298–300. doi: 10.1016/j.cub.2012.12.034.

Dickinson, M. H. and Muijres, F. T. (2016) ‘The aerodynamics and control of free flight manoeuvres in *Drosophila*’, *Philosophical Transactions of the Royal Society B: Biological Sciences*, 371(1704). doi: 10.1098/rstb.2015.0388.

Dill, M. and Heisenberg, M. (1995) ‘Visual pattern memory without shape recognition’, *Philosophical Transactions of the Royal Society of London. Series B: Biological Sciences*, 349(1328), pp. 143–152. doi: 10.1098/rstb.1995.0100.

Dill, M., Wolf, R. and Heisenberg, M. (1993) ‘Visual pattern recognition in *Drosophila* involves retinotopic matching’, *Nature*, 365(6448), pp. 751–753.

Dill, M., Wolf, R. and Heisenberg, M. (1995) ‘Behavioral analysis of *Drosophila* landmark learning in the flight simulator’, *Learning & Memory*, 2(3–4), pp. 152–160. doi: 10.1101/lm.2.3-4.152.

Dreyer, D. *et al.* (2018) ‘The Earth’s magnetic field and visual landmarks steer migratory flight behavior in the nocturnal Australian Bogong moth’, *Current Biology*, 28(13), pp. 2160–2166. doi: 10.1016/j.cub.2018.05.030.

Duistermars, B. J. *et al.* (2007) ‘Dynamic properties of large-field and small-field optomotor

flight responses in *Drosophila*’, *Journal of Comparative Physiology A*, 193(7), pp. 787–799. doi: 10.1007/s00359-007-0233-y.

Duistermars, B. J. (2012) ‘Binocular interactions underlying the classic optomotor responses of flying flies’, *Frontiers in Behavioral Neuroscience*, 6, p. 6. doi: 10.3389/fnbeh.2012.00006.

Dürr, V., König, Y. and Kittmann, R. (2001) ‘The antennal motor system of the stick insect *Carausius morosus*: anatomy and antennal movement pattern during walking’, *Journal of Comparative Physiology A*, 187(2), pp. 131–144. doi: 10.1007/s003590100183.

Dyer, A. G., Paulk, A. C. and Reser, D. H. (2011) ‘Colour processing in complex environments: insights from the visual system of bees’, *Proceedings of the Royal Society B: Biological Sciences*, 278(1707), pp. 952–959. doi: 10.1098/rspb.2010.2412.

Egelhaaf, M. (1985) ‘On the neuronal basis of figure-ground discrimination by relative motion in the visual system of the fly. 2: figure-detection cells, a new class of visual interneurons’, *Biological Cybernetics*, 52(3). doi: 10.1007/bf00364003.

Endler, J. A. (1992) ‘Signals, signal conditions, and the direction of evolution’, *The American Naturalist*, 139, pp. S125–S153. doi: 10.1086/285308.

Faul, F. *et al.* (2007) ‘G*Power 3: A flexible statistical power analysis program for the social, behavioral, and biomedical sciences’, in *Behavior Research Methods*. doi: 10.3758/BF03193146.

Feord, R. C. *et al.* (2020) ‘Cuttlefish use stereopsis to strike at prey’, *Science Advances*, 6(2), p. eaay6036.

Fernald, R. D. (2000) ‘Evolution of eyes’, *Current Opinion in Neurobiology*, 10(4), pp. 444–450. doi: 10.1016/S0959-4388(00)00114-8.

Folkers, E. and Spatz, H. C. (1981) ‘Visual learning behaviour in *Drosophila melanogaster* wildtype AS’, *Journal of Insect Physiology*, 27(9), pp. 615–622. doi: 10.1016/0022-1910(81)90109-8.

Fox, J. L. and Frye, M. A. (2014) ‘Figure-ground discrimination behavior in *Drosophila*. II. Visual influences on head movement behavior’, *Journal of Experimental Biology*, 217(4), pp. 570–579. doi: 10.1242/jeb.080192.

Franceschini, N. (1972) ‘Pupil and pseudopupil in the compound eye of *Drosophila*’, in *Information Processing in the Visual Systems of Anthropods*. Springer Berlin Heidelberg, pp. 75–82. doi: 10.1007/978-3-642-65477-0_10.

Franceschini, N. *et al.* (1991) ‘Vergence eye movements in flies’, in Elsner, N. and Penzlin, H. (eds) *Gottingen Neurobiology Report: Synapse - Transmission Modulation*. Georg Thieme Verlag, Stuttgart, Germany, p. 1.

Franceschini, N. (1997) ‘Combined optical, neuroanatomical, electrophysiological and behavioural studies on signal processing in the fly compound eye’, *Biocybernetics of vision: integrative mechanisms and cognitive processes*, 2, pp. 341–361.

Frederiksen, R. and Warrant, E. J. (2008) ‘Visual sensitivity in the crepuscular owl butterfly *Caligo memnon* and the diurnal blue morpho *Morpho peleides*: a clue to explain the evolution of nocturnal apposition eyes?’, *Journal of Experimental Biology*, 211(6), pp. 844–851. doi: 10.1242/jeb.012179.

Frisch, K. von (1914) ‘Der farbensinn und formensinn der biene’, *Fischer*, 1. doi: 10.5962/bhl.title.11736.

Fujiwara, T. *et al.* (2017) ‘A faithful internal representation of walking movements in the *Drosophila* visual system’, *Nature Neuroscience*, 20(1). doi: 10.1038/nn.4435.

von Gavel, L. (1939) ‘Die “kritische Streifenbreite” als Mass der Sehschärfe bei *Drosophila melanogaster*’, *Zeitschrift für Vergleichende Physiologie*, 27(1), pp. 80–135. doi: 10.1007/BF00340525.

Geurten, B. R. H. *et al.* (2007) ‘Neural mechanisms underlying target detection in a dragonfly centrifugal neuron’, *Journal of Experimental Biology*, 210(18), pp. 3277–3284. doi: 10.1242/jeb.008425.

Geurten, B. R. H. *et al.* (2014) ‘Saccadic body turns in walking *Drosophila*’, *Frontiers in Behavioral Neuroscience*, 8, p. 365. doi: 10.3389/fnbeh.2014.00365.

Giurfa, M. and Sandoz, J. C. (2012) ‘Invertebrate learning and memory: fifty years of olfactory conditioning of the proboscis extension response in honeybees’, *Learning & Memory*, 19(2), pp. 54–66. doi: 10.1101/lm.024711.111.

- Gonzalez-Bellido, P. T., Fabian, S. T. and Nordström, K. (2016) ‘Target detection in insects: optical, neural and behavioral optimizations’, *Current Opinion in Neurobiology*, 41, pp. 122–128. doi: 10.1016/j.conb.2016.09.001.
- Gonzalez-Bellido, P. T., Wardill, T. J. and Juusola, M. (2011) ‘Compound eyes and retinal information processing in miniature dipteran species match their specific ecological demands’, *Proceedings of the National Academy of Sciences*, 108(10), pp. 4224–4229. doi: 10.1073/pnas.1014438108.
- Götz, K. G. (1964) ‘Optomotorische untersuchung des visuellen systems einiger augenmutanten der fruehtfliege *Drosophila*’, *Kybernetik*, 2(2), pp. 77–92.
- Götz, K. G. (1968) ‘Flight control in *Drosophila* by visual perception of motion’, *Kybernetik*, 4(6), pp. 199–208. doi: 10.1007/BF00272517.
- Götz, K. G. and Wenking, H. (1973) ‘Visual control of locomotion in the walking fruitfly *Drosophila*’, *Journal of comparative physiology*, 85(3), pp. 235–266. doi: 10.1007/BF00694232.
- Goulson, D. (1999) ‘Foraging strategies of insects for gathering nectar and pollen, and implications for plant ecology and evolution’, *Perspectives in plant ecology, evolution and systematics*, 2(2), pp. 185–209. doi: 10.1078/1433-8319-00070.
- Guo, A. *et al.* (1996) ‘Conditioned visual flight orientation in *Drosophila*: dependence on age, practice, and diet’, *Learning & Memory*, 3(1), pp. 49–59. doi: 10.1101/lm.3.1.49.
- Hardcastle, B. J. and Krapp, H. G. (2016) ‘Evolution of biological image stabilization’, *Current Biology*, pp. R1010–R1021. doi: 10.1016/j.cub.2016.08.059.
- Hardie, R. C. (1985) ‘Functional organization of the fly retina’, in *Processes in sensory physiology*, pp. 1–79. doi: 10.1007/978-3-642-70408-6_1.
- Hardie, R. C. and Franze, K. (2012) ‘Photomechanical responses in *Drosophila* photoreceptors’, *Science*, 338(6104), pp. 260–263. doi: 10.1126/science.1222376.
- Hardie, R. C. and Juusola, M. (2015) ‘Phototransduction in *Drosophila*’, *Current Opinion in Neurobiology*, 34, pp. 37–45. doi: 10.1016/j.conb.2015.01.008.

Hardie, R. C. and Raghu, P. (2001) 'Visual transduction in *Drosophila*', *Nature*, 413(6852), pp. 186–193.

Haselsteiner, A. F., Gilbert, C. and Wang, Z. J. (2014) 'Tiger beetles pursue prey using a proportional control law with a delay of one half-stride', *Journal of the Royal Society Interface*, 11(95), p. 20140216. doi: 10.1098/rsif.2014.0216.

Von Hassenstein, B. and Reichardt, W. (1956) 'Systemtheoretische Analyse der Zeit-, Reihenfolgen- und Vorzeichenauswertung bei der Bewegungsperzeption des Rüsselkäfers *Chlorophanus*', *Zeitschrift für Naturforschung - Section B Journal of Chemical Sciences*, 11(9–10). doi: 10.1515/znb-1956-9-1004.

Van Hateren, J. H. and Schilstra, C. (1999) 'Blowfly flight and optic flow. II. Head movements during flight', *Journal of Experimental Biology*, 202(11), pp. 1491–1500. doi: 10.1242/jeb.202.11.1491.

Hecht, S. and Wald, G. (1934) 'The visual acuity and intensity discrimination of *Drosophila*', *Journal of General Physiology*, 17(4), pp. 517–547. doi: 10.1085/jgp.17.4.517.

Heesy, C. P. (2009) 'Seeing in stereo: the ecology and evolution of primate binocular vision and stereopsis', *Evolutionary Anthropology: Issues, News, and Reviews*, 18(1), pp. 21–35. doi: 10.1002/evan.20195.

Heisenberg, M. (2015) 'Outcome learning, outcome expectations, and intentionality in *Drosophila*', *Learning & Memory*, 22(6), pp. 294–298. doi: 10.1101/lm.037481.114.

Heisenberg, M. and Buchner, E. (1977) 'The role of retinula cell types in visual behavior of *Drosophila melanogaster*', *Journal of comparative physiology*, 117(2), pp. 127–162. doi: 10.1007/BF00612784.

Heisenberg, M. and Wolf, R. (1979) 'On the fine structure of yaw torque in visual flight orientation of *Drosophila melanogaster*', *Journal of comparative physiology*, 130(2), pp. 113–130. doi: 10.1207/s15327752jpa8302_09.

Heisenberg, M. and Wolf, R. (1984) *Vision in Drosophila: genetics in microbehaviour (Vol. 12), Vision in Drosophila*. Springer-Verlag.

Heisenberg, M. and Wolf, R. (1993) 'The sensory-motor link in motion-dependent flight

control of flies’, *Reviews of Oculomotor Research*, 5, pp. 265–283.

Heisenberg, M., Wonneberger, R. and Wolf, R. (1978) ‘Optomotor-blind H31 - a *Drosophila* mutant of the lobula plate giant neurons’, *Journal of comparative physiology*, 124(4), pp. 287–296. doi: 10.1007/BF00661379.

Henderson, S. R., Reuss, H. and Hardie, R. C. (2000) ‘Single photon responses in *Drosophila* photoreceptors and their regulation by Ca²⁺’, *Journal of Physiology*, 524(1), pp. 179–194. doi: 10.1111/j.1469-7793.2000.00179.x.

Honkanen, A. *et al.* (2014) ‘Cockroach optomotor responses below single photon level’, *Journal of Experimental Biology*, 217(23), pp. 4262–4268. doi: 10.1242/jeb.112425.

Honkanen, A. *et al.* (2018) ‘The role of ocelli in cockroach optomotor performance’, *Journal of Comparative Physiology A*, 204(2), pp. 231–243. doi: 10.1007/s00359-017-1235-z.

Horn, E. (1978) ‘The mechanism of object fixation and its relation to spontaneous pattern preferences in *Drosophila melanogaster*’, *Biological Cybernetics*, 31(3), pp. 145–158. doi: 10.1007/BF00337000.

Horn, E. and Wehner, R. (1975) ‘The mechanism of visual pattern fixation in the walking fly, *Drosophila melanogaster*’, *Journal of comparative physiology*, 101(1), pp. 39–56. doi: 10.1007/BF00660118.

Horridge, A. (2009a) ‘What does an insect see?’, *Journal of Experimental Biology*, 212(17), pp. 2721–2729. doi: 10.1242/jeb.030916.

Horridge, A. (2009b) *What Does the Honeybee See? And how do we know?: a critique of scientific reason*. ANU Press.

Horseman, B. G., Gebhardt, M. J. and Honegger, H. W. (1997) ‘Involvement of the suboesophageal and thoracic ganglia in the control of antennal movements in crickets’, *Journal of Comparative Physiology A*, 181(3), pp. 195–204. doi: 10.1007/s003590050106.

Juusola, M. *et al.* (2017) ‘Microsaccadic sampling of moving image information provides *Drosophila* hyperacute vision’, *eLife*, 6, p. e26117. doi: 10.7554/eLife.26117.001.

Juusola, M. and French, A. S. (1997) ‘Visual acuity for moving objects in first- and second-

order neurons of the fly compound eye', *Journal of Neurophysiology*, 77(3), pp. 1487–1495. doi: 10.1152/jn.1997.77.3.1487.

Juusola, M. and Hardie, R. C. (2001) 'Light adaptation in *Drosophila* photoreceptors: I. Response dynamics and signaling efficiency at 25 C', *Journal of General Physiology*, 117(1), pp. 3–25.

Katsov, A. Y. and Clandinin, T. R. (2008) 'Motion processing streams in *Drosophila* are behaviorally specialized', *Neuron*, 59(2), pp. 322–335. doi: 10.1016/j.neuron.2008.05.022.

Keleş, M. F. and Frye, M. A. (2017) 'Object-detecting neurons in *Drosophila*', *Current Biology*, 27(5), pp. 680–687. doi: 10.1016/j.cub.2017.01.012.

Kemppainen, J. *et al.* (2022) 'Binocular mirror-symmetric microsaccadic sampling enables *Drosophila* hyperacute 3D vision', *Proceedings of the National Academy of Sciences*, 119(12), p. e2109717119.

Kim, A. J. *et al.* (2017) 'Quantitative Predictions Orchestrate Visual Signaling in *Drosophila*', *Cell*, 168(1–2). doi: 10.1016/j.cell.2016.12.005.

Kim, H. G. R., Angelaki, D. E. and DeAngelis, G. C. (2016) 'The neural basis of depth perception from motion parallax', *Philosophical Transactions of the Royal Society B: Biological Sciences*, 371(1697), p. p.20150256. doi: 10.1098/rstb.2015.0256.

Kirschfeld, K. (1967) 'Die projektion der optischen umwelt auf das raster der rhabdomere im komplexauge von *Musca*', *Experimental Brain Research*, 3(3), pp. 248–270. doi: 10.1007/BF00235588.

Kirschfeld, K. (1976) 'The resolution of lens and compound eyes', in *Neural principles in vision*. Springer Berlin Heidelberg, pp. 354–370. doi: 10.1007/978-3-642-66432-8_19.

Kral, K. (2003) 'Behavioural-analytical studies of the role of head movements in depth perception in insects, birds and mammals', *Behavioural Processes*, 64(1), pp. 1–12. doi: 10.1016/S0376-6357(03)00054-8.

Krapp, H. G., Hengstenberg, R. and Egelhaaf, M. (2001) 'Binocular contributions to optic flow processing in the fly visual system', *Journal of Neurophysiology*, 85(2). doi: 10.1152/jn.2001.85.2.724.

Kühn, A. (1927) 'Über den farbensinn der bienen', *Zeitschrift für Vergleichende Physiologie*, 5(4), pp. 762–800. doi: 10.1007/BF00302277.

Kühn, A. and Pohl, R. (1921) 'Dressurfähigkeit der bienen auf spektrallinien', *Naturwissenschaften*, 9(37), pp. 738–740. doi: 10.1007/BF01487183.

Kunze, P. (1961) 'Untersuchung des bewegungssehens fixiert fliegender bienen', *Zeitschrift für Vergleichende Physiologie*, 44(6), pp. 656–684. doi: 10.1007/BF00341335.

de la Flor, M. *et al.* (2017) 'Drosophila increase exploration after visually detecting predators', *PLoS ONE*, 12(7), p. e0180749. doi: 10.1371/journal.pone.0180749.

Land, M. F. (1981) 'Optics and vision in invertebrates', in *Handbook of Sensory Physiology Vol VII/6B*, pp. 471–592. doi: 10.1007/978-3-642-66907-1_4.

Land, M. F. (1992) 'Visual tracking and pursuit: humans and arthropods compared', *Journal of Insect Physiology*, 38(12), pp. 939–951. doi: 10.1016/0022-1910(92)90002-U.

Land, M. F. (1995) 'The functions of eye movements in animals remote from man', in *Studies in Visual Information Processing*. doi: 10.1016/S0926-907X(05)80006-6.

Land, M. F. (1997) 'Visual acuity in insects', *Annual Review of Entomology*, 42(1), pp. 147–177. doi: 10.1146/annurev.ento.42.1.147.

Land, M. F. (1999) 'Motion and vision: why animals move their eyes', *Journal of Comparative Physiology A*, 185(4), pp. 341–352. doi: 10.1007/s003590050393.

Land, M. F. and Eckert, H. (1985) 'Maps of the acute zones of fly eyes', *Journal of Comparative Physiology A*, 156(4), pp. 525–538. doi: 10.1007/BF00613976.

Land, M. F. and Fernald, R. D. (1992) 'The evolution of eyes', *Annual Review of Neuroscience*, 15(1), pp. 1–29. Available at: www.annualreviews.org.

Land, M. F. and Nilsson, D.-E. (2012) *Animal eyes*. Oxford University Press.

Laughlin, S. B. and Weckström, M. (1993) 'Fast and slow photoreceptors - a comparative study of the functional diversity of coding and conductances in the Diptera', *Journal of Comparative Physiology A*, 172(5). doi: 10.1007/BF00213682.

- Lawson, K. K. K. and Srinivasan, M. V. (2018) 'Flight control of fruit flies: dynamic response to optic flow and headwind', *Journal of Experimental Biology*, 220(11), pp. 2005–2016. doi: 10.1242/jeb.189720.
- Lehrer, M. *et al.* (1988) 'Motion cues provide the bee's visual world with a third dimension', *Nature*, 332(6162), pp. 356–357. doi: 10.1038/332356a0.
- Lehrer, M. and Collett, T. S. (1994) 'Approaching and departing bees learn different cues to the distance of a landmark', *Journal of Comparative Physiology A*, 175(2), pp. 171–177. doi: 10.1007/BF00215113.
- Liu, G. *et al.* (2006) 'Distinct memory traces for two visual features in the *Drosophila* brain', *Nature*, 439(7076), pp. 551–556. doi: 10.1038/nature04381.
- Liu, L. *et al.* (1998) 'Conditioned visual flight orientation in *Drosophila melanogaster* abolished by benzaldehyde', *Pharmacology Biochemistry and Behavior*, 61(4), pp. 349–355. doi: 10.1016/S0091-3057(98)00125-7.
- Liu, L. *et al.* (1999) 'Context generalization in *Drosophila* visual learning requires the mushroom bodies', *Nature*, 400(6746), pp. 753–756. doi: 10.1038/23456.
- Maimon, G., Straw, A. D. and Dickinson, M. H. (2008) 'A simple vision-based algorithm for decision making in flying *Drosophila*', *Current Biology*, 18(6), pp. 464–470. doi: 10.1016/j.cub.2008.02.054.
- Maisak, M. S. *et al.* (2013) 'A directional tuning map of *Drosophila* elementary motion detectors', *Nature*, 500(7461). doi: 10.1038/nature12320.
- Maldonado, H. and Rodriguez, E. (1972) 'Depth perception in the praying mantis', *Physiology and Behavior*, 8(4), pp. 751–759. doi: 10.1016/0031-9384(72)90107-2.
- Mallock, A. (1894) 'I. Insect sight and the defining power of composite eyes', *Proceedings of the Royal Society of London*, 55(331–335), pp. 85–90. doi: 10.1098/rsp1.1894.0016.
- Menzel, R. (1979) 'Spectral sensitivity and color vision in invertebrates', in *Comparative physiology and evolution of vision in invertebrates*, pp. 503–580. doi: 10.1007/978-3-642-66999-6_9.

- Mongeau, J. M. and Frye, M. A. (2017) 'Drosophila spatiotemporally integrates visual signals to control saccades', *Current Biology*, 27(19), pp. 2901–2914. doi: 10.1016/j.cub.2017.08.035.
- Morante, J. and Desplan, C. (2005) 'Photoreceptor axons play hide and seek', *Nature Neuroscience*, 8(4), pp. 401–402. doi: 10.1038/nn0405-401.
- Morante, J. and Desplan, C. (2008) 'The color-vision circuit in the medulla of Drosophila', *Current Biology*, 18(8), pp. 553–565. doi: 10.1016/j.cub.2008.02.075.
- Nelson, M. E. and MacIver, M. A. (2006) 'Sensory acquisition in active sensing systems', *Journal of Comparative Physiology A*, 192(6), pp. 573–586. doi: 10.1007/s00359-006-0099-4.
- Nilsson, D.-E. (1989) 'Optics and evolution of the compound eye', in *Facets of Vision*. Springer Berlin Heidelberg, pp. 30–73. doi: 10.1007/978-3-642-74082-4_3.
- Nilsson, D. E. (2013) 'Eye evolution and its functional basis', *Visual Neuroscience*, 30(1–2), pp. 5–20. doi: 10.1017/S0952523813000035.
- Nilsson, D. E. and Ro, A.-I. (1994) 'Did neural pooling for night vision lead to the evolution of neural superposition eyes?', *Journal of Comparative Physiology A*, 175(3), pp. 289–302. doi: 10.1007/BF00192988.
- Nityananda, V., Tarawneh, G., *et al.* (2016) 'Insect stereopsis demonstrated using a 3D insect cinema', *Scientific Reports*, 6(1), pp. 1–9. doi: 10.1038/srep18718.
- Nityananda, V., Bissianna, G., *et al.* (2016) 'Small or far away? Size and distance perception in the praying mantis', *Philosophical Transactions of the Royal Society B: Biological Sciences*, 371(1697), p. 20150262. doi: 10.1098/rstb.2015.0262.
- Nityananda, V. *et al.* (2018) 'A novel form of stereo vision in the praying mantis', *Current Biology*, 28(4), pp. 588–593. doi: 10.1016/j.cub.2018.01.012.
- Nityananda, V. *et al.* (2019) 'Motion-in-depth perception and prey capture in the praying mantis *Sphodromantis lineola*', *Journal of Experimental Biology*, 222(11), p. jeb198614. doi: 10.1242/jeb.198614.
- Nityananda, V. and Read, J. C. A. (2017) 'Stereopsis in animals: evolution, function and mechanisms', *Journal of Experimental Biology*, 220(14), pp. 2502–2512. doi:

10.1242/jeb.143883.

Nordström, K. (2012) ‘Neural specializations for small target detection in insects’, *Current Opinion in Neurobiology*, 22(2), pp. 272–278. doi: 10.1016/j.conb.2011.12.013.

Nordström, K., Barnett, P. D. and O’Carroll, D. C. (2006) ‘Insect detection of small targets moving in visual clutter’, *PLoS Biology*, 4(3), p. e54. doi: 10.1371/journal.pbio.0040054.

Nordström, K. and O’Carroll, D. C. (2009) ‘Feature detection and the hypercomplex property in insects’, *Trends in Neurosciences*, 32(7), pp. 383–391. doi: 10.1016/j.tins.2009.03.004.

Nuutila, J. *et al.* (2020) ‘Effect of stimulus height on cockroach optomotor response’, *Journal of Experimental Biology*, 223(10), p. jeb204768. doi: 10.1242/jeb.204768.

O’Carroll, D. C. and Wiederman, S. D. (2014) ‘Contrast sensitivity and the detection of moving patterns and features’, *Philosophical Transactions of the Royal Society B: Biological Sciences*, 369(1636), p. 20130043. doi: 10.1098/rstb.2013.0043.

Ofstad, T. A., Zuker, C. S. and Reiser, M. B. (2011) ‘Visual place learning in *Drosophila melanogaster*’, *Nature*, 474(7350). doi: 10.1038/nature10131.

Osorio, D. (2007) ‘Spam and the evolution of the fly’s eye’, *Bioessays*, pp. 111–115. doi: 10.1002/bies.20533.

Palavalli-Nettimi, R. and Theobald, J. (2020) ‘Insect neurobiology: how a small spot stops a fly’, *Current Biology*, 30(13), pp. R761–R763. doi: 10.1016/j.cub.2020.05.005.

Pegoraro, M. *et al.* (2020) ‘The genetic basis of diurnal preference in *Drosophila melanogaster*’, *BMC Genomics*, 21(1), pp. 1–11. doi: 10.21203/rs.2.17994/v1.

Peitsch, D. *et al.* (1992) ‘The spectral input systems of hymenopteran insects and their receptor-based colour vision’, *Journal of Comparative Physiology A*, 170(1), pp. 23–40. doi: 10.1007/BF00190398.

Prete, F. R. and Mc Lean, T. (1996) ‘Responses to moving small-field stimuli by the praying mantis, *Spodromantis lineola* (Burmeister)’, *Brain, Behavior and Evolution*, 47(1), pp. 42–54. doi: 10.1159/000113228.

Ptito, M., Lepore, F. and Guillemot, J. P. (1991) ‘Stereopsis in the cat: behavioral

demonstration and underlying mechanisms’, *Neuropsychologia*, 29(6), pp. 443–464. doi: 10.1016/0028-3932(91)90004-R.

Reichardt, W. (1973) ‘Musterinduzierte flugorientierung - verhaltens-versuche an der fliege *Musca domestica*’, *Die Naturwissenschaften*, 60(3), pp. 122–138. doi: 10.1007/BF00594781.

Reichardt, W. and Poggio, T. (1976) ‘Visual control of orientation behaviour in the fly Part I. A quantitative analysis’, *Quarterly Reviews of Biophysics*, 9(3), pp. 311–375. doi: 10.1017/S0033583500002523.

Reichardt, W. and Poggio, T. (1979) ‘Figure-ground discrimination by relative movement in the visual system of the fly - Part I: Experimental results’, *Biological Cybernetics*, 35(2), pp. 81–100. doi: 10.1007/BF00337434.

Reichardt, W., Poggio, T. and Hausen, K. (1983) ‘Figure-ground discrimination by relative movement in the visual system of the fly - Part II: towards the neural circuitry’, *Biological Cybernetics*, 46(1), pp. 1–30. doi: 10.1007/BF00595226.

Reichardt, W. and Wenking, H. (1969) ‘Optical detection and fixation of objects by fixed flying flies’, *Naturwissenschaften*, 56(8), p. 424. doi: 10.1007/BF00593644.

Riabinina, O. *et al.* (2014) ‘Head movements and the optic flow generated during the learning flights of bumblebees’, *Journal of Experimental Biology*, 217(15), pp. 2633–2642. doi: 10.1242/jeb.102897.

Rosner, R. *et al.* (2019) ‘A neuronal correlate of insect stereopsis’, *Nature Communications*, 10(1), pp. 1–9. doi: 10.1038/s41467-019-10721-z.

Rossel, S. (2002) ‘Binocular vision in insects: How mantids solve the correspondence problem’, *Proceedings of the National Academy of Sciences*, 93(23), pp. 13229–13232. doi: 10.1073/pnas.93.23.13229.

Salem, W. *et al.* (2020) ‘Fly eyes are not still: a motion illusion in *Drosophila* flight supports parallel visual processing’, *Journal of Experimental Biology*, 223(10), p. jeb212316. doi: 10.1242/jeb.212316.

Sareen, P., Wolf, R. and Heisenberg, M. (2011) ‘Attracting the attention of a fly’, *Proceedings of the National Academy of Sciences*, 108(17), pp. 7230–7235. doi: 10.1073/pnas.1102522108.

- Schilstra, C. and Van Hateren, J. H. (1999) 'Blowfly flight and optic flow. I. Thorax kinematics and flight dynamics', *Journal of Experimental Biology*, 202(11), pp. 1481–1490. doi: 10.1242/jeb.202.11.1481.
- Schneider, J. *et al.* (2018) 'Can drosophila melanogaster tell who's who?', *PLoS one*, 13(10), p. e0205043. doi: 10.1371/journal.pone.0205043.
- Schnell, B. *et al.* (2012) 'Columnar cells necessary for motion responses of wide-field visual interneurons in Drosophila', *Journal of Comparative Physiology A: Neuroethology, Sensory, Neural, and Behavioral Physiology*, 198(5). doi: 10.1007/s00359-012-0716-3.
- Schultheiss, P. *et al.* (2017) 'Using virtual reality to study visual performances of honeybees', *Current Opinion in Insect Science*, 24, pp. 43–50. doi: 10.1016/j.cois.2017.08.003.
- Seidl, R. and Kaiser, W. (1981) 'Visual field size, binocular domain and the ommatidial array of the compound eyes in worker honey bees', *Journal of comparative physiology*, 143(1), pp. 17–26. doi: 10.1007/BF00606065.
- Sharkey, C. R. *et al.* (2020) 'The spectral sensitivity of Drosophila photoreceptors', *Scientific Reports*, 10(1), pp. 1–13. doi: 10.1038/s41598-020-74742-1.
- Shaw, S. R. (1984) 'Early visual processing in insects.', *Journal of experimental biology*, 112, pp. 225–251.
- Snyder, A. W. and Miller, W. H. (1977) 'Photoreceptor diameter and spacing for highest resolving power', *Journal of the Optical Society of America*, 67(5), pp. 696–698. doi: 10.1364/JOSA.67.000696.
- Snyder, A. W., Stavenga, D. G. and Laughlin, S. B. (1977) 'Spatial information capacity of compound eyes', *Journal of comparative physiology*, 116(2), pp. 183–207. doi: 10.1007/BF00605402.
- Sobel, E. C. (1990) 'The locust's use of motion parallax to measure distance', *Journal of Comparative Physiology A*, 167(5), pp. 579–588. doi: 10.1007/BF00192653.
- Solanki, N., Wolf, R. and Heisenberg, M. (2015) 'Central complex and mushroom bodies mediate novelty choice behavior in Drosophila', *Journal of Neurogenetics*, 29(1), pp. 30–37. doi: 10.3109/01677063.2014.1002661.

- Somanathan, H. *et al.* (2017) ‘Visual adaptations for mate detection in the male carpenter bee *Xylocopa tenuiscapa*’, *PLoS ONE*, 12(1), p. e0168452. doi: 10.1371/journal.pone.0168452.
- Song, Z. *et al.* (2012) ‘Stochastic, adaptive sampling of information by microvilli in fly photoreceptors’, *Current Biology*, 22(15), pp. 1371–1380. doi: 10.1016/j.cub.2012.05.047.
- Spaethe, J. and Chittka, L. (2003) ‘Interindividual variation of eye optics and single object resolution in bumblebees’, *Journal of Experimental Biology*, 206(19), pp. 3447–3453. doi: 10.1242/jeb.00570.
- Spatz, H. C., Emanns, A. and Reichert, H. (1974) ‘Associative learning of *Drosophila melanogaster*’, *Nature*, 248(5446), pp. 359–361. doi: 10.1038/248359a0.
- Srinivasan, M. V. (1977) ‘A visually-evoked roll response in the housefly’, *Journal of comparative physiology*, 119(1), pp. 1–14. doi: 10.1007/BF00655868.
- Srinivasan, M. V. (2010) ‘Honey bees as a model for vision, perception, and cognition’, *Annual Review of Entomology*, 55, pp. 267–284. doi: 10.1146/annurev.ento.010908.164537.
- Srinivasan, M. V. (2011) ‘Honeybees as a model for the study of visually guided flight, navigation, and biologically inspired robotics’, *Physiological reviews*, 91(2), pp. 413–460. doi: 10.1152/physrev.00005.2010.
- Srinivasan, M. V. and Bernard, G. D. (1975) ‘The effect of motion on visual acuity of the compound eye: a theoretical analysis’, *Vision Research*, 15(4), pp. 515–525. doi: 10.1016/0042-6989(75)90029-2.
- Srinivasan, M. V., Poteser, M. and Kral, K. (1999) ‘Motion detection in insect orientation and navigation’, *Vision Research*, 39(16), pp. 2749–2766. doi: 10.1016/S0042-6989(99)00002-4.
- Stange, G. *et al.* (2002) ‘Anisotropic imaging in the dragonfly median ocellus: a matched filter for horizon detection’, *Journal of Comparative Physiology A*, 188(6), pp. 455–467. doi: 10.1007/s00359-002-0317-7.
- Stavenga, D. G. (2003) ‘Angular and spectral sensitivity of fly photoreceptors. I. Integrated facet lens and rhabdomere optics’, *Journal of Comparative Physiology A: Neuroethology, Sensory, Neural, and Behavioral Physiology*, 189(1), pp. 1–17. doi: 10.1007/s00359-002-0370-2.

- Strauss, R. and Heisenberg, M. (1990) 'Coordination of legs during straight walking and turning in *Drosophila melanogaster*', *Journal of Comparative Physiology A*, 167(3), pp. 403–412. doi: 10.1007/BF00192575.
- Takalo, J. *et al.* (2012) 'A fast and flexible panoramic virtual reality system for behavioural and electrophysiological experiments', *Scientific Reports*, 2(1), pp. 1–9. doi: 10.1038/srep00324.
- Tammero, L. F., Frye, M. A. and Dickinson, M. H. (2004) 'Spatial organization of visuomotor reflexes in *Drosophila*', *Journal of Experimental Biology*, 207(1), pp. 113–122. doi: 10.1242/jeb.00724.
- Tanaka, R. and Clark, D. A. (2020) 'Object-displacement-sensitive visual neurons drive freezing in *Drosophila*', *Current Biology*, 30(13), pp. 2532–2550. doi: 10.1016/j.cub.2020.04.068.
- Tang, S. *et al.* (2004) 'Visual pattern recognition in *Drosophila* is invariant for retinal position', *Science*, 305(5686), pp. 1020–1022. doi: 10.1126/science.1099839.
- Tang, S. and Juusola, M. (2010) 'Intrinsic activity in the fly brain gates visual information during behavioral choices', *PLoS One*, 5(12), p. e14455. doi: 10.1371/journal.pone.0014455.
- Taylor, G. J. *et al.* (2015) 'Insects modify their behaviour depending on the feedback sensor used when walking on a trackball in virtual reality', *Journal of Experimental Biology*, 218(19), pp. 3118–3127. doi: 10.1242/jeb.125617.
- Theobald, J. (2019) 'Insect neurobiology: what to make of a small spot?', *Current Biology*, 29(12), pp. R568–R570. doi: 10.1016/j.cub.2019.05.023.
- Timney, B. and Keil, K. (1999) 'Local and global stereopsis in the horse', *Vision Research*, 39(10), pp. 1861–1867. doi: 10.1016/S0042-6989(98)00276-4.
- Toepfer, F., Wolf, R. and Heisenberg, M. (2018) 'Multi-stability with ambiguous visual stimuli in *Drosophila* orientation behavior', *PLoS Biology*, 16(2), p. e2003113. doi: 10.1371/journal.pbio.2003113.
- Trujillo-Cenóz, O. (1965) 'Some aspects of the structural organization of the intermediate retina of dipterans', *Journal of ultrastructure research*, 13(1–2), pp. 1–33. doi: 10.1016/S0022-

5320(65)80086-7.

Viollet, S. (2014) ‘Vibrating makes for better seeing: from the fly’s micro-eye movements to hyperacute visual sensors’, *Frontiers in Bioengineering and Biotechnology*, 2, p. 9. doi: 10.3389/fbioe.2014.00009.

Virsik, R. P. and Reichardt, W. (1976) ‘Detection and tracking of moving objects by the fly *Musca domestica*’, *Biological Cybernetics*, 23(2), pp. 83–98. doi: 10.1007/BF00336012.

Vogt, N. and Desplan, C. (2007) ‘The first steps in *Drosophila* motion detection’, *Neuron*, 56(1), pp. 5–7. doi: 10.1016/j.neuron.2007.09.025.

Waddell, S. and Quinn, W. G. (2001) ‘What can we teach *Drosophila*? What can they teach us?’, *Trends in Genetics*. doi: 10.1016/S0168-9525(01)02526-4.

Wang, X. *et al.* (1998) ‘Relationship between visual learning/memory ability and brain cAMP level in *Drosophila*’, *Science in China, Series C: Life Sciences*, 41(5), pp. 503–511. doi: 10.1007/BF02882888.

Wardill, T. *et al.* (2013) ‘The miniature dipteran killer fly *Coenosia attenuata* exhibits adaptable aerial prey capture strategies’, *Frontiers in Physiology*, 57. doi: 10.3389/conf.fphys.2013.25.00057.

Wardill, T. J. *et al.* (2012) ‘Multiple spectral inputs improve motion discrimination in the *Drosophila* visual system’, *Science*, 336(6083), pp. 925–931. doi: 10.1126/science.1219424.

Wardill, T. J. *et al.* (2015) ‘The killer fly hunger games: target size and speed predict decision to pursuit’, *Brain, Behavior and Evolution*, 86(1), pp. 28–37. doi: 10.1159/000435944.

Wardill, T. J. *et al.* (2017) ‘A novel interception strategy in a miniature robber fly with extreme visual acuity’, *Current Biology*, 27(6), pp. 854–859. doi: 10.1016/j.cub.2017.01.050.

Warrant, E. (2019) *Invertebrate vision*, *Encyclopedia of Animal Behavior*. Elsevier Ltd. doi: 10.1016/B978-0-12-809633-8.01303-0.

Warrant, E. J. (2017) ‘The remarkable visual capacities of nocturnal insects: vision at the limits with small eyes and tiny brains’, *Philosophical Transactions of the Royal Society B: Biological Sciences*, 372(1717), p. 20160063. doi: 10.1098/rstb.2016.0063.

- Warrant, E. J. and McIntyre, P. D. (1993) 'Arthropod eye design and the physical limits to spatial resolving power', *Progress in Neurobiology*, 40(4), pp. 413–461. doi: 10.1016/0301-0082(93)90017-M.
- Warrant, E. J. and Nilsson, D.-E. (eds) (2006) *Invertebrate Vision*. Cambridge University Press.
- Warren, R. M. and Warren, R. P. (1968) 'Helmholtz on Perception: Its Physiology and Development', *The American Journal of Psychology*. doi: 10.2307/1420425.
- Wehner, R. (1972) 'Spontaneous pattern preferences of *Drosophila melanogaster* to black areas in various parts of the visual field', *Journal of Insect Physiology*, 18(8), pp. 1531–1543. doi: 10.1016/0022-1910(72)90232-6.
- Wehner, R. and Horn, E. (1975) 'The effect of object distance on pattern preferences in the walking fly, *Drosophila melanogaster*', *Experientia*, 31(6), pp. 641–643. doi: 10.1007/BF01944603.
- Wehrhahn, C. and Reichardt, W. (1973) 'Visual orientation of the fly *Musca domestica* towards a horizontal stripe', *Die Naturwissenschaften*, 60(4). doi: 10.1007/BF00599440.
- Wiederman, S. D., Shoemaker, P. A. and O'Carroll, D. C. (2008) 'A model for the detection of moving targets in visual clutter inspired by insect physiology', *PLoS ONE*, 3(7). doi: 10.1371/journal.pone.0002784.
- Wiegmann, B. M. *et al.* (2003) 'Time flies, a new molecular time-scale for brachyceran fly evolution without a clock', *Systematic Biology*, 52(6), pp. 745–756. doi: 10.1080/10635150390250965.
- Wijngaard, W. and Stavenga, D. G. (1975) 'On optical crosstalk between fly rhabdomeres', *Biological Cybernetics*, 18(2), pp. 61–67. doi: 10.1007/BF00337126.
- Willmund, R. and Ewing, A. (1982) 'Visual signals in the courtship of *Drosophila melanogaster*', *Animal Behaviour*, 30(1), pp. 209–215. doi: 10.1016/S0003-3472(82)80256-X.
- Wilson, M. (1978) 'The functional organisation of locust ocelli', *Journal of Comparative Physiology*, 124(4), pp. 297–316. doi: 10.1007/BF00661380.

- Wolf, R. *et al.* (1998) 'Drosophila mushroom bodies are dispensable for visual, tactile, and motor learning', *Learning & Memory*, 5(1), pp. 166–178. doi: 10.1101/lm.5.1.166.
- Wolf, R. and Heisenberg, M. (1980) 'On the fine structure of yaw torque in visual flight orientation of *Drosophila melanogaster*. II. A temporally and spatially variable weighting function for the visual field ('visual attention')', *Journal of comparative physiology*, 140(1), pp. 69–80. doi: 10.1007/BF00613749.
- Wolf, R. and Heisenberg, M. (1986) 'Visual orientation in motion-blind flies is an operant behaviour', *Nature*, 323(6084), pp. 154–156. doi: 10.1038/323154a0.
- Wolf, R. and Heisenberg, M. (1991) 'Basic organization of operant behavior as revealed in *Drosophila* flight orientation', *Journal of Comparative Physiology A*, 169(6), pp. 699–705. doi: 10.1007/BF00194898.
- Wolf, R. and Heisenberg, M. (1997) 'Visual space from visual motion: turn integration in tethered flying *Drosophila*', *Learning & Memory*, 4(4), pp. 318–327. doi: 10.1101/lm.4.4.318.
- Xia, S. *et al.* (1997) 'Memory consolidation in *Drosophila* operant visual learning', *Learning and Memory*, 4(2), pp. 205–218. doi: 10.1101/lm.4.2.205.
- Xia, S. Z. *et al.* (1997) 'Nutritional effects on operant visual learning in *Drosophila melanogaster*', *Physiology and behavior*, 62(2), pp. 263–271. doi: 10.1016/S0031-9384(97)00113-3.
- Xia, S. Z., Feng, C. H. and Guo, A. K. (1998) 'Temporary amnesia induced by cold anesthesia and hypoxia in *Drosophila*', *Physiology and Behavior*, 65(4–5), pp. 617–623. doi: 10.1016/S0031-9384(98)00191-7.
- Yack, J. E. *et al.* (2007) 'The eyes of *Macrosoma* sp. (Lepidoptera: Hedyloidea): a nocturnal butterfly with superposition optics', *Arthropod Structure and Development*, 36(1), pp. 11–22. doi: 10.1016/j.asd.2006.07.001.
- Yoon, C. S., Hirosawa, K. and Suzuki, E. (1996) 'Studies on the structure of ocellar photoreceptor cells of *Drosophila melanogaster* with special reference to subrhabdomeric cisternae', *Cell and Tissue Research*, 284(1), pp. 77–85. doi: 10.1007/s004410050568.